INFLUENCE OF CYSTEINE RESIDUES ON MONOAMINE OXIDASES CATALYSIS

By

Ana Paula Barradas Vintém

UNIVERSITY OF ST. ANDREWS

ST. ANDREWS

A thesis presented for the degree of Doctor of Philosophy at the

University of St. Andrews, June 2003

DECLARATION

I, Ana Paula Barradas Vintém, hereby certify that this thesis, which is approximately 32000 words in length, has been written by me, that it is the record of my work carried out by me and that it has not been submitted in any previous application for a higher degree.

Date 17/06/03 Signature of candidate

I was admitted as a research student in September 1999 and as a candidate for the degree of Doctor of Philosophy in September 1999; the higher study for which this record was carried out in the University of St. Andews between 1999 and 2003.

Date 17/06/03 Signature of candidate

I hereby certify that the candidate has fulfilled the conditions of the Resolution and Regulations appropriate for the degree of Doctor of Philosophy in the University of St. Andrews and that the candidate is qualified to submit this thesis in application for that degree.

Date 17/6/03 Signature of supervisor .

In submitting this thesis to the University of St. Andrews I understand that I am giving permission for it to be made available for use in accordance with the regulations of the University Library for the time being in force, subject to any copyright vested in the work not being affected thereby. I also understand that the title and abstract will be published, and that a copy of the work may be made and supplied to any *bona fide* library or research worker.

Date 17/06/03. Signature of candidate .

ACKNOWLEDGEMENTS

Firstly, I would like to express my deep appreciation to Dr. Rona R. Ramsay for her constant support and understanding. Dr. Ramsay, with her high scientific knowledge and intelligence, has given me the best guidance throughout my PhD. I would also like to thank the whole lab group for their help, especially Mrs. Joan Riddell for her technical support.

Especial thanks also to Dr. Nigel Price for introducing molecular biology techniques to me and to Prof. Richard Silverman for his valuable collaboration.

Thank you so much to my family, especially to my parents who have been there for me all of my life and whose support has always been unlimited. During my 3-year stay in Scotland their regular e-mails and phone calls have made the distance to Portugal much shorter and the rainy days more bearable.

To the love of my life, Paulo Oliveira, I would like to thank his constant love and support. I wish that we will never be apart for such long time again.

Thank you to my "Forever friends", Naomi Fawcett and Teresa Carlos, for being with me in the good and the bad times. Thank you also to all the other friends that I have made in St. Andrews.

GRANTS AWARDED:

- Scholarship Praxis XXI from Fundação para a Ciência e a Tecnologia (Portugal) to undertake my PhD studies in the University of St. Andrews, in 1999-2003.
- Moses Madonick travel grant to attend the "9th International Amine Oxidases Workshop" at the Universitat Autònoma de Barcelona, in Barcelona in 2000.

- William Ramsay Henderson Trust Travelling Scholarship of £1000.00 for travel and accommodation expenses of my visit to Prof. Silverman's lab, in Northwestern University, Evanston, USA, in 2001.
- Minshull Fund travel grant of £500.00 for a poster presentation in the "Flavins and Flavoproteins 2002" Conference in Cambridge, in 2002.
- Travel grant from Fundação para a Ciência e a Tecnologia of £500.00 for a poster presentation in the "10th International Amine Oxidases Workshop" in Kadir Has University, Istanbul, Turkey, in 2002.

PUBLICATIONS:

- Medvedev A.E., **Ramsay R.R.**, Ivanov A.S., Veselovsky A.V., Shvedov V.I., Tikhonova O.V., **Barradas A.P.**, Davidson C.K., Moskvitina T.A., Fedotova O.A. & Axenova L.N. (1999). "Inhibition of Monoamine Oxidase by Pirlindole Analogues: 3D-QSAR Analysis" *Neurobiology*, 7, 151-158.
- **Vintém A.P.B.**, Silverman R.B. & **Ramsay R.R.** (2002). "Subtle Differences Between MAO A and its Cysteine 374 Mutant During Mechanism-Based Inactivation by Cyclopropylamines" in *Flavins and Flavoproteins 2002* (Perham, R.N., Chapman, S.K. & Scruton, N.S.), Rudolf Weber, Berlin.
- Silverman R.B., **Vintém A.P.B., Ramsay R.R.**, Lu X., Rodriguez M., Ji H. (2002). "Irreversible Inactivation of Mitochondrial Monoamine Oxidases" in *Flavins and Flavoproteins 2002* (Perham, R.N., Chapman, S.K. & Scruton, N.S.), Rudolf Weber, Berlin.
- **Vintém A.P.B**, **Ramsay R.R.,** Price N., Silverman R.B., (2003). In preparation to submit in *Biochemistry*.

ABSTRACT

Monoamine oxidases (MAO), types A and B, are flavin-containing enzymes important in the regulation of biogenic amines, including the neurotransmitters, serotonin and dopamine. Cysteine modification inactivates MAO and alters the flavin redox properties, yet the crystal structure has shown that there are no conserved cysteines in the active site of MAO B and that the cysteine 365, modified after inactivation by a cyclopropylamine, was on the surface. The aim of this project was to find how the cysteine residues influence MAO catalysis. MAO A and B cysteine mutants to alanine were constructed and expressed in *P. pastoris*. MAO A C374A was purified and characterised kinetically. The mutant was active but had decreased k_{cat}/K_m values with a series of substrates compared to the native enzyme. The K_i values for inhibitors were not changed. Mechanism-based inactivators, cyclopropylamines, showed the same pattern as the substrates. Spectra studies and free thiol counts established that 1-phenylcyclopropylamine (1-PCPA) forms a flavin adduct whereas 2-phenylcyclopropylamine (2-PCPA) and *N*-cyclo-α-methylbenzylamine (N-CαMBA) form adducts with a cysteine in both native and mutant MAO A. Thus, the cysteine modified by N-CαMBA in MAO A is not the 374, as it would be expected by correspondence to the MAO B cysteine 365. For the 1-PCPA and N-CαMBA, the partition ratio was decreased by more than 50%. The data suggest the mutation of cysteine 374 decreases the efficiency of MAO A catalytic process without affecting the ligand binding. A revised mechanism for inactivation of MAO by cyclopropylamines is proposed.

ABBREVIATIONS

A	Adenine
A###G	Alanine number ### mutated to glycine
Ab	Antibody
Abs	Absorbance
Ala	Alanine
AOX	Alcohol oxidase
Arg	Arginine
ATP	Adenosine triphosphate
BCA	Bicinchoninic acid
BSA	Bovine serum albumin
BCIP/NBT	5-Bromo-4-chloro-3-indolyl phosphate / Nitro-blue tetrazolium
C	Cytosine or cysteine
C###A	Cysteine number ### mutated to alanine
C###S	Cysteine number ### mutated to serine
cDNA	Complementary DNA
CIAP	Calf intestinal alkaline phosphate
CNRS	Centre National de la Recherche Scientifique
Cys	Cysteine
DEAE	Diethylaminoethyl
DMSO	Dimethylsulphoxide
DNA	Deoxyribonucleic acid
dNTP	Deoxynucleotide triphosphates
DO	Dissolved oxygen
DPDS	2,2'-Dipyridyl disulphide
dsDNA	double stranded DNA
DTNB	5,5'-Dithio-bis(2-nitrobenzoic acid)
DTT	Dithiothreitol
EDTA	Ethylenediaminetetracetic acid
ESR	Electron spin resonance
FAD	Flavin adenine dinucleotide
FMN	Flavin mononucleotide
G	Guanidine or glycine
GAP	Glyceraldehyde-3-phosphate dehydrogenase
Gly	Glycine
His	Histidine
HPLC	High performance liquid chromatography
HSS	High speed supernatant
HSP	High speed pellet
Ig	Immunoglobulin
Ile	Isoleucine
IPTG	Isopropyl-β-D-thiogalactopyranose
KLH	Keyhole limpets hemocyanin
KPi	Potassium phosphate buffer

L###A	Leucine number ### mutated to alanine
Leu	Leucine
LB	Luria-Bertani broth
LSLB	Low salt LB
LSS	Low speed supernatant
MAO	Monoamine oxidase
MOPS	(3[N-Morpholino]propanesulphonic acid)
MPTP	1-Methyl-4-phenyl-1,2,3,6-tetrahydropyridine
MPP^+	1-Methyl-4-phenylpyridinium
MW	Molecular weight
N-CαMBA	*N*-Cyclopropyl-α–methylbenzylamine
NADH	Nicotinamide adenine dinucleotide, reduced form
NEB	New England Biolabs
1-PCPA	1-Phenylcyclopropylamine
2-PCPA	2-Phenylcyclopropylamine
PCR	Polymerase chain reaction
PEA	β-Phenylethylamine
Phe	Phenylalanine
PLA	Phospholipase A
PLC	Phospholipase C
PLP	Phospholipase pellet
PLS	Phospholipase supernatant
PMSF	Phenylmethylsulphonyl fluoride
Pro	Proline
PVDF	Polyvinylidene fluoride
red	Reduced
SDS	Sodium dodecyl sulphate
Ser	Serine
SPDP	N-succinimidyl-3-(2-pyridyl ditho)propionate
sq	Semiquinone
T	Thymine
TCA	Trichloroacetic acid
Thr	Threonine
Tm	Melting temperature
Trp	Tryptophan
TXP	Triton X-100 pellet
TXS	Triton X-100 supernatant
Tyr	Tyrosine
V###A	Valine number ### mutated to alanine
X-Gal	5-bromo-4-chloro-3-indolyl-β-galactopyranoside

INDEX

1. INTRODUCTION

The aim of this thesis is to report the findings of the author on the influence of the cysteine residues in monoamine oxidases catalysis. Nevertheless, a comprehensive but not exhaustive literature review was thought to be important in order to place the reader in the big context of monoamine oxidases, giving particular emphasis to catalytic mechanisms and the role of cysteine residues in enzymatic reactions. Thus, this chapter starts with a brief overview on the wide family of the monoamine oxidases, the flavoproteins, with the inclusion of a few details somewhat related to this project. The review of the monoamine oxidases starts with a general overview, discusses their substrates and inhibitors properties, structure and mechanism, and ends up with a brief description of their influence in the medical science.

1.1. Flavin and Flavoproteins

Since the discovery of old yellow enzyme (NADPH dehydrogenase) 70 years ago, it has become clear that flavoproteins are involved in a very wide range of biological processes. The most obvious of these are redox reactions that include dehydrogenations, simple electron transfer reactions, monooxygenations and oxidase reactions, but the versatility of the flavin cofactor has allowed its use in the biological sensing and emission of light, redox sensing, DNA repair and other processes. On the other hand, for the vast majority of these enzymes a common feature exists, that at some stage during the catalytic event a transfer of electrons takes place between the substrate and the flavin itself. Flavoenzymes can be grouped into relatively small number of classes, where members within the same class share many common properties differing from those of other classes, including the types of

reaction catalysed, the ability to use molecular oxygen as acceptor and the nature of auxiliary redox centres.

1.1.1. Chemical properties of the flavin

The structure of the redox-active part of the flavin molecule, the 7,8-dimethylisoalloxazine, in its oxidised and fully reduced states, and the numbering of the most important functional groups is shown in Figure 1.1. Reduction of the flavin occurs reversibly by two one-electron steps, or one two-electron step, involving changes which affect particularly the chemistry of the positions N(1), C(4a) and N(5). The potential of this conversion is around –200mV (pH 7) and can be lowered or increased in an approximately 600mV range through interaction with the protein (*1*). The pyrimidine nucleus of the three-membered ring system is electron-deficient and can be viewed as an "electron-sink". The degree to which the negative charge is stabilised or destabilised is an important factor governing the redox potential. A positive charge in the protein around the pyrimidine ring will contribute to increase the redox potential, whereas the presence of negative charge or of a hydrophobic environment will lower it. The thermodynamic stabilisation or destabilisation of intermediate radical forms can be viewed along the same lines. Another important factor affecting the redox potential is the modification of the flavin nucleus through introduction of functional groups and the ionisation states of the substituent (*1*).

Reactions of the flavin nucleus with a given substrate will occur preferentially at specific loci, C(4a) or N(5), depending on the type of reaction. Thus, steric restriction or facilitation of access to the flavin itself or to a specific position can lower or increase the rate of reaction.

Reduced flavin is one of the few biocatalysts, which can efficiently reduce oxygen. The reaction requires the formation of an initial complex of reduced flavin

and O_2, which is the C(4a)-flavin hydroperoxide. An electron is transferred from singlet reduced flavin to triplet O_2 to yield a caged radical pair, which after spin inversion collapses into the flavin hydroperoxide. The latter is unstable in aqueous solution, dissociating heterolytically to H_2O_2 and oxidised flavin (*2*).

Figure 1.1. Structure of the 7,8-dimethylisoalloxazine ring of the flavin.

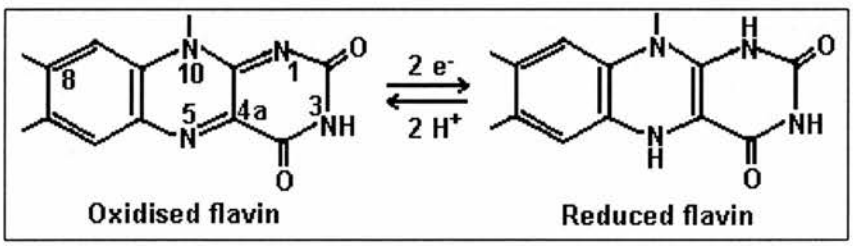

1.1.2. Properties and mechanisms of flavoproteins: a few examples

1.1.2.1. Oxidases

The oxidases, such as D-amino acid oxidase, L-lactate oxidase, glycolate oxidase, react very rapidly with O_2 to yield H_2O_2 and oxidised flavoprotein in a second-order process without observable intermediates (*3*). They all stabilise the red anionic flavin radical on one-electron reduction and most of them stabilise the flavin N(5)-sulfite adduct and the benzoquinoid anion form of the 6- and 8-substituted hydroxy and mercaptoflavins, where the negative charge of the anionic flavin is localised in the N(1)-C(2)O region. In most cases the flavin is well buried in the protein, with only the region around the N(5) accessible to solvent (*4*).

Many flavoprotein oxidases involve oxidation of substrates with electron-withdrawing groups next to the position of dehydrogenation. Such reactions appear to be initiated by abstraction of the relatively acidic α-hydrogen atom as a proton and therefore involve formally a carbanion of the substrate, either as an intermediate or, at least, as a transition state (*5*). An unusual example of a flavoprotein oxidase is the monoamine oxidase where a carbanion may not be involved. The mechanism of MAO is discussed in chapter 1.2.8.

Dihydroorotate dehydrogenases contain FMN as a tightly bound prosthetic group and function in *de novo* synthesis of pyrimidine nucleotides by catalysing formation of the 5,6-double bond of the pyridine ring. The active site is formed by loops that protrude from the barrel structure and contain fully conserved residues. A flexible loop usually covers the active site and contains the active site base (a

cysteine or a serine). This loop must open to allow access of substrate to the active site and close after substrate binding to promote catalysis (*6*).

Semicarbazide-sensitive amine oxidases (SSAO) are copper-containing amine oxidases with high affinity for benzylamine that act only on primary amines. The SSAO are not flavoproteins but contain cupric copper and a carbonyl cofactor (*7*). The reaction consists in the formation of a Schiff base between the primary amino group and the carbonyl group of the enzyme followed by a proton abstraction from the adjacent α-carbon which is the limiting step of the reaction (*8, 9*). Apparently, copper is not involved as a redox catalyst in substrate oxidation, but only in the oxidation of a close-by tyrosine to form the quinone cofactor (*10*).

Plant polyamine oxidases are flavin-containing enzymes that catalyse the oxidation of polyamine substrates spermidine and spermine and have similar structural features with monoamine oxidases (*11, 12*). Although the crystal structure has been solved, the chemical mechanism remains unknown (*13*).

1.1.2.2. Electron transferases

Physiologically, the flavin-containing enzymes of this class are all involved in single-electron transfers, e.g., flavodoxin, ferredoxin-NADP reductase and NADPH-cytochrome P-450 reductase. These enzymes all react sluggishly with O_2 and in the process produce O_2^- and the flavin semiquinone. The semiquinone is also significantly stabilised thermodynamically, generally as the blue neutral radical species. The benzene ring of the flavin is the only part readily accessible to solvent (*4*).

Flavodoxins are low molecular weight, FMN-containing, proteins which function as electron transfer agents in a variety of microbial metabolic processes, including nitrogen fixation. The highly negative redox potential required for the

biochemical activity of the flavodoxins is accomplished by stabilising the semiquinone via hydrogen bond to the N(5) position of the flavin and destabilising the fully-reduced form by constraining it to assume an unfavourable planar conformation. The reactivity of the semiquinone form is lowered by the hydrogen bond, as well as by an interaction with tryptophan residue in the binding site (*14*).

The electron transfer reactions between molecules of flavodoxin from *Megasphaera elsdenii* in different redox states have been investigated by proton nuclear magnetic resonance techniques (*15*). The activation energy for the electron transfer reaction between the semiquinone and hydroquinone state is negligible in contrast to that between the oxidised and semiquinone state. It was suggested that this feature renders *M. elsdenii* flavodoxin to an exclusive one-electron donor/acceptor in the cell, thereby shuttling between the semiquinone and the hydroquinone state.

1.1.2.3. Monooxygenases

The reduced monooxygenase reacts with O_2 to form readily observable flavin C(4a) hydroperoxide intermediates. The physiological reductant is NADH or NADPH. In the absence of further substrate, the flavin hydroperoxide decays non-productively to H_2O_2 and oxidised flavin. However, in the presence of the third substrate the flavin hydroperoxide reacts to transfer an oxygen atom to the substrate, resulting in a C(4a)-hydroxyflavin, which upon dehydration returns the flavin to its oxidised state for the next catalytic cycle. Examples of such enzymes are the *p*-hydroxybenzoate hydroxylase, where the aromatic substrate is hydroxylated at the position ortho to the activating para-substituent; and bacterial luciferase, where the third substrate is a long-chain aldehyde, and the products, fatty acid and H_2O, are formed accompanying emission of visible light (*16*).

1.1.2.4. Disulphide oxidoreductases

This family includes, among others, lipoamide dehydrogenase, glutathione reductase, mercuric reductase and thioredoxin reductase. The discovery of the participation of a redox-active disulphide group in the catalytic mechanism of these enzymes resulted from reductive titrations and its spectral changes and reaction with sulphydryl reagents (*17*).

The proposed mechanism for the disulphide oxidoreductases involves sequential thiol-disulphide interchange reactions in which the interchange thiol of 2-electron reduced enzyme attacks the disulphide of the substrate, forming a mixed disulphide (*18*). This mixed disulphide is then attacked by the electron-transfer thiol of 2-electron reduced enzyme, reforming the active site disulphide and releasing the dithiol form of the substrate. Figure 1.2 shows the mechanism of glutathione reductase and lipoamide dehydrogenase as derived from the respective crystal structures (*19, 20*).

Catalysis by thioredoxin reductase from the malaria parasite *Plasmodium falciparum* involves the flavin and 2 redox active disulphides that are in redox communication: one is made up of Cys88, the interchange thiol, and Cys93, the flavin interacting thiol; the second one, composed of Cys 535' and Cys540', is close to the C-terminus of the other subunit (*21*). The mechanism-based inactivation of thioredoxin reductase by Mannich bases (aminomethylated compounds) involves Michael addition to the reduced enzyme, deamination and addition of a second nucleophile. The reaction of two unsaturated Mannich bases occurred with the C-terminal thiolate(s) rather the interchange thiol, resulting in irreversible or reversible inactivation (by addition of DTT) depending on whether deamination is possible or not. The mechanism proposed for inactivation of this enzyme by unsaturated

Mannich bases involves the formation of an inactive macrocyclic species by bis-alkylation, first of thiol Cys540 and subsequently of Cys535 (*22*).

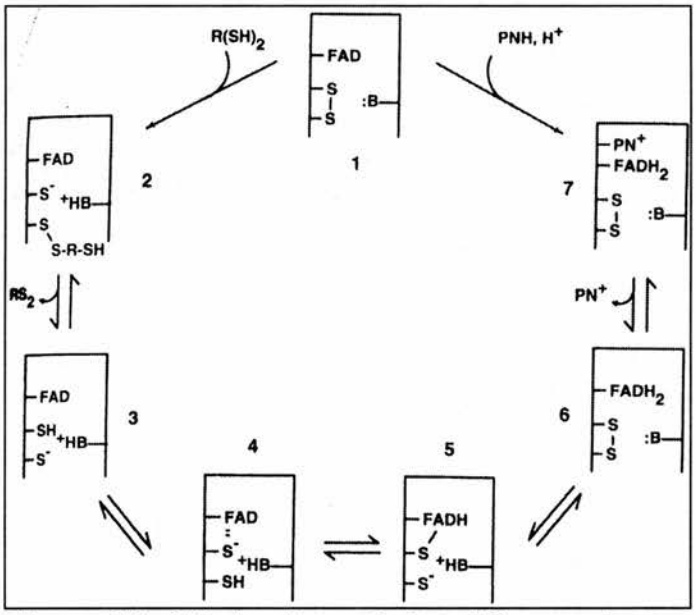

Figure 1.2. Mechanism of glutathione reductase or lipoamide dehydrogenase (*18*). Catalysis starts with species 1 and proceeds clockwise for glutathione reductase and counterclockwise for lipoamide dehydrogenase. Species 2 is the mixed disulphide; species 4 is the thiolate-FAD charge-transfer complex, and species 3 is its prototropic tautomer; species 7 is the $FADH_2$-PN^+ charge-transfer complex (PNH and PN^+, reduced and oxidised pyridine nucleotide); species 5 is a sulphur adduct at the flavin C4a position; the flavin in species 7 (and 6) may be $FADH^-$. The amino acid serving as acid base catalyst is histidine for both lipoamide dehydrogenase and glutathione reductase. The scheme as written applies formally to lipoamide dehydrogenase. One molecule of glutathione reductase departs as species 2 goes to species 3 and the second molecule as species 3 goes to species 4.

1.1.2.5. Heme-containing flavoproteins

Examples of this class are the yeast lactate dehydrogenase (flavocytochrome b_2), which, in addition to the FMN prosthetic group, also contains a b-type cytochrome domain (*23*); and the nitric oxide synthase, which, in addition to containing FAD and FMN, also contains a heme prosthetic group with cytochrome P-450-like characteristics (*24*).

Flavocytochrome b_2 appears to dehydrogenate α-hydroxy acids via a carbanion mechanism, where His373 is the active site base and Ala198 and Leu230 are important for substrate specificity (*25*). Kinetic characterisation of the mutant enzymes L230A and A198G/L230A showed a shift in substrate specificity towards larger substrates compared to the primary substrate lactate. In particular, these mutant enzymes display L-mandelate dehydrogenase activity with an increase of the specificity constant towards L-mandelate up to 80-fold (*26*). The crystal structures of these mutant enzymes allowed visualisation of the increased volume available for binding of larger substrates, and the structure of the phenylglyoxylate-bound L230A enzyme also reveals a mode of binding consistent with the operation of a hydride transfer mechanism for the L-mandelate dehydrogenation and not of a carbanion mechanism (*27*).

1.1.2.6. Metal-containing flavoproteins

The longest known example of a complex flavoprotein is xanthine oxidase that contains molybdenum and iron-sulphur centres in addition to the FAD prosthetic group (*28*). Another example is phthalate oxygenase reductase, which contains both FAD and an iron-sulphur centre (*29*).

Available evidence on the mechanism of xanthine oxidase favors a mechanism in which an active site base abstracts the proton from the Mo-OH group, initiating nucleophilic attack on substrate with concomitant hydride transfer from C-8 of substrate to Mo=S. This yields a complex species with Mo^{IV}, where the product is coordinated to the metal via the newly introduced hydroxyl group (*30, 31*). Reoxidation of the molybdenum centre takes place via electron transfer to the other redox-active centres of the enzyme, ultimately to the FAD where electrons are removed from the enzyme by reaction with dioxygen (*32*). In contrast, it was suggested by others that the reductive half reaction occurs in two consecutive one-electron steps (*33*). To test this hypothesis, the kinetic parameters k_{red} and k_{red}/K_d were determined as well as the one-electron reduction potentials for a variety of substrates. There was no correlation between the kinetic parameters for the reductive half-reaction and the one-electron reduction potentials, as would have been expected if the enzyme were using two one-electron reduction steps (*34*). These results provide additional support for the two-electron reduction mechanism.

1.2. Monoamine Oxidase

1.2.1. Background

Monoamine oxidase (MAO; EC 1.4.3.4) was first described as having tyramine oxidising activity by Mary Hare in 1928 (*35*). Nowadays, it is well known that two forms of the enzyme catalyse the oxidation of primary, secondary and tertiary amines to the corresponding imines, a process important in regulating the level of biogenic amines, such as the amine neurotransmitters norepinephrine, serotonin and dopamine (*36*). MAO is not brain-specific, indeed the highest levels

are in the liver and placenta and the lowest in the spleen (*37*). Intracellularly, it is located on the mitochondrial outer membrane (*38*).

The selective inhibition of MAO by clorgyline and deprenyl demonstrated the presence of two forms of the enzyme. The clorgyline-sensitive form was termed MAO A (*39*) and the deprenyl-sensitive form, MAO B (*40*). They are distinguished by molecular weight, affinity for substrates, sensitivity to inhibitors, tissue distribution and immunological properties (*39, 41-43*). The two forms of MAO have overlapping but distinct substrate and inhibitor specificity and follow the same kinetic and chemical mechanisms (reviewed in (*44-46*)). They are also expressed in different proportions in the various regions and cell types of the central nervous system (reviewed in (*47*)). The A-form predominates in catecholaminergic neurones and the B-form predominates in astrocytes and serotonergic neurones. A few tissues express predominantly or only one form of MAO, such as MAO A in human placenta (*48*) and MAO B in human platelets (*49*), bovine and pig liver (*50, 51*). This suggests that MAO A and MAO B are independently regulated and that cellular distribution may underlie different functions.

The physiological roles of MAO are not entirely clear (*47*). In the gut and circulatory system it probably serves to metabolise amines that could act as false neurotransmitters. Many cell types have adrenergic receptors and systemic sources of MAO may regulate the hormonal actions of biogenic amines released by neurons and chromaffin cells. In neurons and neuroendocrine cells MAO probably has a more specific function in intracellular regulation of amine stores.

Both types of MAO contain 2 identical subunits each with a covalently bound flavin adenine dinucleotide (FAD) cofactor each (*52-55*). FAD is covalently bound to a cysteine group of the enzyme by way of a thioether bond to the 8-position of the

isoalloxazine ring (*56, 57*). There is no evidence for the involvement of any metal ions or lipids, although the presence of lipids or detergents is necessary to avoid aggregation and precipitation (*47*).

The oxidation of the substrates is coupled to the reduction of the FAD. The product of the reaction is the imine of the substrate, which hydrolyses spontaneously to yield the corresponding aldehyde and ammonia. Reoxidation of the enzyme-bound cofactor by molecular oxygen produces H_2O_2.

$R\text{-}CH_2\text{-}NH_2 + E\text{-}FAD \longrightarrow R\text{-}CH{=}NH + FADH_2$

$R\text{-}CH{=}NH + H_2O \longrightarrow R\text{-}CHO + NH_3$

$FADH_2 + O_2 \longrightarrow E\text{-}FAD + H_2O_2$

Compounds that block the catalytic action of MAO A have been shown to exhibit antidepressant activity and are used for the treatment of depression. MAO B inhibition is associated with the enhanced activity of dopamine in the central nervous system, as well as with the decreased production of hydrogen peroxide, a reactive oxygen species (*58*). The MAO B inhibitor deprenyl is marketed as an adjunct to the treatment of Parkinson's disease (*59*).

1.2.2. Substrates

The principle biogenic amines metabolised by MAO A and MAO B are 5-hydroxytryptamine (serotonin), *N*-methyl-2-hydroxy-2-(3,4-dihydroxyphenyl) ethylamine (adrenaline), 2-(3,4-dihydroxyphenyl)ethylamine (dopamine), 2-phenylethylamine, and tyramine (*47*). Many other amines, both aliphatic and aromatic, serve as substrates as well, such as kynuramine, tryptamine, benzylamine (Figure 1.3).

An important structural feature for MAO substrate properties is the stereochemistry of the proton on the α-carbon in amines; aniline and α-methyl-substituted amines, such as amphetamine, are not substrates. Furthermore, both MAO isozymes exhibit the same stereospecificity by abstracting the pro-*R*-hydrogen exclusively from the prochiral methylene group in amine substrates (*60*).

Each of the MAO isoenzymes acts on specific, as well as common substrates. For example, comparing the specificity constant (k_{cat} / K_m) values for some substrates listed in Table 1.1, it can be seen that 5-hydroxytryptamine (serotonin) is more specific for purified MAO A, whereas benzylamine is more specific for purified MAO B.

Substrates of MAO A (serotonin, (nor)adrenaline), because of their chemical structure (catechol, hydroxyindole), are better electron donors for charge transfer interactions than MAO B substrates (benzylamine, phenylethylamine) which are more hydrophobic and characterised by an aromatic ring poorer in electrons (*61*).

MAO B is involved in the conversion of the xenobiotic 1-methyl-4-phenyl-1,2,3,6-tetrahydropyridine (MPTP) to $MPDP^+$, the dihydropyridinium, which is itself a substrate and is oxidised to the very stable product MPP^+ (Figure 1.4) (*62*). This discovery was of major importance since MPP^+ poisoning causes brain lesions and clinical symptoms similar to those of Parkinson's disease.

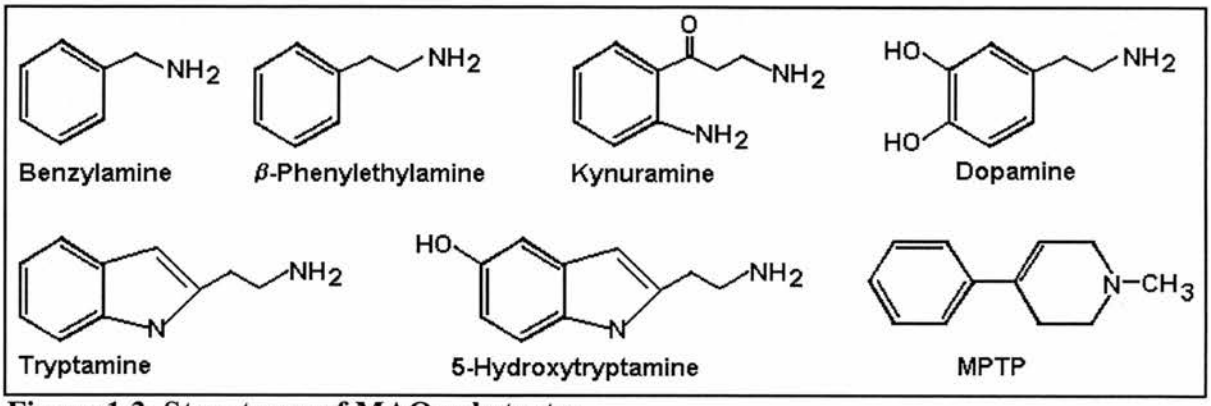

Figure 1.3. Structures of MAO substrates.

Table 1.1. Specificity constants for human liver MAO A and for beef liver MAO B from steady-state experiments*.

	k_{cat} / K_m ($mM^{-1}.s^{-1}$)		
Substrate	**MAO A**	**MAO B**	**MAO B / MAO A**
Kynuramine	17.7	32.7	2
Benzylamine	0.02	27.8	1400
β-phenylethylamine	1.5	54.0	36
Tryptamine	88.3	5.2	0.06
5-hydroxytryptamine	7.0	0.275	0.04
5-methoxytryptamine	9.8	0.75	0.08
MPTP	2.2	4.0	2
$MPDP^+$	0.75	-	-

* Data taken from (*63*).

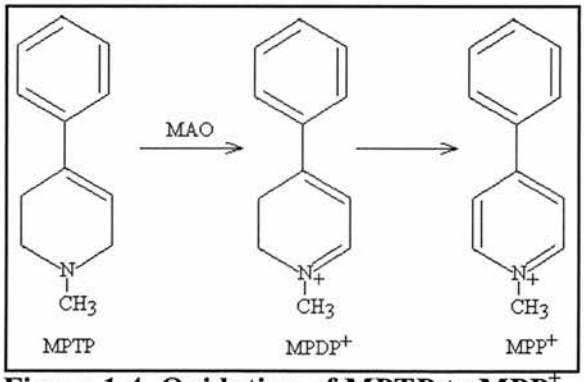

Figure 1.4. Oxidation of MPTP to MPP^+.

Studies on MPTP analogues as substrates of MAO A and B suggested that molecular flexibility enhances reactivity with MAO B but not with MAO A (*64*). Branching and rigidity in this series of tetrahydrostilbazoles were detrimental to the activity as substrates of both forms of MAO. The analogues which contain small electron-withdrawing substituents in the phenyl ring were found to be more selective for MAO B, while those substituted with bulky groups were selectively oxidised by MAO A. The substrate binding site of MAO A probably contains a lipophilic pocket larger than that in a similar site in MAO B. Additional studies on MPTP analogues suggested that the selectivity of these compounds for either MAO A or B is determined by complex interplay of molecular size and flexibility (*65*).

1-Methyl-1,2,3,6-tetrahydrostilbazole and its analogues are oxidised by MAO A at slow rates comparable to that for the structurally similar MPTP, but the rates of oxidation by MAO B vary over a wide range depending on the structure of the analogue (*66*). MAO A oxidation of all of the analogues showed little difference between the *cis* and *trans* isomers. In contrast, MAO B showed distinct stereoselectivity for the *cis* isomers. The stringency of the MAO A active site for the geometry of the substrate molecule is less strict than that of MAO B.

Each form of MAO has been known to have different specificities for different species (*67*). Various C4 substituted 1-methyl-4-phenyl-1,2,3,6-tetrahydropyridinyl derivatives were used as substrates to profile the MAO A and B activities in liver and brain mitochondrial preparations obtained from a variety of mammal species (*68*). MAO B was found to be the principal enzyme present in all tissues. Human and rat liver had the highest levels of MAO A whereas the monkey had very low MAO A activity. A comparison of ratios of the V_{max} / K_m values showed that the rabbit and mouse liver enzymes are particularly poor catalysts for

MPTP relative to the human enzymes. Studies with MAO B inhibitors showed more noticeable differences between different mammalian species (see chapter 1.2.3). These differences between species show the importance of obtaining purified human MAO from heterelogous expression for the studies of the human enzyme.

1.2.3. Reversible inhibitors

Reversible MAO inhibitors can be subdivided further into competitive and slow, tight-binding inhibitors that can be distinguished by the kinetic model in the following equation:

$$E + I \underset{k_{-1}}{\overset{k_1}{\rightleftharpoons}} (E \cdot I) \overset{k_2}{\rightleftharpoons} (E \cdot I^*)$$

According to this expression, the first step in the competitive inhibition process involves the formation of a rapidly reversible complex (E•I). The second step, usually observed with slow, tight-binding inhibitors, involves the slow, time-dependent conversion of the (E•I) complex to an activated complex (E•I*), in which the inhibitor is bound more tightly to the enzyme resulting in a conformational change in the three-dimensional structure of the enzyme.

A number of reversible inhibitors of the enzyme are listed in Table 1.2. Amphetamine and several other α-methyl substituted amines, pirlindole, harmaline, cimoxatone, toloxatone and amiflavine are selective for MAO A. S(+)Amiflavine and S(+)amphetamine are more potent and selective MAO A inhibitors than their R enantiomers (*69*). This highlights the role played by the α asymmetric centre in these two reversible MAO inhibitors. Recently, pyrrole analogues of toloxatone have been shown to be selective for MAO A, the most potent of which was 78-fold more potent than toloxatone (*70*).

Some tricyclic antidepressants are selective inhibitors of MAO B. Caroxazone is preferentially a MAO B inhibitor, although with low selectivity. Examples of potent and reversible competitive MAO B inhibitors are the tetrazoles, ether substituted coumarins (sulfonic acid substituted coumarins are selective for MAO A) and oxadiazolones (*71-73*).

Interestingly, oxadiazolones show remarkable differences in inhibitory potency with MAO B from different mammalian species. Indeed, their inhibitory potency varies by 3 to 4 orders of magnitude between rat and beef liver MAO B, whereas the inhibition of the rat and human liver enzymes is quite similar (*74*). Others have studied the differences of the inhibition of MAO activity by various antidepressants in several mammalian species (*75*). Mouse, rat, dog and monkey brain MAO B activity were inhibited by dicyclic antidepressant zimeldine more potently than MAO A activity. The tetracyclic and non-cyclic antidepressants, maprotiline and nomifensine, inhibited mouse and rat brain MAO B activity more potently than MAO A activity, whereas the inverse was true for dog and monkey brain. The K_i values for the antidepressants studied for monkey brain MAO A and MAO B were low compared to those of mouse, rat and dog. Such differences most likely reflect variations on the structure of the ligand-binding site within the various mammalian species.

Table 1.2. Reversible and competitive inhibition of MAO A and B*

Inhibitor	Source of MAO	K_i (μM)		MAO A Selectivity
		MAO A	MAO B	
S(+)Amphetamine[1]	Rat liver	20	770	39
R(-)Amphetamine[1]	Rat liver	70	600	9
(±)α-methyltryptamine[1]	Rat liver	0.5	1250	2500
S(+)FLA 336 (amiflavine)[1]	Human brain	0.4	210	525
R(-)FLA 336 (amiflavine)[1]	Human brain	0.9	25	28
Harmaline[1]	Rat brain	0.01	200	20000
(±)Toloxatone[1]	Rat brain	1.8	44	24
(±)Cimoxatone[1]	Rat brain	0.004	0.08	20
Caroxazone[1]	Rat brain	12	2	0.2
Pirlindole[1]	Rat brain	0.04	52	1300
Tetrindole[2]	Rat brain	0.4	110	275
N-methylisoquinolium ion[3]	Rat brain	0.81†	36.2†	45
5-[4(phenylmethoxy)phenyl]-2-(cyanoethyl)tetrazole[4]	Rat brain	86†	0.002†	0.000023
7-[3,4-diazol(4-isopropyl)-thiophene]coumarin[5]	Rat brain	>10†	0.0009†	< 0.00009
7-(ethylsulphonyloxy)coumarin[5]	Rat brain	0.008†	5†	625
5-[4-(benzyloxy)phenyl-3-(2-cyanoethyl)-1,3,4-oxadiazol-2(3H)-one][6]	Rat brain	100†	0.0014†	0.00014
(R)-5-methoxymethyl-3(1*H*-pyrrol-1-yl)-2-oxazolidinone[7]	Bovine brain	0.0049	50	10200
MPTP[8]	Human placenta / Bovine liver	18	100	6
$MPDP^+$[8]		2.4	200	83
MPP^+[8]		3	230	77

*Data from: 1-(*69*); 2-(*76*); 3-(*77*); 4-(*71*); 5-(*72*); 6-(*73*); 7-(*70*); 8-(*78*). †IC_{50} values.

MPTP, $MPDP^+$ and MPP^+ are competitive inhibitors of MAO A and B, the former type of enzyme being particularly sensitive (*78*). Both MAO A and B are also irreversibly inactivated by MPTP and $MPDP^+$, but not by MPP^+ (*79*). The inactivation obeys the characteristics of a suicide process and is likely to result from a covalent modification of the enzyme. Analogues of MPTP are also mechanism-based irreversible inhibitors of MAO A and B, whereas their dihydropyridinium and pyridinium oxidation products are potent reversible inhibitors of MAO A but not of MAO B (*64*). Of particular importance is the specificity of the 4'-alkyl substituted MPP^+ analogues: the longer the alkyl chain, the lower is the K_i value for MAO A.

When a series of pirlindole analogues was tested as inhibitors of MAO A and B, rigid analogues exhibited potent and selective inhibition of MAO A (*80*). They have three-dimensional (3D) size limits of 13 angstroms (length) x 7 angstroms (height) x 4.4 angstroms (width). Besides MAO A inhibition, flexible analogues also demonstrated potent inhibition of MAO B and in contrast to rigid analogues their inhibitory activity were not limited by 3D sizes. This and further evidence indicated volume differences between the active sites of MAO A and B. All the compounds studied induced immediate spectral changes in the MAO A. The better inhibitors also showed signs of charge transfer from the inhibitor to the enzyme at 520nm (*80*).

A very potent reversible and selective MAO A inhibitor is befloxatone, an oxazolidinone derivative (*81*). In human and rat brain, heart, liver and duodenum homogenates the K_i values range from 1.9 to 3.6nM for MAO A, which were about 100 times lower than those for MAO B. Befloxatone did not modify the activities of diamine or benzylamine oxidase and did not interact with monoamine uptake mechanisms or with a variety of neurotransmitter or drug receptor sites, which makes it possible to use as an antidepressant.

β-Carboline derivatives, which are heterocyclic, dehydrogenated derivatives of tryptophan, are reversible competitive inhibitors selective for MAO A (*82*). Harmine, 2-methylharminium, 2,9-dimethylharmarinium and harmaline are the most effective of the series and could be endogenous inhibitors of MAO A. The inhibitors interact with the flavin to induce distinct spectral changes, the magnitude of which correlated with the efficacy of the inhibition.

The molecular diversity of reversible inhibitors that is tolerated by MAO greatly complicates the establishment of pharmacophoric elements associated with its inhibition. Nevertheless, a general model was proposed by Wouters (Figure 1.5.A) for the reversible inhibition of MAO A by various families of inhibitors (for example, phenyl oxazolidinones and β-carbolines) *via* long distance, reversible interactions with the enzyme (*61*). It is assumed that the inhibitors are engaged in a molecular association with MAO A through a double attachment at a primary and secondary binding site (Figure 1.5, top). This hypothetical model is consistent with data obtained on different series of reversible inhibitors of MAO A (*61*).

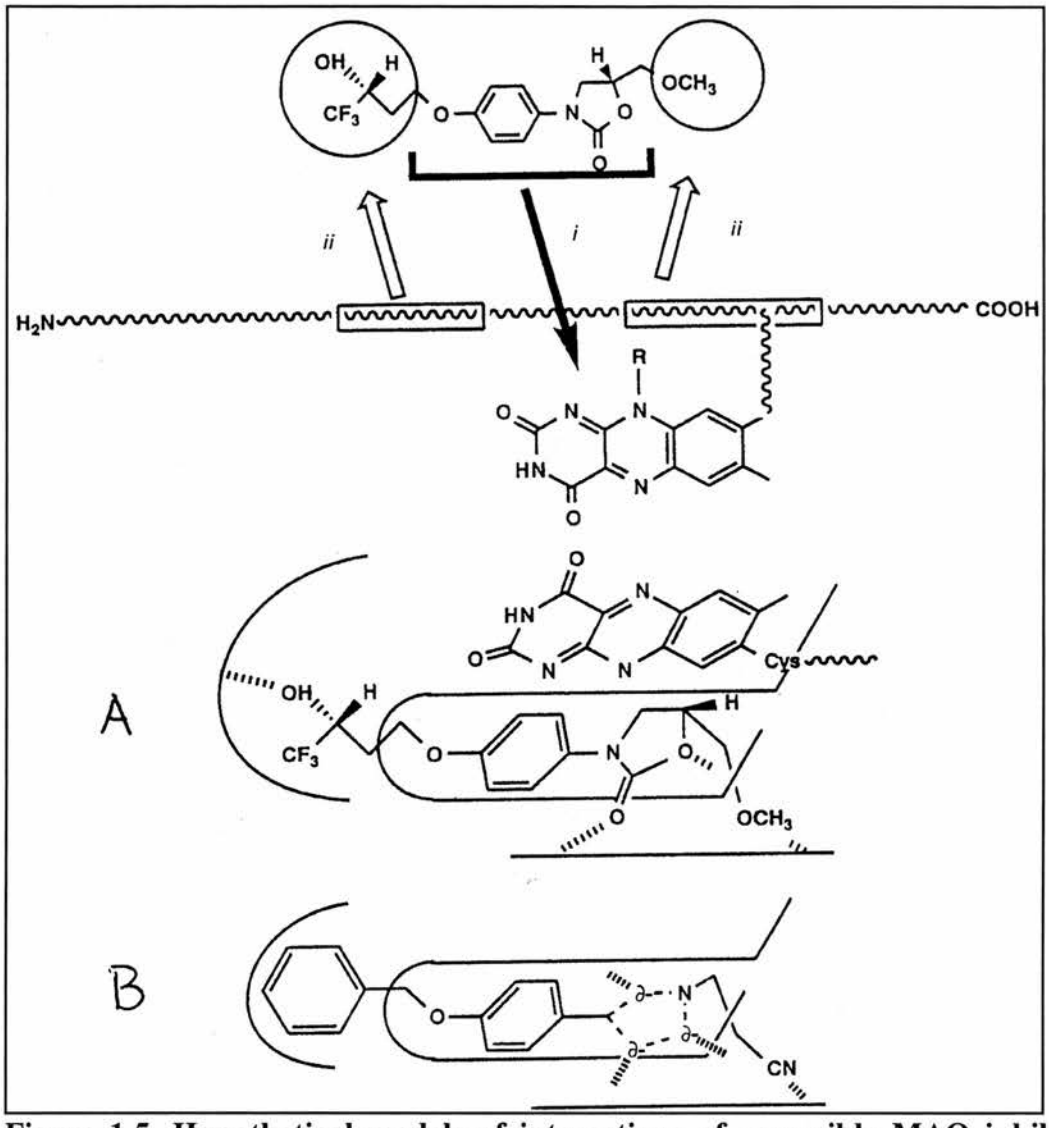

Figure 1.5. Hypothetical models of interactions of reversible MAO inhibitors with the enzyme (*61*). ***(i)*** Stabilisation of a planar electron ring entity (charge transfer interaction with the isoalloxazine ring of the flavin cofactor and additional hydrogen bonds); ***(ii)*** specific interaction of the lateral chains with specific residues. ***A.*** Binding site of reversible MAO A inhibitors illustrated for befloxatone; ***B.*** Binding site of reversible MAO B inhibitors illustrated for diazoheterocyclic derivatives.

The active site of MAO A, in contrast to that of MAO B, can bind positively-charged amines with high affinity, and consequently the basicity of amines can play a significant role in enhancing their selectivity towards MAO A. Inhibitory studies on MPP^+ analogues, revealed that the neutral 4'-pentyl-4-phenylpyridine was about 270 times less effective as a MAO A inhibitor than the positively charged 1-methyl-4'-pentyl-4-phenylpyridine, whereas for MAO B the K_i values are the same for the two compounds (*83*). Studies on the inhibition of MAO by isoquinoline derivatives have shown that besides electrostatic forces, steric, lipophilic and hydrophilic interactions also play an important role in modulating MAO A inhibitory activity (*77*).

Supramolecular models were used to show that flavin hydrogen bonding affects the entire isoalloxazine ring system (*84*). Particularly, specific hydrogen bonds can activate C(8α) towards quinone methide formation and subsequent covalent modification or can provide appropriate conditions for nucleophilic addition to C(4a). Amphetamine, harmine, tetrindole and befloxatone induce a concentration dependent, saturable change in the visible spectrum of the FAD in MAO A (*85*). These spectral changes indicate that the electronic properties of FAD in MAO A are altered by the presence of inhibitor in the active site. In the presence of saturating amounts of inhibitor, the reduction of MAO A by dithionite does not go further than the semiquinone and the changes in the spectra are different for the different inhibitors (*85*). Thus, the spectral and thermodynamic alterations to the flavin as a result of inhibitor binding in MAO A are sensitive to the inhibitor structure.

The charge transfer component seems less important for the reversible inhibition of MAO B, where hydrogen bonding of the inhibitor in a hydrophobic

pocket of the binding site of the protein to fixed anchoring points (Figure 1.5.B) is more important (*61*).

1.2.4. Mechanism-based inactivators

Both MAO A and B are irreversibly inhibited by mechanism-based inactivators from four major classes of compounds: acetylenic amines, allenic amines, substituted hydrazines and arylcyclopropylamines. Although the type of adduct formed is of the same general type with both MAO A and B, considerable selectivity may exist toward one of the two types of MAO, depending on the structure of the inhibitor.

MAO has two nucleophilic centres essential for the mechanism-based inactivation (*86*). One is a -SH group and the other is N(5) or C(4a) of the covalently-bound cysteinyl FAD moiety (Figure 1.6). Alkylation of either the thiol or the flavin results in an immediate inactivation.

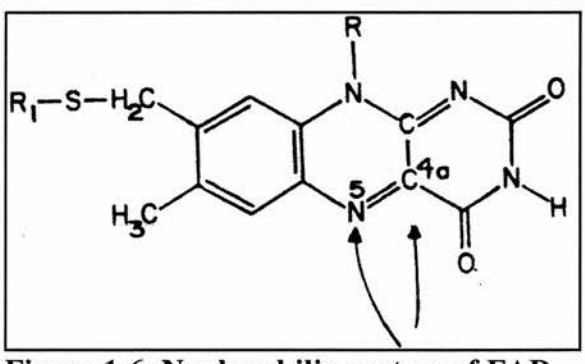

Figure 1.6. Nucleophilic centres of FAD.

1.2.4.1. Acetylenic amines

Acetylenic inactivators of MAO are deprenyl (MAO B), clorgyline (MAO A) and pargyline (both MAO A and B) as they modify the flavin cofactor by the formation of an adduct at the N(5) position, (Figure 1.7). This has established that the ligand-binding site is adjacent to the flavin.

The use of irreversible inhibitors can lead to undesirable side effects. Individuals taking these drugs become susceptible to false amine neurotransmitters in their diet, which are normally degraded by MAO A. These false neurotransmitters, such as tyramine, octopamine and phenylethylamine, can be taken up by adrenegic nerve terminals, act to release and replace the normal transmitter stores in vesicles and thereby compromise synaptic transmission (*87*). For example, disruption of adrenergic input to the heart can lead to cardiac failure. The common side effect of these inhibitors is the "cheese effect", which is a hypertensive crisis induced in patients on a regimen of MAO A inhibitors who consume high amounts of cheese, wine or other foods rich in tyramine.

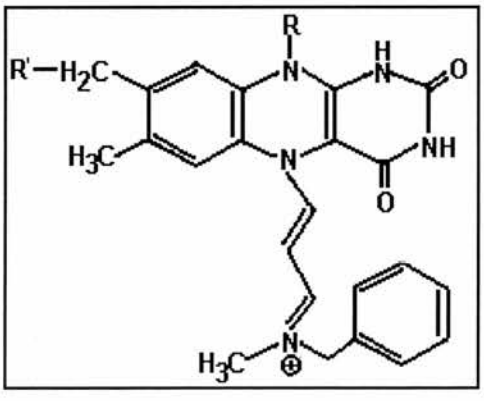

Figure 1.7. Structure of the adduct formed on MAO by suicide inhibition by pargyline.

1.2.4.2. Cyclopropylamines

In the 1960's trans-2-phenylcyclopropylamine (2-PCPA), commonly known as tranylcypromine, was used as an antidepressant. However, the interest in the cyclopropylamines (Figure 1.8), has grown due to their chemical properties as suicide inhibitors of MAO inhibitors.

Although the inactivation of MAO B by 2-PCPA is accompanied by the reduction of the flavin, the imine product does not form an adduct with the flavin but with an amino acid residue, probably a cysteine (*88*). The mechanism proposed for the inactivation of MAO B by 2-PCPA involves a one-electron transfer that leads to rapid homolytic cleavage of the cyclopropyl ring and formation of an adduct with a cysteine radical (*89*).

Interestingly, the inactivation of MAO B by 1-phenylcyclopropylamine occurs in two different pathways derived from a common intermediate (*90*). One pathway leads to irreversible inactivation of the enzyme by formation of a covalent adduct with the N(5) position of the flavin. In addition to formation of this stable covalent adduct, another pathway occurs 7 times as often leading to a covalent adduct with an amino acid residue that is unstable. The amino acid residue was later identified as a cysteine (*91*). The mechanism proposed consists of a one-electron transfer from 1-PCPA to the flavin followed by homolytic cyclopropyl ring opening to the common radical intermediate, which is trapped by two different active site radicals (Figure 1.9). Flavin radical combination yields the stable adduct whereas $S^{\bullet}$ capture produces the labile adduct. Recently, direct evidence for the flavin covalent adduct was obtained by electrospray ionisation mass spectroscopy (*92*). Inactivation of MAO A by 1-PCPA also leads to a covalent adduct to the flavin but there is no evidence that reversible attachment to an amino acid residue occurs (*93*). Although

there are various similarities to the inactivation of MAO A and MAO B by 1-PCPA, differences in the active site environments of the two enzymes might be the reason for the formation of an amino acid adduct in MAO B and not in MAO A.

N-Cyclopropyl-α-methylbenzylamine (N-CαMBA) was shown to inactivate MAO B without attachment to the flavin but presumably to an active site amino acid residue (*94*). In contrast to 2-PCPA, the amino acid adduct formed by N-CαMBA was stable enough to allow its reduction by sodium borohydride and avoid chemical degradation (Figure 1.10). After digestion with Lys-C endopeptidase of the reduced inactivated MAO B by N-CαMBA, HPLC separation of the peptides and sequence analysis, it was possible to identify the modified amino acid as the cysteine 365 (*95*). Inactivation of MAO A by N-CαMBA also yields a cysteine adduct, presumably the cysteine 374 which corresponds to the MAO B cysteine 365 (*93*).

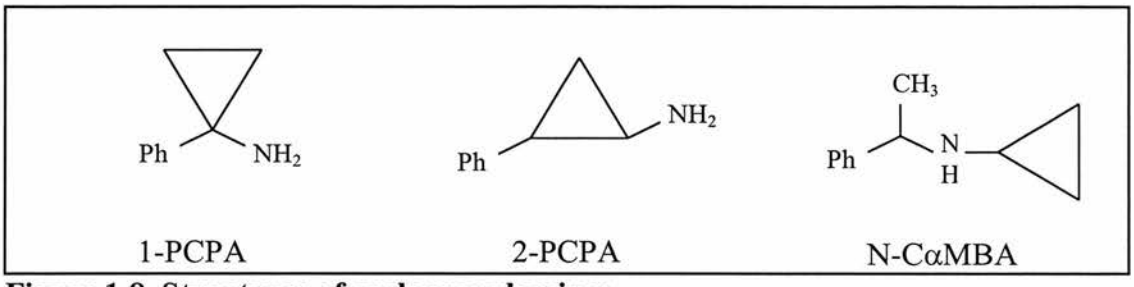

Figure 1.8. Structures of cyclopropylamines.

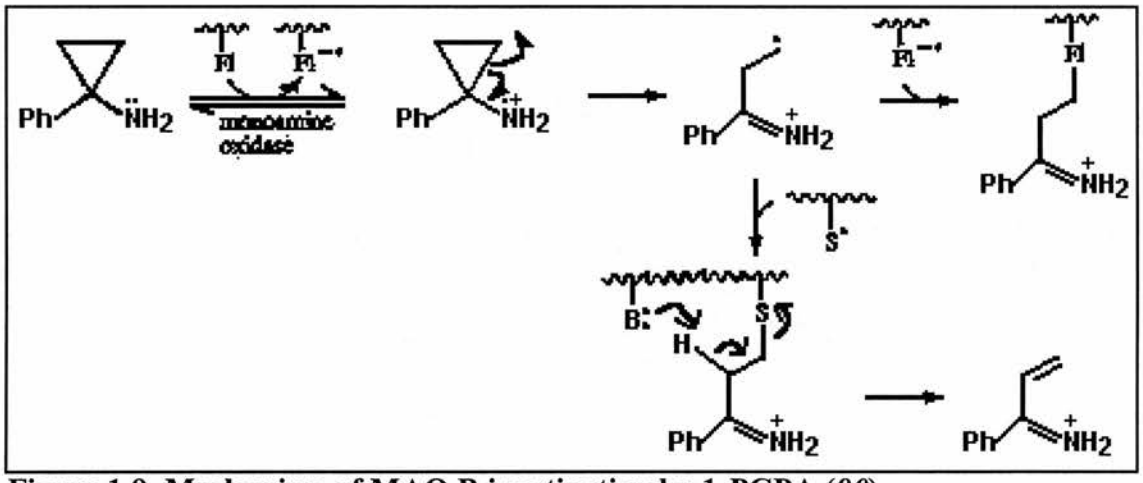

Figure 1.9. Mechanism of MAO B inactivation by 1-PCPA (*90*).

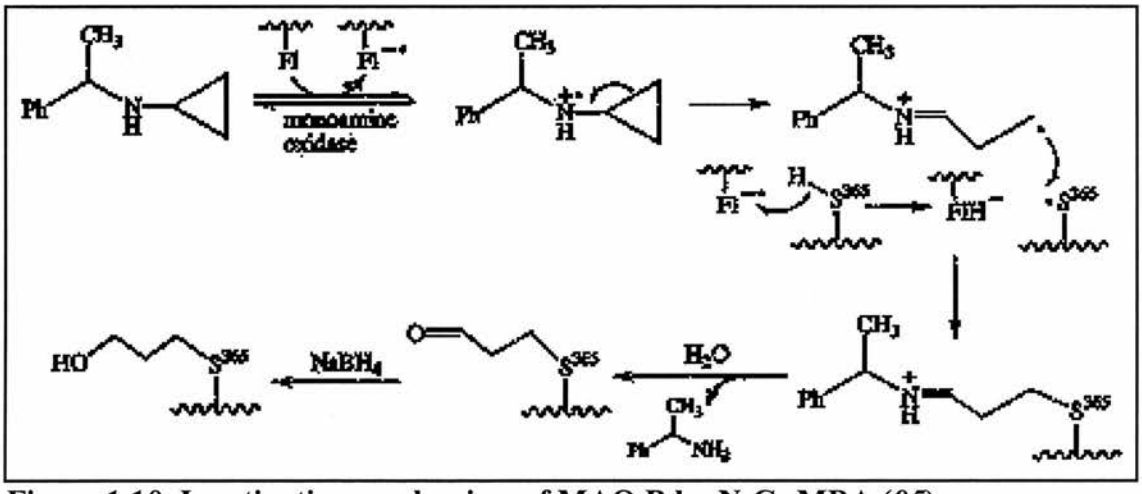

Figure 1.10. Inactivation mechanism of MAO B by N-CαMBA (*95*).

1.2.5. Redox properties

The midpoint potentials for the reduction of FAD in MAO A and B determined in the absence and presence of ligands are listed in Table 1.3 (*96, 97*). The midpoint potentials for the first and second electrons reductions are inverted compared with those for the free FAD (–0.236 V for the first electron and –0.176 V for the second electron (*98*)), indicating that the covalent attachment and/or groups around the flavin have altered the redox properties of the FAD moiety. Substrates but not inhibitors induce a large positive shift in the potential in both MAO A and B, bringing the redox potential to above +0.25 V and closer to the potentials of amine (around +1 V (*99*)) and oxygen (+0.295 V for O_2/H_2O_2 (*99*)). This finding is the first indication of an explanation for the ability of the MAO flavin to oxidise amines. In addition, the reciprocal decrease of the potential of the amine can be speculated, in order to lower the barrier for the transfer of electrons.

The redox potential titrations revealed a puzzling stoichiometry. For the FAD/FAD$^{\bullet}$ couple in the native enzyme, the slope of the double log plot relating the ratio of oxidised to reduced species for enzyme to that for the reporter dye was twice that expected (*97*). In other words, two electrons rather than one were required to obtain the semiquinone. The same conclusion was drawn when human liver MAO A was anaerobically titrated with dithionite (*100*). Four electron equivalents were required for full reduction of the enzyme, two more than expected for a flavin alone. This suggested that there was a redox-active functional group able to accept two extra electrons upon the dithionite titration in the active site of MAO and that these are in close proximity to the flavin. As the flavosemiquinone was formed during titration (strong absorbance at 412nm), this extra redox group interacted with the flavin resulting in some stabilisation of the flavosemiquinone. The low yield of

semiquinone and the four titration phases observed indicated that both the flavin and the second redox group have similar redox potencials. When DPDS-modified enzyme (DPDS modifies free sulphydryl groups) was titrated, no semiquinone was seen and a total of only two electron equivalents were needed to fully reduce the enzyme, the same as expected for the flavin. Apparently, in the modified enzyme there is no interaction between the second redox group and flavin cofactor or the second redox group cannot be reduced. β-Mercaptoethanol, which reduces disulphides, inhibited MAO A by reducing the flavin cofactor. However, no reduction of free riboflavin was observed under the same conditions. This may indicate that β-mercaptoethanol reduces the active site second redox group which, in turn, reduces the cofactor. The results of these experiments using beef liver MAO B were the same. All these data suggested that the redox-active group is a disulphide, which was consistent with the findings of catalytic essential cysteines on MAO (chapter 1.2.6.2). The potential for the cysteine-cysteine redox couple is -220mV close to that for FAD (-208mV) and to that for MAO A and MAO B (Table 1.3).

The four-electron reduction of MAO has raised some controversy. Edmondson found that full reduction of MAO required only one equivalent of substrate, indicating that two electrons were transferred from substrate to give fully reduced flavin (*101*). Later the same group titrated MAO A expressed in *Pichia pastoris* with dithionite and found that again only two electrons were required for full reduction (*102*). The MAO B crystal structure revealed that there were no cysteines in the active site neither any pairs of adjacent cysteines that could form a disulphide group anywhere in the protein.

Table 1.3. Midpoint potentials for MAO A and B in the absence and presence of ligands*

Ligand	Redox couple		Redox potential (mV)	
			MAO A	MAO B
None[(1)]	Oxidised	semiquinone	-159	-167
	Semiquinone	reduced	-262	-275
	Oxidised	reduced	-210	-221
With substrate				
Serotonin	Oxidised	reduced	ND	+194
α-Methylbenzylamine	Oxidised	reduced	-116	+281
Benzylamine	Oxidised	reduced	+263	ND
With other ligands[(1)]				
D-Amphetamine	Oxidised	semiquinone	-176	-119
1-Methyl-4-styrylpyridinium	Oxidised	semiquinone	-158	-162
α-Methylbenzylamine	Oxidised	semiquinone	-130	+245
	Semiquinone	reduced	-102	+317

* Data taken from (*96, 97*). (1) In the presence of xanthine and xanthine oxidase as the reductant system. ND – not determined because the rate of reduction of this enzyme by this substrate was too fast to be certain of equilibrium between the enzyme and the dye.

1.2.6. Structure

1.2.6.1. Primary structure

The amino acid sequences of human liver and placental MAO A, bovine adrenal MAO A, rat liver MAO A, human liver, platelet and frontal cortex MAO B, rat liver MAO B have been deduced from cDNA clones (for human MAO amino acid sequences see chapter 7). These revealed that MAO sequences from different species and of same type (A or B) show more than 85% sequence identity (*e.g.*, human and bovine MAO A are 88% identical (*103*)) and both types of the enzyme are very similar (*e.g.*, human liver MAO A and B are 70% identical (*104*)). MAO A and B consist of 527 and 520 residues and have subunit molecular weights of 59700 and 58800, respectively (*103, 104*).

Both MAO A and B sequences contain the pentapeptide Ser-Gly-Gly-Cys-Tyr, located in the C-terminal region, where the cofactor FAD covalently binds to the cysteine, which corresponds to residues 406 and 397 in MAO A and B, respectively (*56, 57*). A ratio of one FAD per 63 kDa (MAO A) and 57 kDa (MAO B) was determined for the human enzymes (*55*), indicating that there is one FAD per subunit.

Three distinct regions can be delimited along the primary sequence of MAO, the first two of which together form the FAD binding domain of MAO (Figure 1.11): a) a dinucleotide-binding domain region near the N-terminus; b) a FAD domain located near the C terminus, which contains the covalent binding site; c) a third region whose function is not yet well determined and that could confer enzyme specificity (*61, 105*). Another interesting feature of these proteins is the presence of a hydrophobic region (residues 504-521 for MAO A) that is flanked by positively

charged amino acids near the C-termini. This pattern is typical of a membrane spanning helix and so may be important for membrane insertion (see chapter 1.2.6.5). The two types of MAO are derived from separate genes (*104*), which are closely located on the X chromosome at the Xp 11.23 (*106*). These genes have strikingly similar structures both consisting of 15 exons and exhibiting identical exon-intron organisations which suggests that MAO A and B are derived from duplication of a common ancestral gene (*107*). This was later confirmed with the isolation and characterization of an evolutionary precursor of mammalian MAO A and B, the MAO N from *Aspergillus niger* (*108*). The existence of separate genes for both types and their differential expression indicate that they are under separate regulatory controls at the transcriptional level.

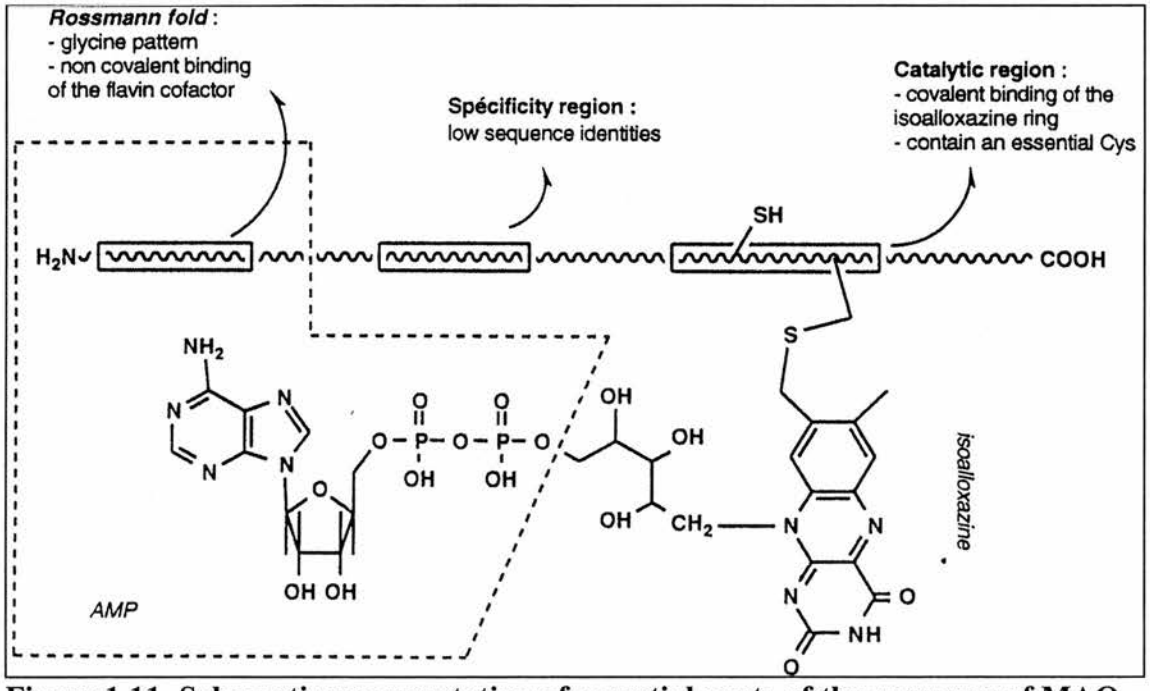

Figure 1.11. Schematic representation of essential parts of the sequence of MAO (*61*). The –SH group indicated is the cysteine 365 of MAO B shown to be modified after inactivation by cyclopropylamines (*95*).

1.2.6.2. Residues important for catalysis

Several studies were carried out in order to identify which residues of the primary structure of MAO are catalyticaly important.

The fact that MAO contains one or more vulnerable cysteine residues was first known in 1945 (*109*). Inactivation experiments on the bovine liver MAO by various sulphydryl reagents as well as protection experiments, kinetics and physicochemical observations suggested that there are only two out of the eight cysteine residues of the enzyme that are required for activity (*110*). Corroborating with this, the kinetics of the inactivation of purified MAO A by DPDS were biphasic and suggested that two cysteine residues are modified before activity disappears (*48*). D-Amphetamine, a competitive inhibitor, protected against the inactivation, suggesting that the groups modified are located in the active site of the enzyme. Further evidence for the participation of a cysteine in the mechanism of MAO was the identification of this amino acid in the labile adduct formed during inactivation of MAO B by 1-phenylcyclopropylamine (*91*). The inactivation site of MAO B by another cyclopropylamine, N-CαMBA, was later identified to be Cys-365, which corresponds to the Cys-374 in MAO A (*95*).

Nine cysteines are found in the deduced amino acid sequences of both human liver MAO A and B. Each of these residues were studied by site-directed mutagenesis, converting them to serines (*111*). Substitution of MAO A Cys-374 and -406 and MAO B Cys-156, -365 and -397 with serine resulted in complete loss of MAO A and B catalytic activity. The seven conserved cysteines between MAO A and B are A165/B156, A201/B192, A306/B297, A321/B312, A374/B365, A398/B389 and A406/B397 (the FAD binding site). The important cysteine residues for catalytic function in MAO A and B are among these conserved residues. The loss

of catalytic activity in the MAO A C406S and MAO B C397S mutants is presumably due to the prevention of covalent binding of the enzyme to the cofactor FAD. The loss of catalytic activity of MAO A C374S and MAO B C156S and MAO B C365S suggests that these cysteines are important for catalytic activity, but whether they were involved in forming the active site or were important for the appropriate conformation of MAO A and B could not be determined in these studies. The fact that there was one additional cysteine residue important in MAO B suggests that there is a structural or conformational difference in the active site of MAO A and B that may confer the different substrate and inhibitor specificities (*111*). Another site-directed mutagenesis study revealed that mutation of MAO B Cys-389 with Ala resulted in complete loss of enzymatic activity (*112*).

Histidine residues may be essential for MAO catalysis as well. Using chemical reagents, 2 histidines residues were shown to be essential for bovine-liver monoamine oxidase activity and protected from modification by active site ligands (*113*). By analysing the activities of a number of mutant MAO B forms expressed in mammalian cells and carrying single amino acid mutation, it was concluded that substitution of His-382 of MAO B with Arg greatly reduced the enzymatic activity, suggesting that this residue represents a nucleophile relevant for the catalytic mechanism (*112*). It was also reported that mutation of MAO B Thr-158 (to Ala) resulted in dramatic loss of enzymatic activity (*112*).

In human MAO A, tyrosyl residues near the FAD binding site were mutated. The lowest specific activities towards kynuramine were exhibited by MAO A Y407F and MAO A Y444F mutant enzymes (*114*). The mutation of Y444F in MAO A resulted in alterations in substrate specificity that are dependent on the size of the aromatic ring and on the alkyl side chain length of various substrates analogues.

However, the mutant exhibits unaltered quantitative structure-activity parameters in the binding and rate of benzylamine analogues, which suggests that its amine oxidation mechanism is identical with that of wild-type MAO A.

The flavin cofactor is essential for MAO activity, as the inactive mutant MAO A apoC406A was expressed in *Saccharomyces cerevisiae* in the absence of riboflavin (*115*). However, addition of FAD (but not FMN or riboflavin) restored catalytic activity. This suggested that the flavin covalent binding to the protein is not an absolute requirement for catalytic activity. In contrast to the serine mutants expressed in mammalian cells (*111*), expression of the C406A mutant in *Saccharomyces cerevisiae* in the presence of riboflavin resulted in the formation of an active enzyme, as found previously with the rat liver enzyme (*115, 116*). Thus, MAO A can be incorporated into the outer membrane of the mitochondrion as an apoprotein, fold to a conformation that binds FAD and has catalytic activity. The major alteration when comparing MAO A C406A with wild-type MAO A is that the activity of the mutant is very labile when the protein is removed from the membrane, whereas the native form is readily solubilised by detergents in a stable, functional form (*115*). This suggests that the covalent linkage of the flavin in MAO A has a role in maintaining the structural integrity of the enzyme.

1.2.6.3. Residues important for ligand specificity

Several studies were done to find the amino acids responsible for the different substrate and inhibitor specificities between MAO A and B. The amino acid residues that are identical in different species in each form can be inferred to have been conserved during evolution because of their functional importance. The residues that are conserved amoung various species but different between the two forms might be those responsible for substrate selectivity of MAO. The regions important for

substrate selectivity are between residues 120 and 220 in rat MAO A and B (*117*) and are within amino acids 215-375 in human MAO A and 206-266 in human MAO B (*118, 119*), as determined using chimeric enzymes constructed by reciprocally switching the corresponding amino acid segments. Using point mutations, it was shown that switching Phe-208 and Ile-199 in rat MAO A and B, respectively, results in a partial inversion of specificities for some substrates and inhibitors (*120*), but the same amino acid substitutions made on human MAO did not result in a change in specificities (*119*). In human MAO, it was the Ile-335 in MAO A and Tyr-326 in MAO B that were shown to have an important function in determining the specificities towards some substrates and inhibitors. This difference between species leads to a reversing of the structural feature responsible for determining specificity. In rat, MAO A has an aromatic ring (Phe-208) and MAO B has an aliphatic side chain (Ile-199), whereas in humans, it is MAO A that has the aliphatic residue (Ile-335) and MAO B has the aromatic residue (Tyr-326).

1.2.6.4. Secondary structure

Results of infrared spectroscopy (FTIR) on both forms of MAO were described in (*121*), which provided information on the secondary structure of this enzyme. Assignment of the secondary structure to the sequences of MAO was performed using the statistical GOR method (*121*). The deduced folding of the two forms of MAO is shown in Figure 1.12.

Comparison of the secondary structure of both forms of MAO shows differences in the folding of the protein, in particular between residues 100-200 of the aligned sequences. The differences in this part of the sequence could reflect different folding of the tridimensional structure of the protein. These structural changes may alter the binding of substrate and/or inhibitor to the enzyme, thus

conferring the specificities of MAO A and B (*121*). More details of the secondary structure of MAO A obtained by homology modelling can be found in (*61*).

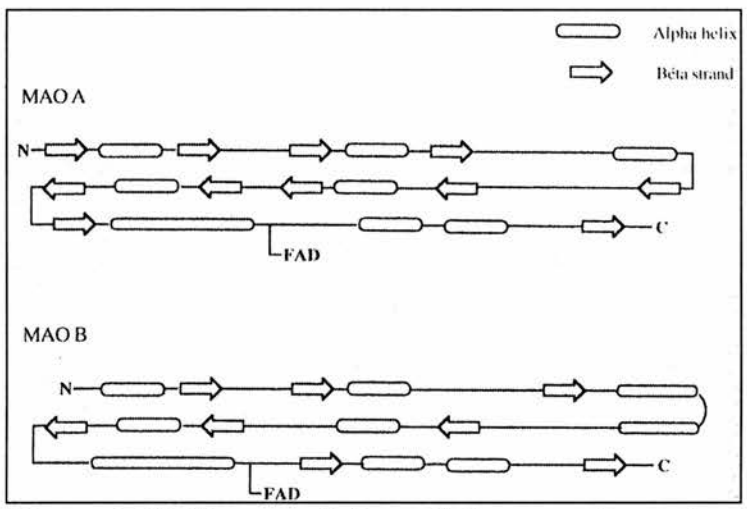

Figure 1.12. Representation of the secondary structure (α helix or β strand) attributed to the amino acid sequence of MAO A and MAO B. The position of the covalently bound FAD cofactor is indicated as well (*121*).

1.2.6.5. Tertiary structure

It took almost 20 years, since MAO was first purified with high yield (*48*), to obtain the X-ray 3D structure of MAO B (*122*). This delay may be explained by the fact that purified protein must be maintained in the presence of a detergent to prevent aggregation and precipitation (*47, 123*), which makes crystallisation procedures more difficult than for soluble proteins. In recent years computer modelling was the chosen tool to get some insights on the overall and especially the active site structure.

The crystal structure of MAO B was revealed very recently broadening the knowledge on MAO characteristics (*122*). The 520 amino acids of MAO B fold into a compact structure with the closest structural matches to L-amino acid oxidase (*124*) and polyamine oxidase (*13*). The enzyme is dimeric with extensive monomer-monomer interactions, as 15% of monomer accessible surface is buried upon dimer formation (Figure 1.13.A.).

The C-terminal residues form an extended polypeptide chain (amino acids 460-488) that traverses the monomer surface and is followed by an α-helix that initiates at Val 489 (Figure 1.13.B.) (*122*). These C-terminal amino acids 461-520 were previously shown to be responsible for membrane attachment (*125*) and the residues 489-515 were predicted to form a transmembrane helix (*126*). It is suggested that the dimer binds to the membrane with its two-fold axis perpendicular to the membrane plane and the C-terminal helices inserted in the lipid bilayer. In addition to the C-terminal helical segment, the structure shows that other protein regions may be involved in membrane binding. In residues 481-488 of the elongated polypeptide stretch, several hydrophobic side chains point towards the membrane. At the end of loop 99-112, Pro 109 and Ile 110 are surface-exposed in a position that could allow interaction with the membrane.

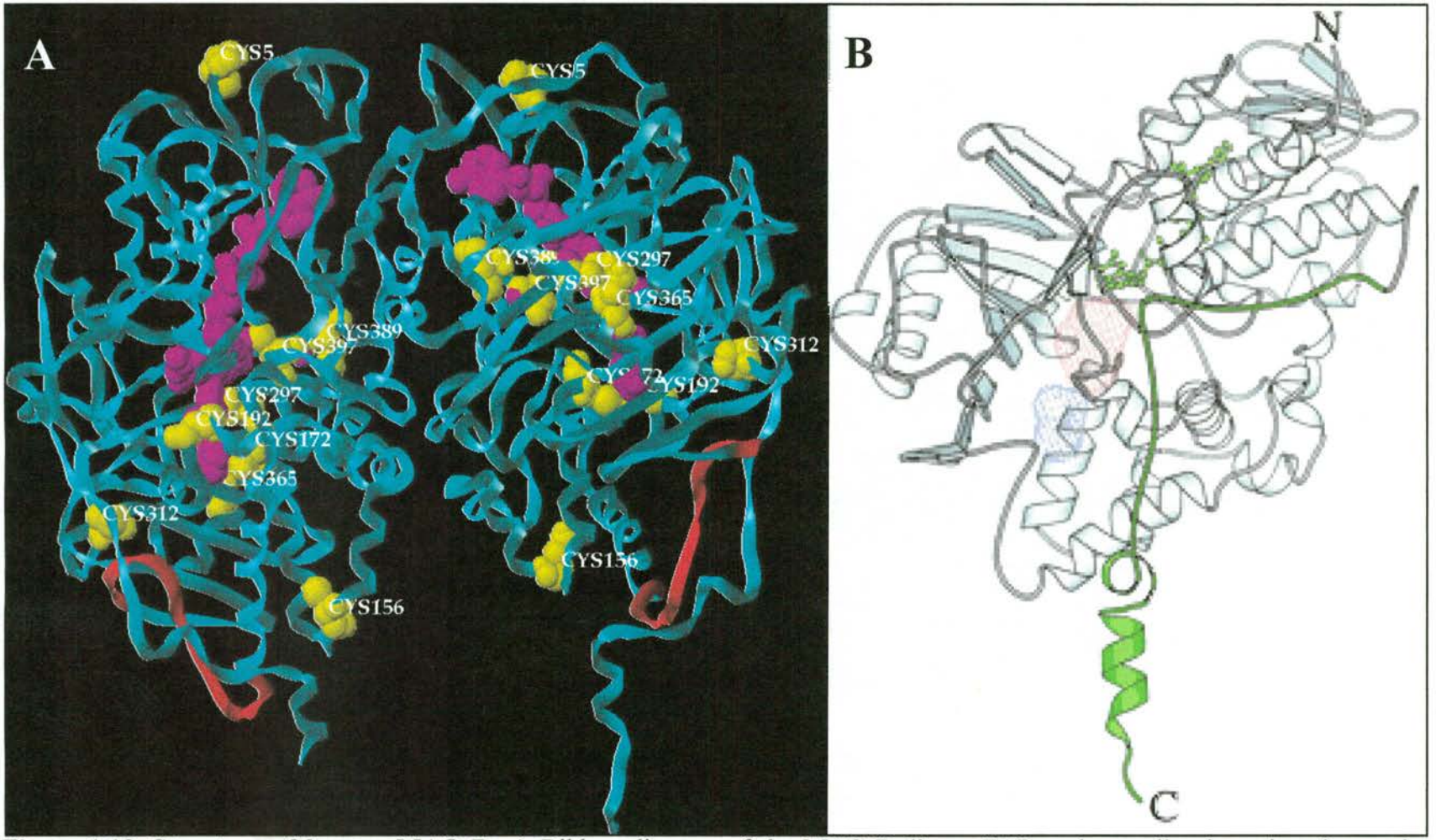

Figure 1.13. Structure of human MAO B. ***A.*** Ribbon diagram of the MAO B dimer. FAD and pargyline in active site are in pink and the cysteines are in yellow. The red ribbon is the loop 99-112. ***B.*** Cavities constituting the substrate path from the protein surface to the flavin in the MAO B monomer. Adjacent to the active site cavity (cyan) is the entrance cavity (blue). The C-terminal is in green (*122*).

The MAO B crystal structure also shows that pargyline covalently binds to the N(5) on the *re* side of the flavin in a solvent inaccessible environment (Figure 1.13.A.) (*122*). The substrate-binding site is formed by a cavity (420Å^3) lined by a number of aromatic and aliphatic amino acids, providing a highly hydrophobic environment. Adjacent to this is a separate, smaller hydrophobic cavity (290Å^3) situated between the active site and the protein surface, that is shielded from solvent by loop 99-112 (Figure 1.13.B.). Residues Tyr-326, Ile-199, Leu-171 and Phe-168 are the side chains that separate the two cavities. These observations suggest a mechanism for admission of the substrate into the active site that initially involves the movement of loop 99-112 to open access to the smaller cavity and then the transient movement of the four residues separating the two cavities.

The authors suggest that the amine substrate binds between the phenolic side chains of Tyr-398 and Tyr-435 that, together with the flavin, form an aromatic caged environment that is responsible for recognition of the amino group (*122*).

There are no active site residues that could act as bases to function in proton abstraction from the α-C of the substrate (*122*). Moreover, there are no conserved cysteines in the active site. Cysteine 365, the site of modification by cyclopropylamines (*95*), is at the surface of the protein, some 20Å away from the loop 99-112.

The crystal structure of MAO A is not available yet. A partial 3D model of human MAO A was proposed (*105*), which shows two alpha/beta domains (the FAD-binding N-terminal and central domains) and an alpha+beta domain. The C-terminal region is predicted to be responsible for anchoring the protein into mitochondrial membrane and was not modelled.

To have a spatial idea of the MAO A active site, a mold of the substrate-binding region was designed using data of the enzyme interaction with reversible competitive inhibitors and the analysis of their 3D structures (*127*). The superimposition of rigid ligands in biologically active conformations allowed the determination of the shape and dimension of the active site cavity accommodating these compounds.

A more recent and detailed model of the MAO A active site was obtained based on the polyamine oxidase 3D structure (*128*). It was suggested that Lys-305, Trp-397 and Tyr-407 may be involved in the non-covalent binding to FAD. Tyr-407 and Tyr-444 in MAO A (Tyr-398 and Tyr-435 in MAO B) may form an aromatic sandwich which stabilises the substrate binding.

Another theoretical model, supported by spectral and kinetic evidence, suggests that MAO A inhibitors strongly interact with the flavin (*129*). The model is based on the energetically favourable stacking of the ring systems of the flavin and inhibitor found in solution, where their orientation can be predicted based on molecular orbital calculation and electrostatic potential (*130*). The inhibitor efficacy will depend on the complementarity of the atomic charges (*129*).

1.2.7. Kinetic mechanism

Kinetic mechanisms are investigated to determine the nature of the intermediates and the rate-limiting steps in order to explain how catalysis is achieved and why some substrates are oxidised better than others. The values of the rate constants have implications for metabolic regulation, such as the influence of anoxia on the rate of disposal of different amine substrates. Ultimately, understanding the mechanism of catalysis permits the design of inhibitors to give the specific modulation of enzyme activity *in vivo*.

Several studies were made to determine whether MAO follows a ping-pong mechanism (transfer of a group from the donor to the enzyme, followed by dissociation of the donor and a second transfer from enzyme to acceptor) or a ternary-complex mechanism (transfer occurs while both donor and acceptor are in the active site of the enzyme). Major variations in the mechanism, depending on the substrate used, were observed using steady-state and stopped-flow techniques, as well as studying isotope effects on MAO B (*131*). With benzylamine as substrate, a very large kinetic isotope effect was found, while phenylethylamine showed almost no kinetic isotope effect in steady-state assays. On the other hand, at high O_2 concentrations phenylethylamine was a far better substrate than benzylamine. It was concluded that with phenylethylamine, a binary complex mechanism operates and with benzylamine a ternary complex is involved. Tyramine and tryptamine are also oxidised by a binary complex mechanism (*132*).

Stopped-flow studies on the mechanism of oxidation of MPTP by bovine liver MAO B revealed that both benzylamine and MPTP form ternary complexes, not only of reduced enzyme, oxygen and product but also of reduced enzyme, oxygen and substrate (*133*). However, the mechanism for a given substrate is not exclusive but, rather, is determined by competition between the alternate pathways as a result of different rate constants for the oxidation of the reduced enzyme, the reduced enzyme-product complex and the reduced enzyme-substrate complex, as well as the different dissociation constants (Figure 1.14). When the reoxidation of the reduced enzyme is by a ternary-complex mechanism, the rate is much faster than by the binary one (*133*). Other studies on MAO A opened the hypothesis of a ternary-complex mechanism for it as well (*134*). It was also suggested that, for the A enzyme, the ternary complex with substrate, but not product, is reoxidised at faster

rate than the free, reduced enzyme. Moreover, the rate of the ternary complex pathway is dependent on the nature of the substrates (*63*). This means that substrate binding alters the observed rate constant for the reoxidation step, because the reduced enzyme-substrate complex reacts with oxygen faster than the free reduced enzyme.

In the steady state for MAO A, the reduction of the flavin is rate limiting in all cases and the K_m for O_2 is very low (*63, 134*). For MAO B, the reoxidation is rate-limiting and the K_m for O_2 is high and varies with the substrate (*131*). In situ, MAO A is responsive to changes in concentration and type of amine present, whereas MAO B is responsive to changes in the O_2 concentration. The different substrate specificities of MAO A and B and their different localization in specific brain regions enhanced by variations in O_2 tension may be a way of regulating the level and type of biogenic amines in brain compartments (*135*).

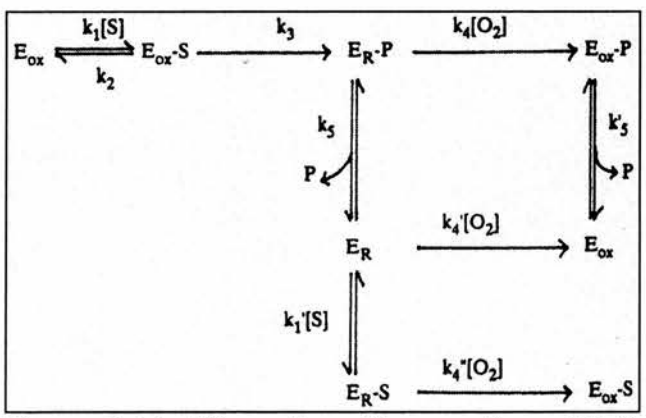

Figure 1.14. Alternate pathways of reoxidation of reduced MAO via binary or ternary complexes (*134*).

1.2.8. Chemical mechanism

Despite the intense interest in this enzyme for several decades, the chemical mechanism of MAO is still not completely understood. The reaction catalysed by MAO consists of a reductive and oxidative half reaction (Figure 1.15). In the reductive half-reaction the amine substrate is oxidised and the FAD is reduced to the hydroquinone. In the second half-reaction the FAD is reoxidised by molecular oxygen with formation of H_2O_2. The primary substrate oxidation product is an imine that is spontaneously hydrolysed to the final product aldehyde, either on the enzyme surface or after it has dissociated from the enzyme. Steady-state kinetic studies of product inhibition in MAO B suggested that hydrolysis occurs before product dissociation and that only the complex E_{red}–NH_3 could bind O_2 (*136*). In contrast, stopped-flow kinetic studies on *para*-substituted benzylamine analogues suggested that amine oxidation to the imine results in a kinetically stable reduced-enzyme-imine complex that reacts with O_2 at rates consistent with catalysis. If so, imine hydrolyis would occur after release from the oxidised form of the enzyme (*137*).

The oxidative deamination with electron transfer to the FAD could follow a deprotonation (carbanion), hydride transfer, polar nucleophilic addition or an electon transfer (radical cation) mechanism.

The deprotonation mechanism is not reasonable because of the high pK_a of the methylene protons of the substrate and the fact that the oxidation of 2-chloro-2-phenylethylamine does not involve a carbanion intermediate (*138*). Moreover, the crystal structure of MAO B has revealed that there is no active site base that could remove the methylene protons (*122*).

The hydride transfer mechanism involves a rate limiting $H^{\bullet}$ abstraction from the α-carbon of the amine substrate leading to the α-aminyl radical (bypassing

intermediate 3 in Figure 1.16). Rapid electron transfer from the α-aminyl radical results in the protonated iminium species and the flavin hydroquinone. Direct hydrogen abstraction is inconsistent with all of the studies of MAO-catalysed oxidations of cyclopropylamines and a cyclobutylamine (*139*). In some of these examples there is no α-hydrogen atom and several of the flavin adducts that were isolated could not arise from direct cyclopropyl or cyclobutyl cleavage by oxidised flavin.

A reformulation of the Hamilton's original polar nucleophilic mechanism (*140*), was proposed by Miller and Edmondson (*101*). The mechanism involves a nucleophilic attack to the flavin at the C(4a) position (Figure 1.17). The formation of the 4a-alkylated isoalloxazine ring leads to a very strong base at N(5) of the flavin with a pK_a that is expected to be in the range of the anilines (pK_a of ~30). Thus, a concerted transfer of the benzyl proton to N(5) of the 4a-alkyl flavin should be facilitated. Following this concerted addition –αC-H bond cleavage reaction, elimination would occur producing the protonated imine product and the reduced flavin cofactor.

This mechanism was proposed to accommodate the QSAR analysis of para-substituted benzylamines oxidation by MAO A (*101*), which strongly supports a proton abstraction mechanism of αC-H bond cleavage. This rules out any mechanisms involving hydride transfer or hydrogen atom abstraction and supports the polar nucleophilic mechanism and the one-electron transfer mechanism (Figure 1.16). However, contrary to the one-electron transfer mechanism, the polar nucleophilic mechanism is not consistent with the studies with the cyclopropylamines. Two highly sterically-hindered amines were shown to be oxidised by MAO B, making it difficult to imagine how they could undergo

nucleophilic addition at C4a of the flavin (*141*). Furthermore, cinnamylamine-2,3-oxide underwent chemistry indicative of a radical reaction, not of a nucleophilic reaction when incubated with MAO B (*142*).

The one-electron transfer mechanism was the most extensively studied hypothesis for MAO amine oxidation (Figure 1.16) (*139*). One-electron transfer from the substrate amino group to the oxidised flavin (Fl) gives the amine radical cation **3** and the flavin semiquinone ($Fl^{\bullet-}$). Loss of a proton (pathway **a**) gives the α-amino radical **4**, which can either transfer the second electron to the flavin semiquinone to give reduced flavin (FlH^-, pathway **b**) or undergo radical combination with an active site radical (pathway **c**) to give a covalent adduct **5**, which should decompose by β-elimination to give the iminium ion. The X group could be either the flavin semiquinone generated in the first step or an amino acid radical formed by hydrogen atom transfer from the amino acid to the flavin semiquinone. Experiments identified the X group being a cysteine residue (*46*).

The initial electron transfer to generate an aminyl radical cation **3** is consistent with the mechanism-based inactivators properties of cyclopropylamines and cyclobutylamines. All of the cyclopropylamines studied inactivated MAO B, resulting in cyclopropyl ring opened adducts which supports the intermediacy of a cyclopropylaminyl radical (*46*). Furthermore, 1-phenylcyclobutylamine underwent chemistry from a known one-electron rearrangement upon one-electron oxidation by MAO B (*143*).

Trans-1-(aminomethyl)-2-phenyl cyclopropane and (aminomethyl)cubane were used as probes to differentiate a proton/second electron transfer mechanism (pathway **a**) from a hydrogen atom transfer mechanism (pathway **d**) (*139*). The

results strongly argue against a transfer of a hydrogen atom from the amine radical cation (pathway **d**) and support the proton/electron transfer mechanism (pathway **a**).

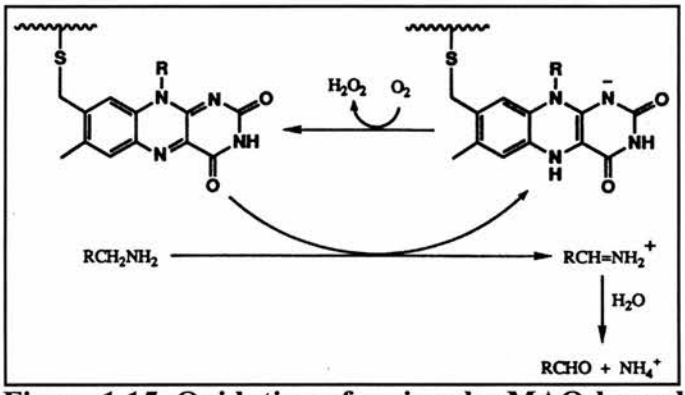

Figure 1.15. Oxidation of amines by MAO-bound FAD.

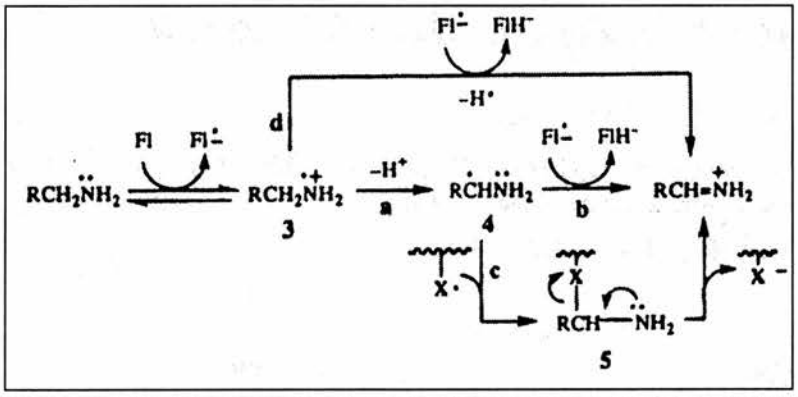

Figure 1.16. One electron transfer mechanism for MAO catalysis (*139*).

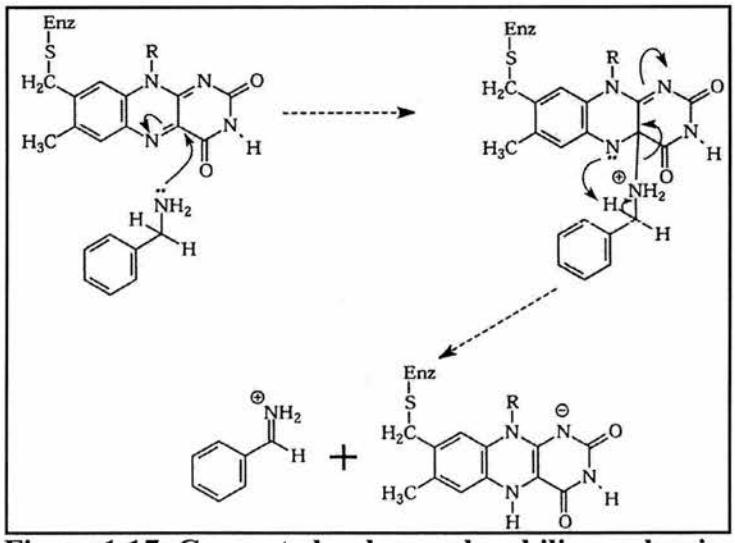

Figure 1.17. Concerted polar nucleophilic mechanism for MAO catalysis (*144*).

One aspect of this mechanism that requires rationalisation is the thermodynamic barrier of the initial electron transfer. However, the difference in the redox potentials of the flavin and the amine substrate can be lowered during catalysis, as discussed in chapter 1.2.5. Moreover, distortion of the planar oxidised flavin structure to a bent reduced flavin structure would lower the LUMO energy of the flavin, making acceptance of an electron a lower energy process. In fact, the flavin in human MAO B is known to bend along the N5-N10 axis by about 30° (*122*), indicating that it is being forced into the shape of a reduced flavin, making it a much stronger oxidant. Another important factor in amine oxidation is the solvent effect. The $E_{½}$ of an organic compound can change by 0.5 V just by changing from water to mixtures of water and organic solvents (*145*). Because the active site of MAO is highly hydrophobic, the redox potentials are more related to those in organic solvents than in aqueous medium, again suggesting a strong change in redox potentials.

No radical intermediates (flavosemiquinone or substrate amino radical) were detected by rapid-scan stopped flow and magnetic field independence during the reductive half-reaction of MAO B with substrates (*146*). However, the formation of an ESR-detectable substrate radical was detected during the oxidation of 1-amino-1-benzoylcyclobutane in the presence of a spin trap (*147*). On the other hand, it was reported that during the oxidation of a number of *para*- and *meta*-substituted benzylamines by MAO B, no evidence for a radical mechanism could be detected (*148*), although, in view of the large kinetic isotope effects, one would expect the transient accumulation of flavin semiquinone, under conditions when cleavage of the C-H bond is rate limiting if the one-electron transfer mechanism applies.

1.2.9. MAO in health and illness

Although the main interest on MAO is the development of the best antidepressants without side effects, there are other areas on the medical field that this enzyme is involved in.

1.2.9.1. Parkinson's and Alzheimer's diseases

Idiopathic Parkinson's disease is an age-related neurodegenerative disorder characterised by slowness, stiffness, resting tremor, gait impairment and postural instability. The MAO B inhibitor *l*-deprenyl is an effective dopamine-sparing adjunct when used in combination with L-dopa for the treatment of this disease and delays the progression of symptoms (*59*). Rasagiline is 5-10 times more potent than deprenyl as a MAO B inhibitor and anti-parkinson drug (*149, 150*). However, these drugs have neuroprotective effects that are not related to MAO B inhibition (*151, 152*). Another link between MAO B and PD is the neurotoxin MPTP. MAO B converts MPTP to the toxic metabolite MPP^+, which selectively destroys nigrostriatal neurons (*153*). The similarity between the neurodegeneration induced by MPTP and the neuronal damage in PD (*154*) has provided animal models for parkinsonism and the hope that elucidation of the mechanism of the neurotoxicity of MPTP may yield clues to some of the causes of idiopathic PD.

Alzheimer's disease (AD) is a neurodegenerative illness characterised by a progressive decline in cognitive function mostly in elderly people. The treatment of this disease is based on acetylcholinesterase inhibitors, but MAO B inhibitors are also beneficial. MAO B activity can increase up to 3-fold in the temporal, parietal and frontal cortex of AD patients compared with controls. This increase in MAO B activity produces an elevation of brain levels of hydroxyl radicals, which has been correlated with the development of the AD characteristic amyloid β-peptide plaques

(*155*). *l*-Deprenyl was shown to increase the life span of AD patients supposedly through, among other actions, enhancement of nitric oxide-mediated mechanisms in vascular and neural tissue (*156*). A recent approach of drug designing for the treatment of AD is, based on rasagiline, to combine the propargyl group of a MAO B inhibitor and a carbamate moiety for cholinesterase inhibition (*157*). In the same line of thought, the MAO B inhibitors coumarins have been shown to also exhibit acetylcholinesterase inhibition (*158*).

1.2.9.2. Behavioural changes

The clearest genetic evidence that MAO regulates human behaviour comes from a study on the abnormal aggressiveness in males from a Dutch family with a complete MAO A deficiency caused by a point deletion in the gene encoding MAO A (*159*). MAO A deficiency and aggression has also been confirmed in studies of MAO A-deficient mice. MAO A knock-out (KO) pups have elevated brain levels of serotonin and a distinct behavioural syndrome, including enhanced aggression, is manifested by adult males (*160*). Elevated levels of serotonin may also be important in the enhanced emotional learning that adult MAO A KO mice exhibit (*161*). Besides serotonin, the levels of norepinephrine and dopamine are also increased in MAO A KO mice (*160*). Conversely, only levels of phenyethylamine are increased in MAO B KO mice (*162*). Since norepinephrine and dopamine mediate the stress response and their action is potentiated by phenylethylamine, it is not surprising that MAO A-deficient mice and MAO B-deficient mice show an increase reactivity to stress in forced-swim test (*160, 162*).

1.2.9.3. Cigarette smoke

There is a dramatic decrease in the MAO A and B activities in the brains of smokers relative to non-smokers or former smokers (*163, 164*). It has been suggested that, since pulmonary MAO is mainly responsible for metabolising plasma serotonin, its inhibition by cigarette smoke promotes cigarette-associated lung disease (*165*). Tobacco may contain a substance or substances with antidepressant and/or neuroprotective properties, which, by virtue of MAO A inhibition, may contribute to the addiction liability of tobacco in patients suffering from depression and, by virtue of MAO B inhibition, could be linked to the reported low risk that smokers have for developing Parkinson's disease (*166*).

1.3. Aims of the Project

Understanding the catalytic mechanism of monoamine oxidases is of major importance for the rational design of new, potent, reversible and selective inhibitors that can improve human life quality and increase the life span. At the start of this project, the 3D structure of MAO was not known and the evidence that one or two cysteines were involved in the MAO catalysis, described in chapters 1.2.4, 1.2.5 and 1.2.6.2, was compelling. It was hypothesised that a disulphide was located at the active site as a second redox group, in addition to the flavin, and that could interact with the cofactor. By investigating the role of the putative disulphide in MAO catalysis an important step towards obtaining the complete knowledge of the chemical mechanism could be made.

The experimental approaches chosen in order to explore the cysteine residues and their involvement in the MAO chemical mechanism were:

- Construct single and double cysteine mutants to alanine: MAO A C374 and C398 and the correspondent MAO B C365 and C389;

- Characterise the mutants and identify the kinetic, spectral and redox differences to the native enzymes;
- Perform mechanistic target experiments using the mechanism-based inactivators cyclopropylamines.

2. METHODS AND MATERIALS

2.1. MAO Cloning and Expression in *Pichia pastoris*

2.1.1. Basic techniques

I learned basic molecular biology techniques in the Hannah Research Institute under the supervision of Dr. Nigel Price. MAO A, MAO B and mutant MAO B C389S genes cDNAs cloned in the vector pYEDP60 were supplied by Dr. P. Urban (CNRS, France). The sequences of the cDNAs were downloaded from the GeneBank™ database. Location of restriction enzyme cleavage sites and development of cloning strategies were performed with the aid of Lasergen MapDraw software (DNAstar).

The strategies to excise MAO genes from the vector pYEDP60 and to clone them into the vector pGAPZ as well as constructions of the mutants were based on the information available about these vectors and on the map sequences of the cDNAs and respective amino acids, including the cleavage sites of the restriction enzymes that cut once or twice in the genes and not the pGAPZ vector. These maps are shown in chapter 7.

2.1.1.1. Plasmid DNA extraction and purification

Plasmid DNA was purified from 2mL of overnight bacterial cell culture using a Strataprep™ Plasmid Miniprep Kit (Stratagene) or Wizard® Plus SV minipreps DNA purification system (Promega). DNA was eluted in 100μL of TE buffer (10 mM Tris-HCl, pH 8.0, 1 mM EDTA) or nuclease-free water to give a final concentration of 0.1-0.2 μg/μL.

DNA for sequence analysis (~15 μg) was sent to MWG-Biotech as a dried pellet following ethanol precipitation. The DNA was ethanol precipitated by adding TE buffer to 400 μL, followed by 40 μL (1/10 volume) of 4 M NaCl and 800 μL (2X volume) of 100% ethanol. After mixing, the solution was put at -20°C for 1 h (30 min in -70°C) and spun at 14000 g, -4°C for 10min. The supernatant was discarded and the pellet was washed in 600 μL of 70% (v/v) ethanol. The precipitate was then dried.

The extraction and purification of plasmid DNA from agarose gel slices was done using a Strataprep™ DNA Gel Extraction Kit (Stratagene) or QIAquick® gel extraction kit (Qiagen).

2.1.1.2. Digests with restriction enzymes

Table 2.1 lists all the restriction enzymes used as well as their specifications and suppliers.

The digests were done in two different reaction volumes, 20 μL (small digests), for analytical purposes, or 50 μL (big digests) where DNA was used for subsequent cloning (Table 2.2). Digests were incubated at the optimum temperature for at least 1 hour. In the case of *Bst*AP I, a drop of oil was added to prevent evaporation at 60°C. When found necessary, extra enzyme (0.5 μL) was added and the incubation continued.

Where digestion with two enzymes requiring different buffers was necessary, the digests were performed sequentially with an intermediate ethanol precipitation step (chapter 2.1.1.1).

Following digestion, DNA samples were analysed by agarose gel electrophoresis.

Table 2.1. Restriction enzymes used, specifications and suppliers[1]

Enzyme	Stock conc. (u/μL)[2]	Cleavage site	Reaction temperature (°C)	Supplier
Avr II	4	C∨CTAGG	37	NEB
*Bst*AP I	5	GCANNNN∨NTGC	60	NEB
*Csp*45 I	10	TT∨CGAA	37	Promega
Dpn I	10	GA^{me}∨TC	37	Promega
*Eco*R I	10	G∨AATTC	37	Promega
*Hin*d III	10	A∨AGCTT	37	Promega
Kas I	10	G∨GCGCC	37	NEB
Pst I	10	CTGCA∨G	37	Promega
Sac I	10	GAGCT∨C	37	Promega
Sca I	10	AGT∨ACT	37	Promega

(1) The buffers were supplied along with the respective enzymes in a 10X concentration to be used in the digest. (2) u is activity unit defined as the amount of enzyme required to digest 1 μg of DNA in 1 hour at the reaction temperature in a total volume of 50 μL.

Table 2.2. Restriction enzymes reaction mixture in digestions

Reaction components	Small digest	Big digest
Sterile distilled water	9.3 μL	23.5 μL
Restriction enzyme 10X buffer	2 μL	5 μL
100X BSA, acetylated (Promega)	0.2 μL	0.5 μL
DNA sample	8 μL (0.8-1.6 μg)	20 μL (2-4 μg)
Restriction enzyme	0.5 μL (2-5 u)[1]	1 μL (4-10 u)
Final volume	20 μL	50 μL

(1) u is defined in Table 2.1.

2.1.1.3. Agarose gel electrophoresis

Samples were analysed in 1% (w/v) agarose (Boehringer Mannheim) gels containing 0.5μg/ml ethidium bromide (Sigma) prepared in TAE buffer (40 mM Tris base, 0.1% (v/v) glacial acetic acid, 1 mM EDTA, pH 7.2). Samples were mixed with sample buffer (10 mM Tris-HCl, pH 7.5, 50 mM EDTA, 10% Ficoll®, 0.25% bromophenol blue, 0.4% Orange G) and electrophoresed alongside DNA size markers (Promega 1 kb DNA ladder), in a horizontal gel electrophoresis apparatus (Hybaid (BioRad) or Hoefer™ Minnie (Pharmacia Biotech)) typically at 100 V for 1 h. Images of ethidium bromide stained gels were recorded using a UV transilluminator and gel imaging system (Herolab E.A.S.Y. store or BioRad Gel Doc 2000).

2.1.1.4. Dephosphorylation of the vector

After digesting a vector to use later in a ligation it is advantageous to treat it with an alkaline phosphatase to remove the phosphate groups from the 5'-ends and prevent self-ligation of the vector. The enzyme used was the Calf Intestinal Alkaline Phosphatase (CIAP) purchased from Promega. Before dephosphorylation the restriction enzyme was heat killed at 65°C for 15min. The procedure to dephosphorylate 5'-protruding ends and 5'-recessed or blunt ends (in digests from *Pst* I, *Sac* I and *Sca* I) was as described in (*167*). After dephosphorylation the DNA solution was run on an agarose gel to isolate and purify the linearized vector. The vector was then ready for ligation to the insert.

2.1.1.5. Polymerase chain reaction

The PCRs were done using a Hybaid Omn-E apparatus or a Progene (Techne). The reagents were dNTPs (Pharmacia), oligonucleotide primers from

MWG-Biotech or Oswel DNA Service designed with the help of the PrimerSelect software, *Pfu*Turbo DNA polymerase (2.5 u/μL) and respective 10X buffer (Stratagene). In some cases, addition of DMSO (Sigma), which acts to reduce DNA secondary structure, was necessary to achieve successful amplification. Supercoiled plasmid DNA was used as template. Where direct restriction digestion of PCR primers was intended, at least 4 extra bases were added to the 5'-end of the primer.

After the PCR was completed, the reaction solution was run in an agarose gel to check the results and purify the product. PCR products were either digested directly with appropriate restriction enzymes, or via an intermediate cloning step into pGEM-T vector (Promega).

The pGEM-T vector is specially designed for cloning of PCR products generated by certain thermostable polymerases, such as *Taq* polymerase. *Taq* polymerase adds a single deoxyadenosine (A) to the 3'-ends of the amplified fragments, so the vector is supplied already linear with added thymidine (T) to both ends. As *pfu* polymerase originates blunt ends, the PCR products are first treated with *Taq* polymerase (Promega) as shown in Table 2.3. The ligation set up of the tailed PCR product to the pGEM-T vector is also shown in Table 2.3.

After the ligation incubation, the ligase was heat-killed at 65°C for 15 min and the DNA was transformed into bacterial cells (chapter 2.1.1.7). After transformation and bacterial growth, the plasmid DNA was extracted, purified and digested with the proper enzymes to obtain the fragment of interest.

After digestion of the PCR products, either from direct approach or from the pGEM-T system, the DNA was run on a gel to isolate and purify the fragment. The fragment was then ready for ligation to the vector.

Table 2.3. Cloning of PCR products into pGEM-T vector.

PCR product tailing		pGEM-T ligation	
Components	**Volume (μL)**	**Components**	**Volume (μL)**
PCR product	4[1]	2X T4 DNA ligase buffer	5
10X *Taq* polym. Buffer	1	pGEM-T vector	1
2 mM dATP	1	Tailed PCR product	2
25 mM $MgCl_2$	0.6	Sterile distilled water	1
Sterile distilled water	2.4	T4 DNA ligase (3 u/μL)[3]	1
Taq polymerase (5 u/μL)[2]	1		
Final volume	10	Final volume	10
Incubation conditions	70°C, 15-30 min	Incubation conditions	4°C, overnight

(1) Usually 1-7μL, depending on concentration of DNA. (2) One unit of *Taq* polymerase, u, is defined as the amount of enzyme required to catalyse the incorporation of 10 nanomoles of dNTPs into acid insoluble material in 30 min at 74°C. (3) 0.01 Weiss unit of T4 DNA ligase is defined as the amount of enzyme required to catalyse the ligation greater than 95% of the *Hind* III fragments of 1 μg of Lambda DNA at 16°C in 20 min.

Table 2.4. Example of a ligation protocol

Components	**Ligation**	**Control**
Sterile distilled water	7 μL	11 μL
10X T4 DNA ligase buffer	2 μL	2 μL
Vector	6 μL	6 μL
Insert	4 μL	0 μL
T4 DNA ligase (3u/μL)[1]	1 μL	1 μL
Final volume	20 μL	20 μL
Incubation conditions	Room temperature for 3 h or 4°C overnight	

(1) Unit u defined in Table 2.3.

2.1.1.6. Ligation of plasmid vector and insert DNA

The amounts of vector and the insert DNA used were estimated from the intensity of the ethidium bromide stained DNA band on the gel used. A molar ratio of vector:insert in the range 1:1 - 1:3 was used, with approximately 100ng of vector DNA. An example ligation protocol is shown on Table 2.4. A control was always performed to check on the religation of the vector.

After the ligation incubation, the ligase was heat-killed at 65°C for 15 min and the DNA was transformed into bacterial cells.

2.1.1.7. Bacterial transformation and subsequent growth

Unless stated otherwise, transformation of cells of *E. coli* XLI Blue was performed by electroporation (BioRad *E. coli* pulser, Equibio Easyject Plus and 0.2 cm gap cuvettes) using approximately 10 ng of plasmid DNA and a voltage of 2.5 V. Bacteria containing the plasmids pYEDP60, pBluescript SK (Stratagene) or pGEM-T (Promega) were grown in LB (10 g/L NaCl, 10 g/L tryptone, 5 g/L yeast extract) liquid medium or LB agar (LB plus 15 g/L agar) containing 0.1 g/mL carbenicillin (Melford). For blue/white screening of PCR products cloned into pGEM-T, the agar plates also contained 0.1 mM IPTG (Melford) and 40 μg/mL X-Gal (Melford). In the case of *E. coli* containing the pGAPZ plasmid, low salt LB (LSLB: LB but 5 g/L NaCl) was used as higher salt concentrations reduce effectiveness of the added 25 μg/mL zeocin (Invitrogen).

When the method for transformation was heat-shock, the bacterial cells *E. coli* XLI Blue were first made competent. The bacteria were grown overnight in 5 mL LB liquid medium containing 0.1 g/mL carbenicillin, 37°C with shaking at 200 rpm. A dilution of 1/100 in 100 mL of the same medium was shaken at 200 rpm and

37°C until the absorbance at 600 nm reached 0.6 (3-4 h). The culture was cooled down in ice and then centrifuged at 3000 g, 4°C. The pellet was resuspended in 15 mL of filter-sterile TFB1 (30 mM potassium acetate, pH 5.8, 10 mM $CaCl_2$, 50 mM $MnCl_2$, 100 mM RbCl, 15% glycerol) and kept in ice for about 10 min. The cells were centrifuged again and the pellet resuspended in 2 mL of filter-sterile TFB2 (100 mM MOPS, pH 6.5, 75 mM $CaCl_2$, 10 mM RbCl, 15% glycerol). Aliquots of 100 µL were transferred into 0.5 mL tubes and then frozen in dry-ice and stored at –70°C. To perform the transformation, 5 and 10 µL of the PCR products were mixed with ice-thawed 100 µL of competent cells and left on ice for 30 min. As a control, 1 µL of plasmid DNA (145 ng) of known concentration was also used. The mixtures were incubated for 1 min at 42°C in a water-bath and placed on ice for 2 min. 1 mL of ice-cold LB was added and the culture shaken at 200 rpm, 37°C for 1 h. The 1 mL cultures with PCR products and 10 µL of the control culture were plated out in LSLB-agar (LSLB plus 15 g/L agar) with 25 µg/mL zeocin and incubated at 37°C overnight. The control was used to check the transformation efficiency. Single colonies of the PCR products transformants were chosen to incubate in 5 mL of LSLB with 25 µg/mL zeocin and the cultures were grown overnight in a 37°C shaker. The DNA was extracted and checked with the appropriate restriction enzymes (chapters 2.1.1.1 and 2.1.1.2).

2.1.1.8. Transformation of the genes into yeast

To increase the efficiency of transformation and integration into the *Pichia pastoris* genome the DNA was linearized using *Avr* II. This enzyme cuts with the pGAPZ, but does not cut the MAO cDNA inserts. The linearized plasmid integrates into *Pichia* genome by homologous recombination. Approximately 30 µg of plasmid

DNA was digested with 4 units of enzyme at 30°C in a volume of 100 µL DNA solution. After overnight digestion, the DNA was purified (gel purification kit). After ethanol precipitation, the DNA was resuspended in 10.2 µL of sterile, distilled water. 0.2 µL of this DNA solution was analysed by gel electophoresis to confirm complete linearization.

The *Pichia pastoris* were transformed by electroporation (Bio-Rad GenePulser II or Equibio EasyJect Plus, with 0.2 cm path electroporation cuvettes) as described in the Invitrogen product manual. Briefly yeast cells (*Pichia pastoris*, strains X33 (wild type) and SMD 1168 kexl::SUC2 (protease deficient, (*168*)) were grown to an Abs of 1.3-1.5, harvested by centrifugation (4°C) and washed several times with decreasing volumes of ice-cold water. After final resuspension using 1/250 of the original culture volume of 1 M Sorbitol (Merck), 80 µl aliquots were used for each transformation. A modification of this method to improve competence of the cells was the incorporation of a DTT treatment before the washes. The cells were resuspended in 40 mL sterile ice-cold water and after addition of 10 mL 10X TE buffer (100 mM Tris-HCl (Sigma) pH 7.5, 10 mM EDTA (Sigma)) and 10 mL of 1M lithium acetate (Acros), the solution was gently shaken for 45 min at 30°C. 2.5 mL of 1 M DTT (Sigma) was added and the solution was gently shaken again for 15 min at 30°C. The cells were pelleted again and washed as before.

The electroporation conditions used were 1.5 kV of charging voltage, 25 F of capacitance and 400 Ω of resistance for the Bio-Rad GenePulser II and 329 Ω for the Equibio EasyJect Plus. Immediately after pulsing (time constant typically 8-10 ms), cells were mixed with 1mL of ice-cold 1 M sorbitol, transferred to 15 mL tubes and placed at 30°C. After 1 h, 1 mL of pre-warmed YPD (1% yeast extract, 2% peptone, 2% dextrose) was added and incubation was continued with shaking at 200 rpm.

After 4 h the transformed cells were plated out by spreading 250 μL on YPDS agar plates (YPD containing 2% agar and 1 M sorbitol) containing zeocin and grown at 30°C for 3-5 days until colonies appeared. The zeocin concentrations ranged from 0.1 to 8 mg/mL.

2.1.1.9. Testing the clones

To ensure the clones were zeocin resistant, they were streaked out for single colonies on YPD plates containing zeocin (0.1 to 8 mg/mL) and grown for 24 h.

The clones were grown in 5 mL YPD (200 rpm, 30°C) containing zeocin (0.1 to 4 mg/mL) for two days and then transferred to 50 mL YPD without antibiotic and incubated again for three days. The cultures were pelleted at 3000 g for 5 min, 4°C and washed twice with distilled water. The pellets were weighed and resuspended in 5 mL of ice-cold breakage buffer (0.1 mM Tris-HCl, pH 7.5, 1 mM EDTA, 0.5 mM PMSF (Sigma), 3 mM DTT). 5mL of cold, acid-washed glass beads (425-600 microns) from Sigma were added and allowed to stand for 2 min. The mixture was vortexed for 1min and chilled on ice for at least 30 s. This cycle was repeated 4 times. To separate the glass beads and the cells debris from the enzyme suspension, the mixture was spun at 3000 g for 10 min at 4°C. MAO assays were then performed on the final supernatant and the expression level in U/g_{yeast} calculated. The definition of activity unit (U) is μmol(product)/min using 1 mM kynuramine (Sigma) as substrate.

The clone found to have the highest expression level was used for further transformation and selection in increasing zeocin concentrations (up to 8 mg/mL) in order to obtain higher expression levels.

Glycerol stocks of the cells clones were made from overnight 5 mL YPD culture. Culture aliquots (1 mL) with 25% glycerol were snap frozen in liquid nitrogen and stored in -70°C.

2.1.2. Cloning into pGAPZ

pGAPZ was available in three forms, a, b or c, the only difference being one restriction site on end of the polylinker, which was *Apa* I, *Xba* I or *Sna*B I, respectively. In case of later wanting to insert something on this site, it should be chosen the one with the enzyme that does not cut MAO genes. It was the case of pGAPZa and pGAPZb, the former being the one used.

The polylinkers of pYEDP60 and pGAPZa consist of the restriction sites of *Bam*H I/ *Sma* I/ *Kpn* I/ *Sac* I/ *Eco*R I (*169*) and *Sfu* I/ *Eco*R I/ *Pml*I/ *Sfi* I/ *Bsm*B I/ *Asp*718 I/ *Kpn* I/ *Xho* I/ *Sac* II/ *Not* I/ *Apa* I (Invitrogen product manual), respectively, being the underlined one located immediately downstream of the promoter. Using this information, it was decided to use *Eco*R I to cut the gene in the pYEDP60 after the 3'-end and to clone the gene in pGAPZa between *Sfu* I and *Eco*R I.

All PCR were checked for errors by sequencing in MWG-Biotech. The pGAPZa with the MAO genes were then electroporated into *Pichia* and the respective expression levels were checked.

2.1.2.1. MAO A

The strategy to get the MAO A gene from pYEDP60 and clone it into pGAPZ is described schematically in Figure 2.1. As there is no appropriate restriction enzyme site on the 5'-end to cut the whole gene between it and *Eco*R I, an enzyme that cuts ahead was chosen in order to the fragment be long enough to be

obtained by PCR. Such enzyme was *Kas* I. The PCR, under the conditions shown in Table 2.5 was performed using as template the cloned pYEDP60, as sense primer 5'-GTATTCGAACAAGATGGAAAACCAAGAAAAGGC-3' and as antisense primer 5'-CTGGAATTCAGGCGCCCCGAAATGGATA-3' (Table 2.6). These were designed to introduce a *Csp*45 I restriction site (isoschizomer of *Sfu* I) and a *Eco*R I restriction site, respectively. This way the fragment could be introduced in the vector pGAPZa after being digested with *Csp*45 I and *Eco*R I and dephosphorilated.

2.1.2.2. Removal of the MAO A 3' untranslated end

The strategy to remove the 3' untranslated region on the MAO A cDNA was to obtain by PCR the fragment between *Hind* III and the stop codon, including the restriction site for *Eco*R I immediately after the latter. This fragment could then replace the one with the extra base pairs (Figure 2.2).

The PCR, was set up with the sense primer 5'-CTTGCCCGGAAAGCTGATCGAC-3' and the antisense primer 5'-CGTGTGAATTCTCAAGACCGTGGCAGGAGC-3' (Table 2.5 and Table 2.6). The former was designed to be located before the *Hind* III cleavage site in MAO A gene and the latter to have the cleavage site of *Eco*R I just after the stop codon.

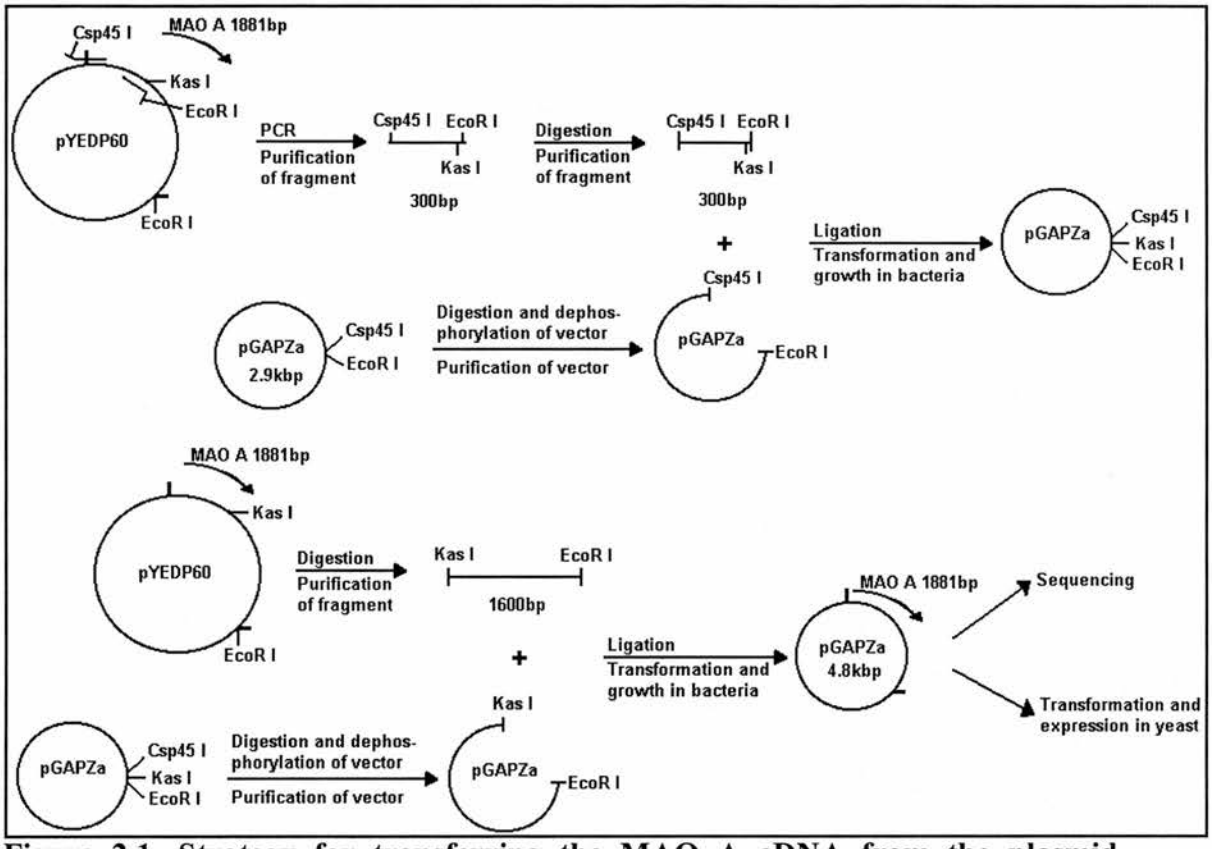

Figure 2.1. Strategy for transferring the MAO A cDNA from the plasmid pYEDP60 to the plasmid pGAPZa. The techniques used in each step are described in chapter 2.1.1.

Table 2.5. PCR program using the Hybaid Omn-E apparatus

Stage	Temperature (°C)	Time (min:s)	Number of cycles
1	95(1)	05:00(1)	1
	85	hold(2)	
2	95	01:00	20(4)
	56.5(3)	01:00	
	72	00:45(5)	
3	72(6)	10:00(6)	1

(1) Denaturation of DNA; (2) Addition of polymerase; (3) Optimal annealing temperature, depending on the primer pair used (as suggested by primer design software); (4) The lowest number of cycles possible was used to minimize PCR errors, typically 20; (5) The amplification time is dependent on the length of the PCR product: 1min per 1kbp; (6) PCR product extension.

Table 2.6. Components and quantities in a PCR set up using DMSO[1].

Components[2]	Quantities (μL)		
	0% DMSO	5% DMSO	10% DMSO
10X polymerase buffer	5	5	5
10mM dNTP	1	1	1
50μM sense primer[3]	1	1	1
50μM antisense primer[3]	1	1	1
DMSO	0	2.5	5
1/300 template[4]	41.5	39	36.5
Polymerase[5]	0.5	0.5	0.5
Final volume	50	50	50

(1) DMSO (Sigma) reduces DNA secondary structure; (2) The components were assembled in the order shown. Two drops of mineral oil were added to avoid evaporation; (3) Where direct restriction digestion of PCR primers was intended, at least 4 extra bases were added to the 5'-end of the primer; (4) Supercoiled plasmid DNA was used as template; (5) The enzyme was added last at 85°C, during stage 1 of the PCR program (Table 2.5).

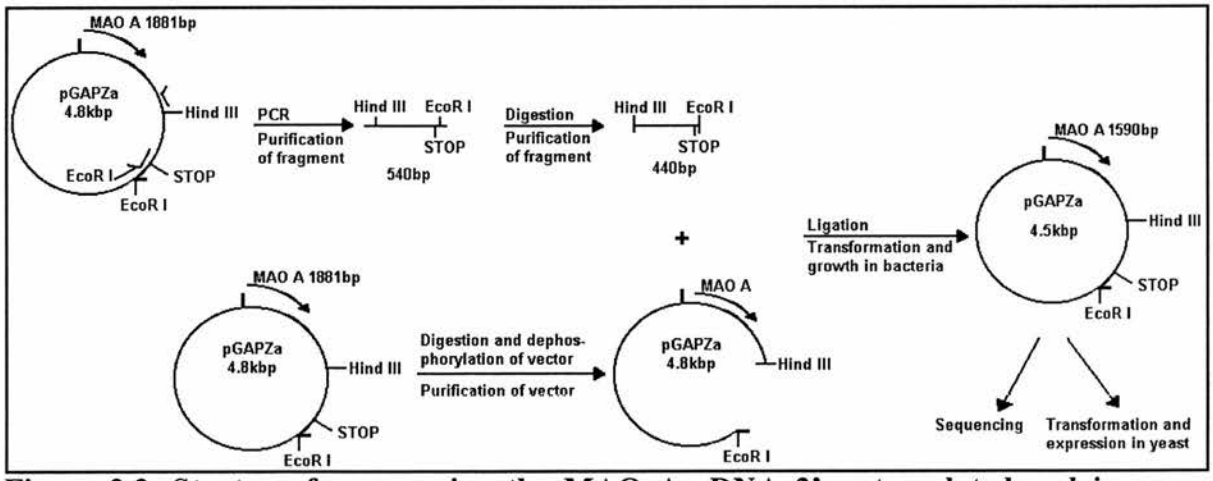

Figure 2.2. Strategy for removing the MAO A cDNA 3' untranslated end in pGAPZa. The techniques used in each step are described in chapter 2.1.1.

2.1.2.3. MAO B and the mutant MAO B C389S

The strategy to clone MAO B and the mutant MAO B C389S into pGAPZ, schematicaly described in Figure 2.3, was similar to the one for MAO A except the use of the fact that there was the restriction site of *Bsp*AP I at the 5'-end. In this case the whole gene could be cut from the vector pYEDP60 and then cloned into pGAPZa after creating the *Bsp*AP I restriction site in the latter. Two oligos were designed to have, after annealing, the ends corresponding to the restriction sites of *Csp*45 I and *Eco*R I and in the middle the restriction site of *Bsp*AP I. Their sequences were: sense 5'-CGAAGATGAGCAACAAATGCG-3' and antisense 5'-AATTCGCATTTGTTGCTCTCTTT-3'.

2.1.3. MAO mutants construction

All mutants were done making a mutation of the target cysteine to an alanine in the MAO genes in the plasmid pGAPZa. The incorporation of the mutation was checked by sequencing in MWG-Biotech. The mutated genes were transformed into *Pichia* and the respective expression levels checked.

2.1.3.1. MAO A C374A

The mutant MAO A C374A could be constructed using the PCR technique, as the codon for C374 is adjacent to the restriction site for *Sac* I, which cuts twice on the gene. The steps used to construct this mutant are described in Figure 2.4.

The PCR was done using the sense primer 5'-ACAAAATCTGCTGGACAAAGACTGCTAGG-3' and the antisense primer 5'-GGGGGGGGA**GCT**CAGCGATTTTCTTCTTCCTT-3' (Table 2.5 and Table 2.6). The sense primer was designed to be located before the first cleavage site of *Sac* I in MAO A gene and the antisense primer to have the second cleavage site of *Sac* I

and the mutation cysteine 374 to alanine (in bold). This way, after digestion with *Sac* I, the mutant fragment could replace its analogue on the wild type MAO A gene. But as this fragment is located at the central part of the gene and the sequencing procedure can only start from the gene ends, it would be difficult to sequence it. Therefore, it was decided to clone the mutant fragment into a common replicative vector in *E. coli* that had the restriction site for *Sac* I in its polylinker, and use this to send for sequencing. A ligation was set up to clone the fragment with the mutation in the pBluescript SK vector, which did not work (no colonies grew on selective media). As it could have been a problem in the insert, the PCR was repeated but this time the product was cloned into the pGEM-T vector. This vector was designed especially to clone PCR products and could also be used to send for sequencing the fragment. To check on the ligation, the plasmids from four clones were digested with *Sac* I.

The vector from the correct clone was then digested with *Sac* I to recover the mutated fragment and use it to replace the wild type fragment in the pGAPZ with MAO A gene. After checking the ligation, it was necessary to check if the orientation of the fragment on the MAO A gene was correct, as both ends had the same restriction site. To do this another PCR was performed using the same primers as above. This PCR would only work if the fragment was in the correct orientation.

At this stage it was discovered that, due to a designing error, the sense primer of the first PCR (Figure 2.4) was downstream from the first *Sac* I restriction site instead of upstream, which means that the mutant fragment did not have this restriction site on the 5'-end. This explains why the ligation with the pBluescript did not work. The digestions of the cloned pGEM-T could not reveal this error because pGEM-T had one *Sac* I restriction site that was only 39bp distant from the insertion

point of the fragment. Moreover, the PCR for checking the mutated fragment orientation after insertion in the pGAPZ-MAO A gene was not dependent on the orientation because both sense and antisense primers were inside the fragment.

The mistake on the sense primer resulted in the incorporation of a small fragment from the vector pGEM-T in the pGAPZ-MAO A gene. Instead of trying to remove the extra small fragment, it was easier to remove a fragment that would include only the desired mutation and replace the analogue on the wild type pGAPZ-MAO A. To do this it was used the *Vsp* I that cuts once between the two mutations and once the pGAPZ downstream from the 3'-end of the MAO gene. This step is schematicaly explained in Figure 2.5.

Only the clones with the fragment in the correct orientation would grow because the *Vsp* I restriction site on pGAPZ was located in the ColE1 origin, which allows replication and maintenance of the plasmid in *E. coli*.

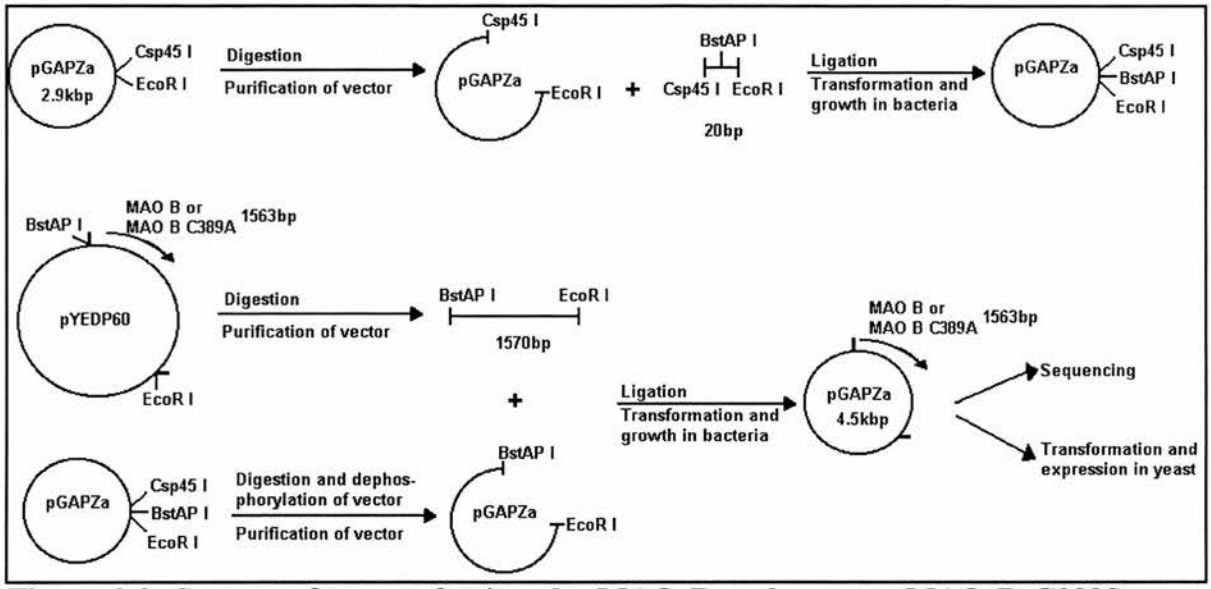

Figure 2.3. Strategy for transferring the MAO B and mutant MAO B C389S cDNAs from the plasmid pYEDP60 to the plasmid pGAPZa. The techniques used in each step are described in chapter 2.1.1.

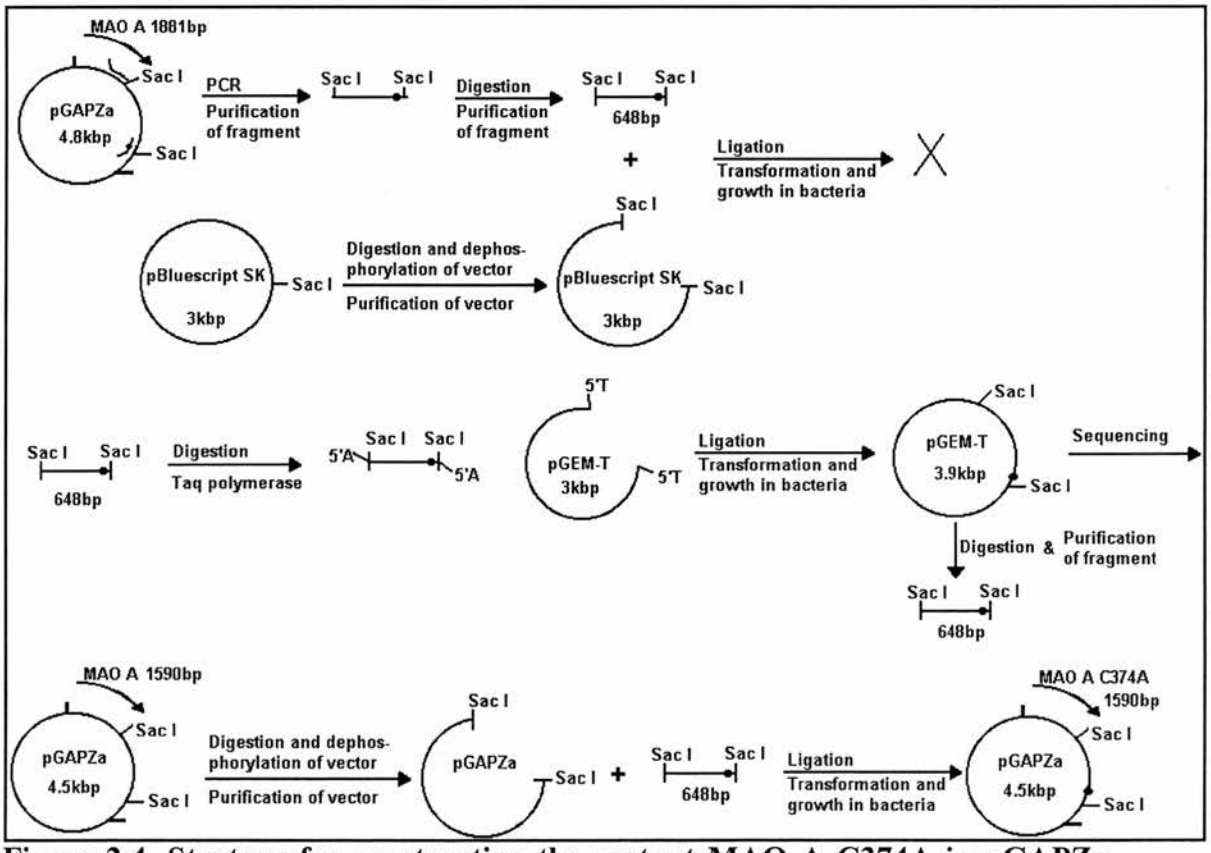

Figure 2.4. Strategy for constructing the mutant MAO A C374A in pGAPZa. The techniques used in each step are described in chapter 2.1.1.

2.1.3.2. ***MAO B C389A***

The principle used to design the strategy of construction of mutant MAO B C389A was similar to the one for mutant MAO A C374A (Figure 2.6).

The PCR was done using the sense primer 5'-GGCCATTCCCACCTGTAT-3' and the antisense primer 5'-CCGAGTACT**GCT**CCTCAGCCCAGTTCTTTTCTTC-3' (Table 2.5 and Table 2.6). The sense primer was designed to be located before the cleavage site of *Pst* I in MAO A gene and the antisense primer to have the cleavage site of *Sca* I and the mutation cysteine 389 to alanine (in bold). This way, after digestion with *Pst* I and *Sca* I, the mutant fragment could replace its analogue on the wild type MAO B gene. There is no evidence that *Sca* I efficiently cuts close to the end of a DNA fragment, so it was safer to clone the fragment first into the vector pGEM-T. Both *Sca* I and the PCR originate blunt ends, which means that in the case of non-efficient cutting the fragment would ligate anyway to the blunt ended gene and create an error only detectable by sequencing.

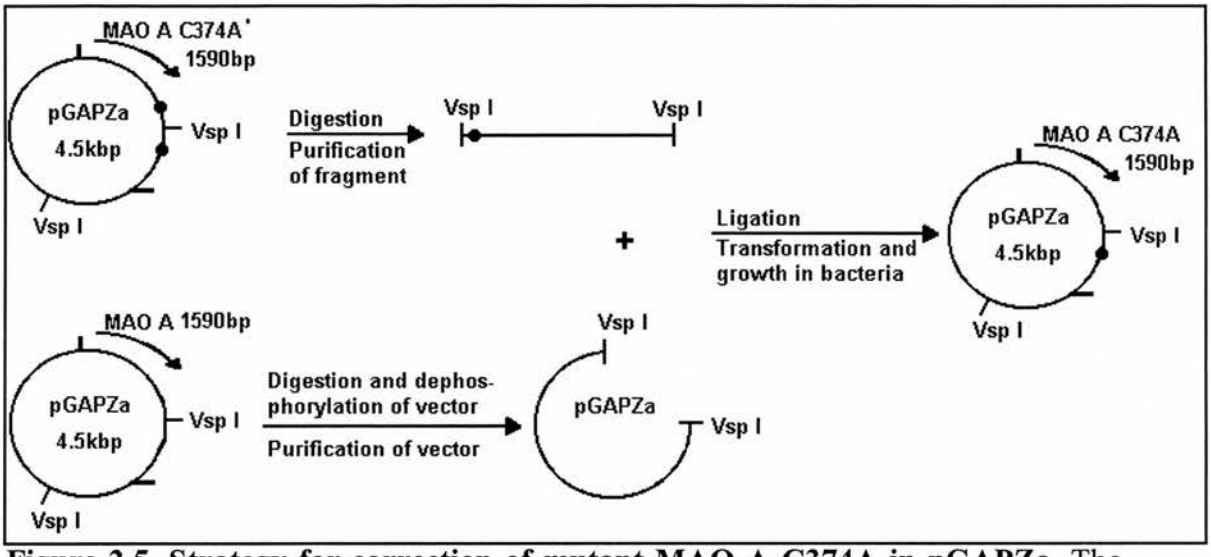

Figure 2.5. Strategy for correction of mutant MAO A C374A in pGAPZa. The techniques used in each step are described in chapter 2.1.1.

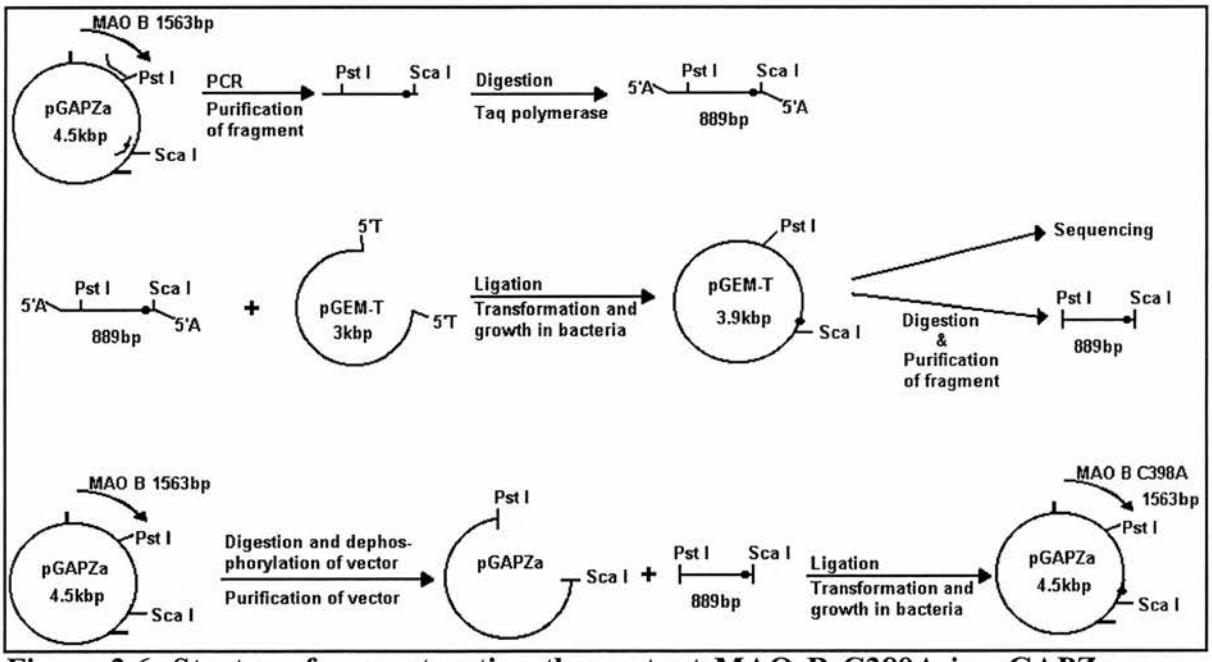

Figure 2.6. Strategy for constructing the mutant MAO B C389A in pGAPZa. The techniques used in each step are described in chapter 2.1.1.

2.1.3.3. MAO A C398A and MAO A C374A & C398A

The principle of the method used to insert the mutation MAO A C398A and MAO A C374A & C398A was the same as described in previous chapters (2.1.3.1 and 2.1.3.2). The cysteine 398 is close to the restriction site of *Sca* I, so the antisense primer was designed to have this cleavage site and the mutation (in bold) and the sense primer was designed to be located before the restriction site *Kas* I, 5'-CCCCCAGAGTACT**GCT**CCTCAGCCCAGTTCTTCTC-3' and 5'-GGGGAAAACATATCCATTTCGGGGCGCC-3', respectively. The primers were ordered from Oswel DNA Service. The templates for the PCR were pGAPZa with MAO A for preparing of the single mutant MAO A C398A and pGAPZa with MAOA C374A for the double mutant MAO C374A & C398A. The PCR products were run on an agarose gel and the respective bands purified. The DNA was treated with *Taq* polymerase to be ligated to the pGEM-T plasmid. The pGEM-T with the PCR product incorporated was transformed into electrocompetent XL1-Blue cells. While the pGEM-T with the PCR product was sent to sequence to MWG-Biotech, the piece of DNA without the mutation in the templates was replaced by the PCR product with the mutation.

2.1.3.4. Correction of the MAO B mutation V489A

The technique to correct the mutation MAO B V489A was different from the above because the mutation site does not have a unique restriction site close by. It consisted in designing the primers with the desired mutation that would anneal to the same sequence on opposite strands of the template. The PCR, using *Pfu* Turbo DNA polymerase, is done on the whole of the plasmid, including the MAO gene and the incorporation of the mutation, resulting in nicked circular bands. The methylated,

nonmutated parental DNA template is then digested with *Dpn* I and the circular nicked dsDNA is transformed into electrocompetent XL1-Blue cells. After transformation the cells repair the nicks in the mutated plasmid, which can be recovered and analysed.

The PCR set up and programme are shown in Table 2.7 and Table 2.8, respectively. The primers with the mutation (in bold) used were 5'-GACATTTGCCCTCC**GTG**CCAGGCCTGCTCAGGC-3' and 5'-GCCTGAGCAGGCCTGG**CAC**GGAGGGCAAATGTC-3'. The components were assembled in the order shown. Supercoiled plasmid DNA was used as template.

Table 2.7. Components and quantities the PCR set up for correction of the MAO B mutation V489A.

Components	Quantities (μL)	
10X polymerase buffer	5	5
2mM dNTP (Pharmacia)	5	5
Sense primer	(1)	(1)
Antisense primer	(1)	(1)
Template	0.7[2]	1.4[2]
Water	(3)	(3)
Polymerase[4]	1	1
Final volume	50	50

(1) Calculated from the primer stock concentration to give 0.5μM; (2) Calculated to give about 100 and 200 ng, respectively; (3) Calculated to give a final volume of 50 μL; (4) Added only at 85°C (see Table 2.8).

Table 2.8. PCR programme using the Progene PCR machine[1].

Prog	Segment	Temperature (°C)	Time (min:s)	Number of cycles
1	1	95[2]	05:00[2]	1
	2	85	02:00[3]	
2	1	95	01:00	20[5]
	2	(4)	01:00	
	3	72	(6)	
3		72[7]	10:00[7]	1

(1) PCR composition as in Table 2.7; (2) Denaturation of DNA; (3) Addition of polymerase; (4) Optimal annealing temperature, depending on the primer pair used - T = Tm(lower of the pair) - number base mismatch x 3°C - 6°C; (5) The lowest number of cycles possible was used to minimize PCR errors; (6) The amplification time is dependent on the length of the PCR product: 1 min / 1 kbp; (7) PCR product extension.

2.1.3.5. MAO B C365A and MAO B C365A & C389A

The technique for the construction of the cysteine to alanine mutations MAO B C365A and MAO B C365A & C389A was the same as described above (chapter 2.1.3.4). After several failed attempts using PCR conditions as in Table 2.7 and Table 2.8, new primers were designed and PCR conditions optimised. The sense and antisense primers were 23 bases long, complementary to each other and with the same sequence of the targeted region of the MAO B gene except for the inclusion of the mutation cysteine to alanine at position 365. The primer sequences containing the mutation (in bold), ordered from Oswell DNA service, were

5'-CATAGAGTTC**AGC**AAGTTTCTTC-3' and

3'- GTATCTCAAG**TCG**TTCAAAGAAG - 5'.

To increase the yield on PCR products, the temperature of annealing of the first PCR cycles was low and increased after every cycle, until the desired high temperature was achieved to obtain high specificity (PCR ladder technique). The templates used for the construction of the MAO B C365A and MAO B C365A & C389A mutants were MAO B cDNA and MAO B C389A cDNA in the pGAPZa plasmid, respectively.

The PCR ladder set up and programme are shown in Table 2.9 and Table 2.10, respectively. The components were assembled in the order shown. Supercoiled plasmid DNA was used as template.

Table 2.9. Components and quantities in a PCR ladder set up.

Components	Quantities (μL)
10X polymerase buffer	5
2mM dNTP (Pharmacia)	5
Sense primer	3.5[(1)]
Antisense primer	1.8[(1)]
1/10 diluted template	1
Water	32.7
Polymerase[(2)]	1
Final volume	50

(1) Calculated from the primer stock concentration to give 0.5 μM; (2) Added only at 85°C (see Table 2.10).

Table 2.10. PCR ladder programme using Progene PCR machine[(1)].

Prog	Segment	Temperature (°C)	Time (min:s)	Number of cycles
1	1	95	05:00	1
	2	85	02:00[(2)]	
2	1	95	00:30	4
	2	47 + 4x2[(3)]	00:45	
	3	72	05:00	
3	1	95	00:30	20
	2	55	00:45	
	3	72	05:00	
4		72	10:00	1

(1) PCR composition as in Table 2.9; (2) Addition of polymerase; (3) The temperature was increased 2°C every cycle for 4 cycles.

2.1.4. Check of expression of inactive mutants

In order to check if the inactive clones were expressing the enzyme, MAO A and B antibodies were produced and used in western blots.

2.1.4.1. Production of MAO A and B antibodies

Two polyclonal anti-peptide antibodies were produced, one against MAO A only (Ab A) and another against both MAO A and B (Ab A&B). The antigens chosen were the N-terminal of MAO A for Ab A and an internal completely homologous sequence of MAO A and MAO B for Ab A&B. The peptides MENQKASIAGHMFC (N-terminal) and CGAVEAGERAARE (internal) were synthesised by Dr. Kemp in the Centre for Biomolecular Sciences, St. Andrews.

A cysteine was added to one of the ends of both peptides to be coupled to a carrier via SPDP. The carrier chosen was KLH (Keyhole Limpets Hemocyanin) from Sigma. To 2 mL of KLH (10 mg/mL in 0.1 M phosphate, 0.1 M NaCl, pH 7.5) were added 450 μL of 20 mM SPDP (225 μL per mL of KLH) dropwise. The solution was mixed for 30 min at room temperature and then dialysed in 500 mL PBS (8 g/L NaCl, 0.2 g/L KCl, 1.44 g/L Na_2HPO_4, 0.24 g/L KH_2PO_4, pH 7.4) for 2 h and again overnight at 4°C. The activation of the carrier could be estimated by taking the absorbance at 343 nm (ε = 8080 $M^{-1}.cm^{-1}$) of an aliquot in PBS with 30 mM DTT, as DTT displaces an equimolar amount of pyridine-2-thione.

1mL of each peptide (6.9 mg/mL internal and 4.6 mg/mL N-terminal in PBS) were added to 1.5 mL of activated KLH and left mixing at room temperature for 1 h and then at 4°C overnight. The amount of peptide coupled could be calculated from the absorbance at 343 nm, as coupling of the peptide releases an equimolar amount

of pyridine-2-thione. The solutions were dialysed as before and mixed together. Aliquots of 500 and 250 μL were stored at –20°C.

One aliquot of 500 μL and four aliquots of 250 μL of the conjugated peptides were sent to MicroPharm, Limited for production of antisera by sheep for 14 weeks with two bleeds (200-300 mL) at weeks 10 and 14.

2.1.4.2. Purification of MAO A and B antibodies

The sheep antisera were purified and the antibodies separated by peptide affinity chromatography.

1 g of activated Thiol-Sepharose 4B (Sigma) were swollen in 200 mL of Affinity Column Buffer (50 mM Tris, 0.5 M NaCl, 1 mM EDTA, pH 7.5) for 15 min at room temperature. The resin was collected on a sintered filter and washed with 100 mL of Affinity Column Buffer, removing most of the liquid without letting it over dry. 5 mg of peptide were dissolved in 5 mL of Affinity Column Buffer and, after taking an aliquot of 100 μL to freeze, the remainder was immediately added to the washed resin in a 15 mL plastic tube. The solution was mixed at room temperature for about 2 h and allowed to settle to remove the supernatant. Coupling of the peptide could be checked by taking the absorbance of the supernatant at 343 nm, as it displaces the resin protective group. The resin was washed three times with Affinity Column Buffer and stored at 4°C (for long storage 0.02% azide was added).

A 3 cm x 100 cm column was packed with the peptide-activated resin and washed with 10 column volumes of Affinity Column Buffer. 20 mL of antiserum were centrifuged at 48000 g, 4°C for 20 min and the supernatant was loaded into the column at 1 mL/min while 4 mL fractions were being collected. After the wash was repeated, the peptide specific antibody was eluted with 0.1 M Glycine/HCl, pH 2.5. Prior to elution 0.5 mL of 1 M Tris were added to each fraction collector tube.

Fractions of 3 mL were collected and immediately mixed for pH checking (should be between 5 and 9).

The elution of the serum proteins and then the specific antibodies was followed by reading the absorbance at 280 nm. Aliquots of 15 µL of the acid-eluted fractions were loaded on 15% polyacrylamide-SDS gels (*170*) to check the purification of the antibodies. The two fractions with higher amounts of specific antibodies were pooled together and stored in 50% glycerol, 1 mg/mL BSA and 0.01% azide, in aliquots of 1.5 mL at –20°C.

2.1.4.3. Western blot

7.5 and 10% polyacrylamide-SDS gels were run with the MAO samples and pre-stained large-range protein markers (NEB) and cut to the desired size.

The transfer was the semi-dry electrophoretic using the Semi-Dry Blotter II KemEnTec. The electrode plates of the transfer apparatus were wet with transfer buffer (25 mM Tris-base, 25% methanol (Fisher)). 18 sheets of absorbent paper (Whatman 3MM) and one sheet of PVDF membrane (Millipore) were cut to the size of the gel (typically 9 cm x 6 cm). The membrane was soaked first in methanol and then in transfer buffer. The absorbent paper was also wet by soaking in transfer buffer. The gel, membrane and paper were assembled as follows:

Top plate (cathode)

9 layers of absorbent paper soaked in transfer buffer

Polyacrylamide gel slightly wetted in transfer buffer

The membrane soaked in transfer buffer

9 layers of absorbent paper soaked in transfer buffer

Bottom plate (anode)

The sandwich was carefully checked for air bubbles, which were gently removed by rolling a clean test tube over it. Using a pastette, transfer buffer was put on top of the sandwich, but without flooding the apparatus. The transfer was run for 30 min.

The membrane was blocked with 20mL of 5% (w/v) skimmed milk powder in PBS for 1 h on the shaking platform.

After rinsing with water the membrane was cut in as many strips as the desired number of dilutions of the primary antibody. The strips were then put in capped tubes with the primary antibody at the appropriate dilutions in 2mL 5% (w/v) skimmed milk powder in PBS. The tubes were put on a roller-rock for 1 h.

The strips from the different dilutions were washed separately 4 times for 10 min with 0.2% Tween 20 (Sigma) in PBS, rocking and then could be put together to incubate with the alkaline phosphatase-conjugated secondary antibody at a dilution of 1/2000 in 2 mL 1% (w/v) skimmed milk powder for 1 h. The secondary antibody used was an anti-sheep IgG alkaline phosphatase conjugated developed in donkey and was purchased from Sigma. The strips were washed 4 times as before and one last time with PBS only.

For detection, the strips were washed for 5min in alkaline phosphatase buffer (Sigma) and 10 mL of Sigma BCIP/NBT liquid substrate system (developing reagent) were added and incubated at room temperature until the bands were coloured enough (purple). The reaction was stopped by rinsing with 20 mM EDTA in PBS.

2.2. Fermentation

2.2.1. *Saccharomyces cerevisiae*

Human liver MAO A was over-expressed in *Saccharomyces cerevisiae*. The fermentation, performed as described in (*171*), was characterised by cell growth on glucose followed by induction of enzyme expression by galactose. The fermentation conditions were 30°C, agitation of 200 rpm and air supply of 2 vvm (2 L air/L media/min), using a 12 L Microferm fermentor (New Burnswick Scientific) with automatic temperature control and agitation and aeration manual controls. The fermentation stages were monitored by sampling and measuring the Abs_{600nm}. After harvesting, the cells were weighed and frozen at -70°C.

2.2.2. *Pichia pastoris*

The fermentation protocol for an inducible system of *Pichia pastoris* is extensively described in (*172*). For the constitutive expression system it is suggested to start the fermentation with glycerol at the batch phase and followed by a fed-batch phase using a 40% glucose solution (*172*).

Pichia fermentations can reach very high cell densities (final Abs_{600nm} of 400 or higher) and have a high demand of oxygen, which should be monitored by measuring the dissolved oxygen (DO) concentration. There were no facilities available for oxygen supplementation or direct monitoring of the DO. The alternative was to follow the protocol for a fermentation at moderate cell density, where a final Abs_{600nm} of 50 could be reached. The main conditions should be 30°C, agitation at 400rpm and automatic control of DO at 35% and pH at 5.0.

The first fermentations were with the wild type strain X33. They were started with a fermentor basal salts (*172*) media volume of 6 L with a glycerol concentration

of 1%. 4 L of 40% glucose were prepared to start the fed-batch stage at a rate of 1 mL/L/h for adaptation to the new carbon source, which could take approximately 2 h. Then the rate could be increased to 2 mL/L/h for 4 h and increased again to 3 mL/L/h for 2 h. Finally, the rate could be increased and maintained at 4 mL/L/h.

The fermentor available did not have automatic controls of dissolved oxygen or pH. To have an idea if oxygen was limiting or not, an oxygen electrode connected to a chart recorder was set up next to the fermentor. A sample was taken from the fermentor and placed in the closed chamber. The oxygen comsuption was followed until exhaustion of substrate in the sample. A small volume of glucose was then added and if oxygen consumption was registered then the dissolved oxygen was not limiting. The pH was controlled manually by sampling regularly. It was maintained just above 5 by adding filter sterilised ammonia (35%) to the media.

When the *Pichia* pastoris strain was changed from the wild type X33 to the protease deficient SMD 1168 kexl::SUC2 (*168*), the fermentation conditions had to be changed to obtain a good growth and a standard procedure was reached.

Starting with single colonies a succession of duplicate volumes of 5 mL (with 1 mg/mL zeocin), 50 mL and 500 mL of YPD media were inoculated and shaken at 200 rpm and 30°C. The whole of the final culture (1 L) was used to inoculate the fermentation medium.

The fermentation medium (10 L total volume) was prepared using the basal salts medium with the addition of 2 mL/L of trace salts (*172*), 0.5% yeast extract, 1% peptone and 2% glucose. A 35% ammonia solution was filter sterilised and added to the media until pH was just above 5. The fermentation was set at 30°C, 400-450 rpm and was started at about 6 L/min. Whenever possible and with minimal intervals of 1-2 h, samples of about 3 mL were taken to monitor the Abs and the pH. When the

first stationary phase was reached, 500 mL of a 40% glucose solution with 2 mL/L trace salts was added and the aeration turned to 14 L/min. The cells were harvested when the second stationary phase was reached.

A further improvement on the cell weight yield was obtained increasing the pH to 6-7.

The cells were harvested by centrifugation at 3000 g, 0°C for 10 min. To wash the cells, the pellets were resuspended in a volume 4X the cells dry weight of Cell Wash Buffer (0.1 M Tris-HCl, pH 7.5). The pellets were stored at -70°C.

2.3. MAO Purification

The purification method for MAO A from *Sacharomyces cerevisiae* was established before (*48, 171*). The same method was used to purify MAO expressed in *Pichia* but alterations had to be made to improve the extraction of the enzyme.

The cells were thawed and washed again in Cell Wash Buffer. The cell suspension was centrifuged at 3000g, 0°C for 10min and the supernatant was discarded. The pellet was resuspended in a volume 1X the cells dry weight of Cell Breakage Buffer (0.1 M Tris-HCl, pH 7.5, 1 mM EDTA, 3 mM DTT, 0.5 mM PMSF (all from Sigma)). Aliquots of about 10 mL of the cell suspension were added to about 10 mL of glass beads (acid-washed, 425-600 microns, from Sigma) ice-chilled in 40 mL capped centrifuge tubes (Nalgene). The cells were broken in 6 cycles of vortexing the tubes for 1 min and chilling on ice. The mixture was filtered through one layer of muslin in a Büchner funnel to separate the beads. The tubes were rinsed with cell breakage buffer. The filtrate was centrifuged at 3000 g, 0°C for 10 min. The supernatant was kept and the pellets resuspended with cell breakage buffer in a volume 1X the original cells dry weight, already used to rinse the beads. This wash

of the beads and the resuspension of the pellets would normally recover about 10-20% more of the total enzyme activity.

The total supernatant of the low speed spin was ultracentrifuged at 33krpm (50.2Ti rotor, Beckman), 0°C for 40 min. The pellets were resuspended in Extraction Buffer (0.1 M Triethanolamine (Sigma) / HCl, pH 7.2). The membrane suspension was diluted to a protein concentration of 12 mg/mL and brought to 30°C in a water bath, with continuous stirring. Then were added 25 mM $CaCl_2$, 100 mg/L of Phospholipase C (Sigma) and 255 μL/L of Phospholipase A (1603200 U/mL from *N. naja* venom). The pH was monitored and adjusted to 7.2 with 2 M NH_4OH. After a 60 min incubation the material was centrifuged at 48000 g, 4°C for 30 min. The pellets were resuspended in Extraction Buffer and the suspension diluted to a protein concentration of 15 mg/mL. Triton X-100 (Sigma) was added to 0.5% and the material stirred for 30 min at 30°C in a water bath. The material was centrifuged at 48000 g, 4°C for 30 min. The yellowish supernatant was retained.

The Triton extract was loaded onto a column using a BioRad chromatography system with a 1000 cm x 2 cm column of DEAE sepharose CL-6B (Sigma) at a maximum speed of 1 mL/min. The column was washed with 300 mL of degassed Buffer A (20 mM KPi, pH 7.0, 20% glycerol, 0.5% Triton-X100 and 3 mM DTT) before and after loading the Triton extract. Elution was done with linear gradient of Buffers B (20 mM KPi, pH 7.0, 20% glycerol, 0.5 mM D-amphetamine (Sigma), 0.8% β-octylglucoside (Fisher), 0.5 mM PMSF and 3 mM DTT) and C (225 mM KPi, pH 7.0, 20% glycerol, 0.5 mM D-amphetamine, 0.8% β-octylglucoside, 0.5 mM PMSF and 3 mM DTT) using the BioRad Econosystem's gradient former function. 10 mL fractions were collected and assayed for MAO activity and the absorbance measured at 456 and 280 nm. The active fractions were pooled considering the purity

analysed by the graphs of MAO activity and the ratio of absorbance 456/280 versus the fraction number. The pooled fractions were concentrated to a small volume (1-2 mL) using Amicon concentrators with YM-10 membranes (Millipore).

The final material was characterised by the spectrum at 300 – 600 nm. A diluted sample was made anaerobic in a quartz cuvette fitted with a silicone stopper, in an argon/vaccum gas train. Spectra were recorded of the sample alone; after reduction with anaerobic 1 mM kynuramine; and, after full reduction with solid dithionite (Sigma) quickly mixed in. The percentage of active enzyme was calculated as the difference of absorbance at 456 nm upon reduction with kynuramine divided by the total difference of absorbance upon reduction with dithionite and multiplied by 100. The final product, after addition of 50% glycerol, was stored at -20°C.

MAO A activity was assayed spectrophotometrically at 314 nm, using 1 mM kynuramine in a 1 mL system containing Assay Buffer (50 mM KPi, pH 7.2, 0.2% Triton X-100), equilibrated with air at 30°C. Protein quantity was determined by the BCA (Pierce) and Peterson-Lowry methods.

2.4. MAO Titrations

2.4.1. Reductive titrations with dithionite

Purified MAO was titrated with standardised dithionite (Sigma), the procedure based on (*100*). Briefly, all the experiments were carried out anaerobically at 20°C in 50 mM KPi, pH 7.2, containing 0.1% Brij-35 (Sigma). The titrations with sodium dithionite were carried out in a custom-made quartz anaerobic cuvette with a side arm, in an atmosphere of high purity argon. To make sure of consumption of any residual oxygen, 20 mM glucose and 5 μL glucose oxidase/catalase mixture was added. The glucose oxidase/catalase mixture consists of 10 μL catalase (Sigma) and

10 μL glucose oxidase (Sigma) in 500 μL water. Dithionite standardised by titration of riboflavin, was added via a gas-tight syringe attached to the cuvette. The spectra were recorded in a Shimadzu UV-2101PC spectrophotometer. For the enzyme titration, the spectra were recorded 30min after each dithionite addition to ensure that equilibrium was established.

2.4.2. Redox potential

For the calculation of redox potentials the enzyme was titrated with standardized dithionite as described above (chapter 2.4.1) but in the presence of a reporter dye, indigo disulphonate at a concentration similar to the enzyme. Alternatively, the reduction of the enzyme could be done with xanthine and xanthine oxidase as described in (*97*).

2.5. Steady-State Kinetics

2.5.1. Substrates

The initial rates of oxidation of a range of concentrations of kynuramine (0.1 to 0.9 mM), benzylamine (0.2 to 0.8 mM) and MPTP (Sigma) (0.02 to 0.5 mM) were measured spectrophotometrically at 314, 250 and 343nm, respectively, in Assay Buffer at 30°C using a 6-cell changer spectrophotometer Shimadzu UV-2101PC. The initial rates of oxidation of a range of concentrations of β-phenylethylamine (PEA, from Sigma) (0.2 to 2.5 mM) and serotonin (Sigma) (0.3 to 1.8 mM) were measured polarographycally in Assay Buffer at 30°C, using the Digital Oxygen System model 10 (Rank Brothers, Ld.) connected to a chart recorder from Graphics 1000 Lloyds Instruments. The Michaelis-Menten parameters K_m and k_{cat} were calculated using the Hanes plot.

2.5.2. Competitive inhibitors

The competitive inhibition constant, K_{ic}, for D-amphetamine, MPP^+ and Harman (Sigma) was calculated plotting the K_m/V_{max} apparent values for kynuramine (0.1 to 0.9 mM) in the presence of inhibitor against the concentration of the inhibitor ([I]). K_{ic} = - [I], where K_m/V_{max} apparent equals zero.

2.6. Mechanism-Based Inactivation by Cyclopropylamines

2.6.1. Inactivation constant and rate

The inactivation constant, K_I, and the inactivation rate, k_{inact}, were calculated for the mechanism-based inactivators, 1-phenylcyclopropylamine (1-PCPA), *N*-cyclopropyl-α-methylbenzylamine (N-CαMBA) supplied by Prof. Silverman and 2-phenylcyclopropylamine (2-PCPA, from Sigma).

The enzyme was incubated with a range of concentrations of 1-PCPA (0.8 to 5 mM) or N-CαMBA (0.125 to 0.6 mM) in Incubation buffer (100 mM KPi, pH 7.2, 20% glycerol, 0.2% Triton X-100) at 25°C. An aliquot was taken at timed intervals and assayed for residual enzyme activity with 1mM kynuramine in Assay Buffer at 25°C. In the case of 2-PCPA, the incubation was set up in 6 cuvettes at 25°C with Incubation buffer and inactivator and the enzyme added at different time points. The Assay buffer was then added and the 6 assays were run at the same time in the 6-cell changer spectrophotometer. This was done for a range of concentrations of the inactivator from 12 to 100 μM.

The logarithm of the percentage of activity remaining was plotted against time to calculate the half-life time $t_{1/2}$ for each inactivator concentration. The $t_{1/2}$ vs. the reciprocal of the inactivator concentration (Kitz & Wilson plot) gives a straight

line where the intercept over the slope gives the K_I and the reciprocal of the slope gives the k_{inact}.

2.6.2. Competitive inhibition constant

The competitive inhibition constant, K_{ic}, for 1-PCPA, N-CαMBA and 2-PCPA was obtained as described in chapter 2.5.2.

2.6.3. Partition ratio

A constant amount of enzyme (about 2 μM) was incubated with 10 different concentrations of inactivator in Incubation buffer, to a total volume of 400 μL (see Table 2.11 for detailed quantities). The solutions were incubated at 25°C for up to 15 days. Aliquots of 20 μL were removed periodically and assayed for residual activity. Activity was expressed relative to the control solution without inactivator. The PR was then determined graphically (see Figure 4.8)

Table 2.11. Incubation contents for the determination of MAO A and MAO A C374A partition ratio for cyclopropylamines.

Concentration (μM)	N-CαMBA	2-PCPA	1-PCPA
MAO A	1.04	1.01	6.0
MAO A C374A	0.82	0.72	4.6
Inactivator	0 – 6.25	0 – 6.0	0 – 80

2.6.4. Flavin spectra change by inactivation

The cyclopropylamines inactivate MAO A by forming adducts to the flavin and/or to a cysteine. Reoxidation of the flavin is observed after denaturation if the adduct is not formed on the flavin. 125 μL of MAO A (56 μM) and 200 μL of MAO A C374A (28 μM) were dialysed against 0.5 L of Dialysis Buffer (50 mM KPi, pH 7.2, 0.1% Brij-35) with 2 changes every 45 min. The enzyme was centrifuged at 14000 g, 4°C for 10 min to separate any precipitate and the supernatant was transferred to a quartz cuvette. After the first spectrum was run (300 to 600 nm) and the enzyme assayed, 2-PCPA, 1-PCPA or N-CαMBA were added to the final concentrations of 1 mM, 5 mM and 2 mM, respectively. More spectra were run periodically until no change was seen and the enzyme was less than 5% active. To 350 μL of inactivated enzyme was added 350 μL of saturated urea (11-12 M) for complete denaturation. Spectra were run periodically to check for reoxidation of the flavin.

2.6.5. Sulphydryl titration

Sulphydryl titrations of 1-PCPA- and N-CαMBA-inactivated MAO A and mutant MAO A C374A were performed to count the free cysteines. Aliquots (200 μL) of 28 μM MAO A or 20 μM MAO A C374A were added to 200 μL aliquots of a solution of 1-PCPA (final concentration of 0 or 5 mM) or N-CαMBA (final concentration of 0 or 2 mM) in Incubation Buffer and incubated overnight at room temperature. Aliquots were taken for enzyme activity and protein assays. Each enzyme solution was dialysed for 3 h against three changes (500 mL each) of Incubation Buffer and spun at 14000 g, 4°C for 10 min. Aliquots were taken for enzyme activity and protein assays.

The sulphydryl titrations were performed with DTNB (Sigma) that reacts with –SH groups with a change of absorbance at 412 nm (ε = 13600 $M^{-1}.cm^{-1}$, pH 7-8). A 100μL aliquot of inactivated MAO A or MAO A C374A was added to a solution of 480μL of distilled water with 200μL of 100mM KPi, pH 8. The reference cuvette contained the same solution but the Dialysis Buffer substituted the enzyme. After autozero against the reference cell, 20 μL of 4 mg/mL DTNB in 100 mM KPi, pH 8 were added to the reference cuvette and then to the enzyme solution. The reaction was followed at 412 nm until no change was observed. The number of free cysteines is $N_{cys} = C_{412nm} / C_{enz}$, where $C_{412nm} = Abs_{412nm} / \varepsilon$.

2.6.6. Identification of the cysteine modified by N-CαMBA

MAO A was inactivated with N-CαMBA and the adduct bound to a cysteine stabilised to be sent to the Harvard Microchemistry Institute for analysis. To 50 μL of 56 μM MAO A were added 200 μL of N-CαMBA (final concentration of 0 and 8 mM) in 50 mM Tris buffer, pH 8 and the mixture was incubated at room temperature in the dark. When inactivation was 95% compared with control, 250 μL of 0.2 M sodium borate buffer, pH 8, with 17 μL of sodium borohydride (1 mg / 10 μL) in 10 mM NaOH, were added to each enzyme solution. After a 2 h incubation at room temperature and in the dark, the enzyme was precipitated with 70 μL of 55% TCA on ice for 15 min. After centrifuging for 10 min at 10000 g and 0°C, the supernatant was discarded and the pellets dissolved in 10 μL of 1 M NaOH. Aliquots of 150 μL of 0.5 M Tris buffer, pH 6.8 were added to each solution. The resulting MAO A modified solution was run on 7.5% polyacrylamide-SDS gels in a BioRad electrophoresis mini-system, along with protein markers Mark 12® MW Stand (Invitrogen). Anything that was in contact with the gels was carefully rinsed with HPLC grade

water to minimize keratin contamination. After staining (commassie blue) and destaining, the gels were rinsed in HPLC grade water and the bands correspondent to MAO A were excised and put in eppendorf tubes. The bands were washed twice with 50% acetonitrile (HPLC grade) by inverting the tubes for 2-3 min. The excess of liquid was discarded and the gel bands stored at –20°C until they were sent to the Harvard Microchemistry Institute.

3. EXPRESSION AND PURIFICATION OF MAO AND ITS CYSTEINE MUTANTS IN *PICHIA PASTORIS*

MAO A and B cysteine mutants were constructed and constitutively expressed in *Pichia pastoris*. The expression levels were analysed by measuring MAO activity and by western blots. *Pichia pastoris* cells expressing MAO A and the single mutants MAO A C374A, MAO A C398A and double mutant MAO A C374A & C398A were grown by fermentation and the enzymes extracted and purified.

3.1. MAO Cloning and Expression in *Pichia pastoris*

MAO cDNA was obtained from Dr. P. Urban (CNRS, France) in the plasmid pYEDP60, a replicative vector for *Saccharomyces cerevisiae*. Apart from MAO A and B genes, a MAO B mutant gene was also available, where the cysteine 389 had been replaced by a serine (MAO B C389S). The goal of the cloning experiments was to transfer these MAO genes to the plasmid pGAPZ, a vector that enables constitutive expression of the recombinant protein in *Pichia pastoris* using the promoter GAP (*173*), and then construct other mutants of interest. The work was started in the Hannah Research Institute under the supervision of Dr. Nigel Price and continued in St. Andrews.

3.1.1. Sequencing results

MAO A and B and the mutant MAO B C389S were cloned into pGAPZa as described in Methods and Materials, chapter 2.1.2. To check the cloning techniques had been successful, especially the PCRs, the genes were sent to sequence.

MAO A was sequenced at the 5'-end (650 bp) and, after the removal of the 3' untranslated end, at the new 3'-end (650 bp). All was correct except a mutation that

translated a serine at position 3 instead of an asparagine. The base pairs responsible for this were located on the sense primer used for the PCR (Figure 2.1), indicating that the error was either originated by the oligos supplier company or during the PCR. To correct the error the same primer was re-ordered and used to repeat the PCR. The fragment with the mutation was then replaced by the new one and further sequencing revealed no errors.

MAO B and MAO B C389S sequences at the 5'-end (650 bp) had no errors. The 3'-end (800 bp) of the mutant was also sequenced to confirm the mutation. It was found that besides the expected mutation C389S the mutant had a mutation V489A located near the C-terminal. It was later found that this mutation came from the original MAO B gene, which was corrected as described in chapter 2.1.3.4.

All the PCR products on the construction of the mutants MAO A C374A, MAO A C398A, MAO A C374A & C398A, MAO B C365A, MAO B C389A and MAO B C365A & C389A (chapter 2.1.3) were sequenced, confirming the inclusion of the mutations and revealing no errors at the MAO genes.

3.1.2. Expression levels

The highest expression levels obtained from the clones of MAO A and B and the mutants are listed in Table 3.1.

In contrast to published reports (*111, 112*), the mutants MAO A C374A, the correspondent MAO B C365A and the MAO B C389A are active. In the published work, clones of MAO A C374S and MAO B C365S were inactive and the clone of MAO B C389S was partially active (*111*). MAO B cysteine 389 was also mutated to alanine and expressed in mammalian cells which resulted in complete loss of activity (*112*). The main difference in methods between the published work and the reported here is the expression system, mammalian in the previous and yeast in the latter.

There are other discrepancies on the MAO mutant expression systems. The MAO B cysteine 397 (flavin attachment site) was mutated to serine, alanine and histidine giving inactive clones expressed in mammalian cells (*111, 174*). However, when the mutant MAO A C406A (correspondent to MAO B C397) was expressed in *Saccharomyces cerevisiae*, the clone was fully active (*115, 116*).

The fact that the mutants were active showed that the MAO A cysteine 374 and the MAO B cysteines 365 and 389 were not essential for activity. In fact, the crystal structure of MAO B (*122*) showed that C365 and C389 are located on the surface of the protein.

The MAO A and B expression levels (Table 3.1) are very low compared with the 2-3 U/g_{yeast} obtained expressing MAO A inducibly in *Saccharomyces* and the very high expression levels obtained expressing MAO A and B inducibly in *Pichia* (*102, 175*). To obtain higher expression, more transformations were tried and also increasing zeocin concentrations up to 8 mg/mL were used. However, the clones that had their resistance to zeocin increased did not have higher MAO activity levels. As the system is constitutive, there probably is a limitation on the number of gene copies that the *Pichia* strain genome can take and also a limit on the quantity of enzyme that it can produce while growing. Although, there are examples of good expression of other enzymes using the GAP promoter (constitutive) compared with the AOX promoter (inducible), including membrane bound enzymes (*173, 176*), this was not found for MAO.

Nevertheless, even with low expression levels, it was possible to obtain good purified MAO A and MAO A C374A, which permitted the continuation of the project. Changing to the *Pichia* inducible system was not considered due to time constraints and the more complex apparatus required for optimal growth conditions.

Table 3.1. pGAPZa cloned MAO activity expression levels in *Pichia pastoris* SMD 1168 kex1::SUC2

MAO A	Expression (U/g_{yeast})*	MAO B	Expression (U/g_{yeast})*
Native	0.2	Native	0.3
C374A	0.2	C365A	0.07
C398A	0	C389A	0.4
C374A & C398A	0	C365A & C389A	0

*The definition of activity unit (U) is μmol/min using 1 mM kynuramine (MAO A) or 3 mM benzylamine (MAO B) as substrates.

3.1.3. Check of expression of inactive mutants

The mutant clones of MAO A C398A, MAO A C374A & C398A and MAO B C365A & C389A do not show any activity. This could be due to the mutations or to very low expression levels. To check the expression levels, western blots were run on the mutant samples using a commercial human MAO monoclonal antibody from mouse (Biogenesis). Each western blot was loaded with purified MAO A and cell lysates expressing MAO A as controls and cell lysates of clones expressing the inactive mutants.

Several dilutions, from 1:100,000 to 1:100, of the commercial monoclonal primary antibody were used but no bands appeared after 1h of exposure time to the development reagent. The same antibody was then used at a very low dilution of 1/5, but only non-specific binding was seen and there was no binding to purified MAO A (not shown).

As the commercially available MAO monoclonal antibody did not work in the western blots, it was decided to produce MAO polyclonal antibodies. The production and purification of polyclonal MAO A & MAO B and MAO A only antibodies is described in chapter 2.1.4.

3.1.3.1. Purification and characterization of MAO A and B antibodies

The antibodies against a peptide sequence specific to MAO A only (Ab A) and a peptide sequence common to both MAO A and B (Ab A&B) were raised in sheep using activated peptides (chapter 2.1.4.1). The same peptides were used to purify the antibodies by affinity chromatography (chapter 2.1.4.2). By loading the antiserum on the column, the specific antibodies against the peptide linked to the resin would bind while the other proteins were washed through. The specific

antibodies could later be eluted out of the column under low pH conditions, taking care to immediately neutralise the eluate to prevent denaturation. The protein content of the fractions was monitored by the absorbance at 280nm.

There were two bleeds taken from the sheep at the 10^{th} (1^{st} bleed) and 14^{th} (2^{nd} bleed) weeks after the first immunization. Each antiserum from the two bleeds could be run on two columns, one activated with the internal peptide to purify Ab A&B and the other with the N-terminal peptide to purify the Ab A. Figure 3.1 illustrates one of the four purifications performed.

The acid eluted fractions were run on 15% polyacrylamide-SDS gels to check the purification of the antibodies. The fractions with higher antibody content were pooled and stored. Figure 3.2 shows the gel photo with the fractions 42 to 51 of Figure 3.1. Fractions 45 and 46 were pooled together as they contain the purified specific antibody, seen by the bands at 50 and 25 kDa, correspondent to the heavy and light chains, respectively. The band at 68 kDa corresponds to albumin, a common contamination. The presence of albumin is actually beneficial, as it stabilises the antibody in solution and that is why BSA is added for storage (chapter 2.1.4.2).

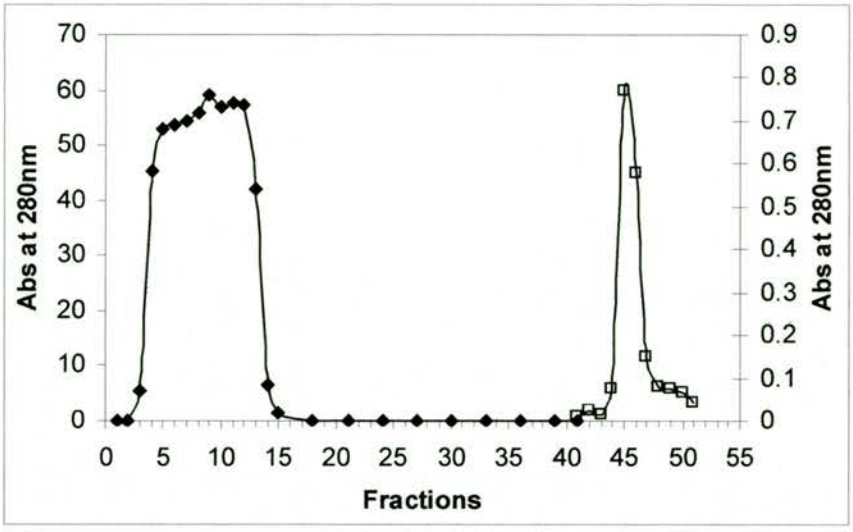

Figure 3.1. Affinity column chromatogram of antibody purification. (◆) Fractions 1 to 18 of 4mL each: MAO antiserum with high protein content passing through the column; fractions 19 to 41 of 8mL each: wash with 50mM Tris, 0.5M NaCl, 1mM EDTA, pH 7.5; (□) fractions 42 to 51 of 3mL each collected into 0.5mL 1M Tris: elution of the specific antibodies by 0.1M Glycine/HCl, pH 2.5.

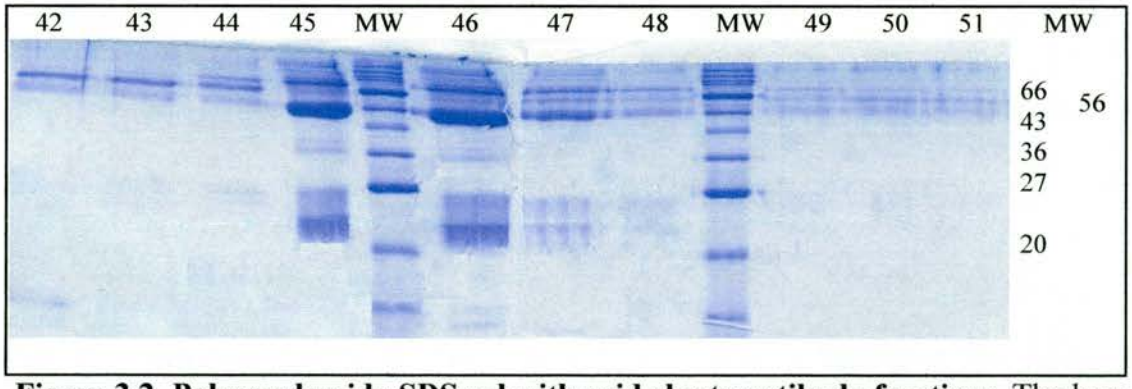

Figure 3.2. Polyacrylamide-SDS gel with acid eluate antibody fractions. The lane numbers correspond to the fraction numbers on Figure 3.1. MW: protein markers (kDa). The bands at the molecular weights of 68, 50 and 25kDa correspond to albumin and antibody heavy and light chains, respectively. The fractions pooled were 45 and 46.

After purification, the antibodies from 1st and 2nd bleeds were tested on purified MAO A and B. They were used with dilutions from 1/100 to 1/100,000 on western blots loaded with about 2 μg of purified enzyme. Figure 3.3 shows the test of Ab A and A&B from 2nd bleed on MAO A. Using the Ab A, a gradient of light purple bands, with increasing primary antibody concentrations, were observed at the MW of around 60kDa (MAO A MW is 59.7 kDa (*103*)) after an exposure time of 2 min (Figure 3.3.A). The same bands appeared using Ab A&B but in a much stronger colour and a more evident fade with increasing primary antibody dilutions (Figure 3.3.B). This shows that the Ab A&B has a stronger interaction with MAO A protein than the Ab A. At the lower dilution of Ab A&B two other bands appeared, at MW between 33 and 48 kDa (Figure 3.3.B, lane 1), which could be proteolytic products of MAO A at low concentrations, as they do not show with the higher primary antibody dilutions. This result shows that both antibodies work well with MAO A up to the highest dilution tested. When high specificity on purified MAO A is needed the Ab A (Figure 3.3.A) is the best to use as with the time of exposure of 2 min, no other bands were present at any dilution tested. Moreover, the Ab A did not recognize MAO B (not shown as membranes were blank).

The Ab A&B was also tested with MAO B at the same dilutions (Figure 3.4). Single bands of purple appeared at around 60 kDa (MAO B MW is 58.8 kDa (*104*)), the colour fading with increasing primary antibody dilutions, as expected. The antibody was very specific at all dilutions and with short exposure times.

The results with the antibodies from the 1st bleed were the same as described for the 2nd bleed.

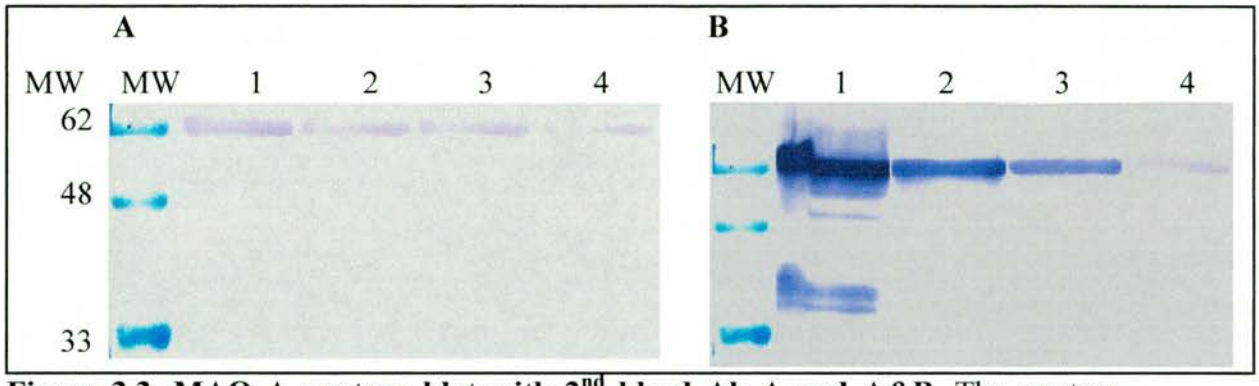

Figure 3.3. MAO A western blot with 2nd bleed Ab A and A&B. The western blots were performed as described in 2.1.4.3. ***A.*** MW: pre-stained protein markers (kDa); lanes 1-4: Ab A at the dilutions 1/100, 1/1,000, 1/10,000 and 1/100,000, respectively. The times of exposure of lane 1 was about 1min and of lanes 2, 3 and 4 were about 2 min. ***B.*** MW: pre-stained protein markers; lanes 1-4: Ab A&B at the dilutions as above. The times of exposure of lanes 1 and 2 were about 10 s and of lanes 3 and 4 were about 30 s.

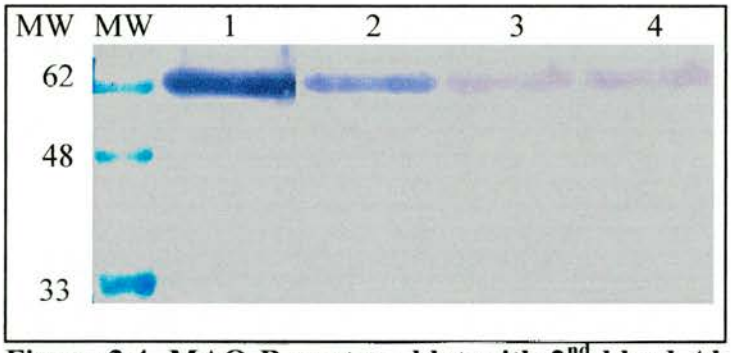

Figure 3.4. MAO B western blot with 2nd bleed Ab A&B. The western blot was performed as described in 2.1.4.3. MW: pre-stained protein markers (kDa); lanes 1-4: Ab A&B at the dilutions 1/100, 1/1,000, 1/10,000 and 1/100,000, respectively. The exposure times of lane 2 were about 10 s, lane 3 about 20 s and lanes 4 and 5 were about 1 min.

3.1.3.2. *Western blots on inactive mutants*

Using the purified anti-peptide antibodies, it was possible to perform western blots on the cell lysates of the inactive mutants. The cell lysates of the inactive clones MAO A C398A, MAO A C374A & C398A and MAO B C365A & C389A and the active clones MAO B C389A, MAO B C365A and MAO A (control) were prepared as described in chapter 2.1.1.9. The protein content and activity were checked for each, the only ones active being MAO A (0.18 U/g_{yeast}) and MAO B C389A (0.23 U/g_{yeast}). Some activity was also expected from the clone expressing MAO B C365A, which had previously shown an expression level of 0.07 U/g_{yeast} (Table 3.1). This was disappointing but not very surprising, as loss of activity of clones stored for a long time at –70°C had been experienced before.

Samples of 40 µg of protein from each clone cell lysate were used for the western blot with the Ab A&B at a dilution of 1/500. The MAO A C398A and MAO A C374A & C398A were also used with Ab A at a dilution of 1/100. The results are shown on Figure 3.5 and Figure 3.6. The band at about 60 kDa can be seen for MAO A (Figure 3.5, lane 1) and MAO B C389A (Figure 3.6, lane 1) as expected from the MAO activity results (Table 3.1). For the mutants that showed no activity, there are no distinguishable bands at 60 kDa (Figure 3.5 and Figure 3.6, lanes 2 and 3). However, there are two bands at the MW between 48 and 33 kDa, which are common for MAO A and B mutants and do not show for samples containing active enzyme. These bands, also detected in purified MAO A with Ab A&B at the lower dilution of 1/100 (Figure 3.3.B), could be MAO degradation products as they are recognised by both antibodies in the case of the MAO A mutants. This degradation could be the reason of the low expression levels obtained (Table 3.1). Apparently, the mutant clones that were inactive had unstable enzymes as they do not show the

whole protein but only the proteolytic products. This is more evident with the fact that the clone expressing MAO B C365A lost activity after storage for longer than 1 month, which was never recovered even after repeated transformations and fresh growth. Native MAO A and MAO B and other active mutant clones maintained their expression levels constant after storage for almost 2 years.

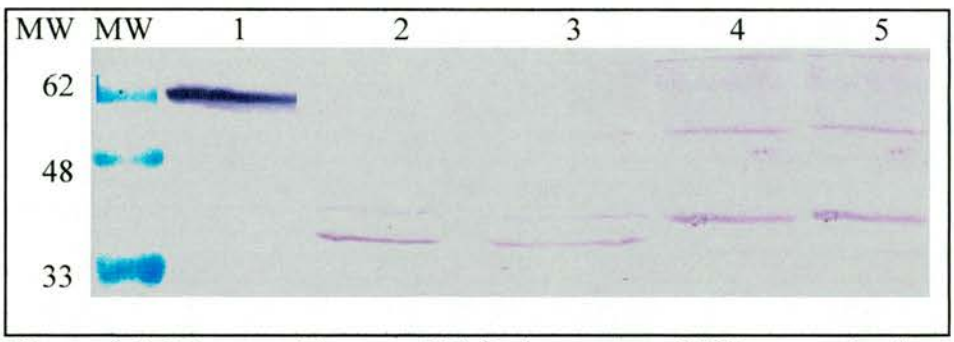

Figure 3.5. Western blots on MAO A mutants. MW: pre-stained markers (kDa); lanes 1-3: 40μg of protein from cell lysates of MAO A, MAO A C398A and MAO A C374A & C398A, respectively, with Ab A&B at 1/500; lanes 4 and 5: 40 μg cell lysates MAO A C398A and MAO A C374A & C398A, respectively, with Ab A at 1/100.

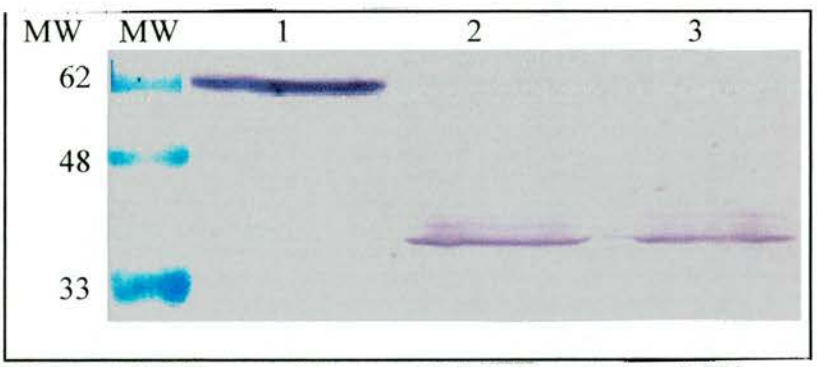

Figure 3.6. Western blots on MAO B mutants. MW: pre-stained markers (kDa); lanes 1-3: 40 μg of protein from cell lysates of MAO B C389A, MAO B C365A, MAO B C365A & C389A, respectively, with Ab A&B at 1/500.

3.2. Fermentation of *Pichia pastoris*

The first fermentations were done with the wild type strain X33 expressing MAO A. It started with a batch stage with glycerol and then upon depletion of this, the carbon source was changed to glucose in a fed-batch manner.

The wild type fermentations had high yield reaching an Abs_{600nm} of 96.5 (Figure 3.7). At 25 h the glycerol was exhausted and the glucose feeding was started at a rate of 1 mL/L/h. The growth was left overnight at a glucose feed rate of 2 mL/L/h and at 40 h was increased to 3 mL/L/h. There was no evidence of oxygen limiting the growth. The last 2 hours of fermentation the glucose feed rate was at 4 mL/L/h, obtaining 366 g of cell dry weight at harvest, which corresponded to a yield of 61 g_{yeast}/L.

The initial pH was 5.40, which dropped to below 5 at 19, 40 and 45 hours, when around 10 mL filtered sterilised ammonia was added.

Due to problems in the MAO purification (chapter 3.3), the *Pichia* strain was changed to the protease deficient SMD 1168 kex1::SUC2 (*168*). This strain was found to have a very slow growth in glycerol and starting the fermentation with glucose was considered. If glucose is in excess, yeast produces ethanol, which is harmful for the cells specially when high cell densities are reached. However, *Pichia*, with enough aeration supplied, prefers the oxidative metabolism (*176*) and for moderate cell densities the aeration supply available was found not to be limiting the growth. Moreover, for the constitutive system, glucose was found to give a better yield than glycerol (*176*). Hence, glucose could be used for all growth.

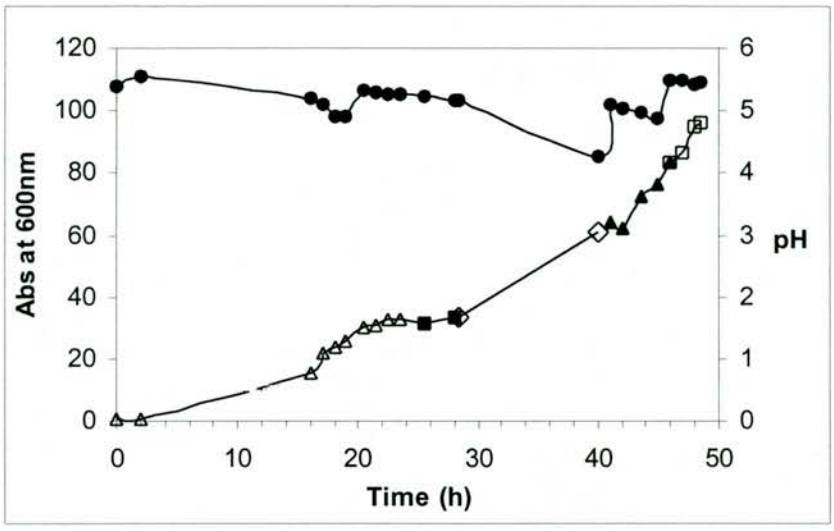

Figure 3.7. Fermentation of wild type *Pichia* expressing MAO A. Fermentation at 30°C using basal salts media. The batch phase with 1% glycerol (△) was followed by the fed-batch phase with additions of 40% glucose with 2 mL/L of trace salts at the feed rates of 1 mL/L/h (■), 2 mL/L/h (◇), 3mL/L/h (▲) and 4 mL/L/h (⊟). The pH (●) was maintained around 5 with additions of 10mL of 35% filter sterilized ammonia at 19, 40 and 45 h. The air supply was 6 L/min with the agitation at 400 rpm. The cells were harvested at an Abs_{600nm} of 96.5.

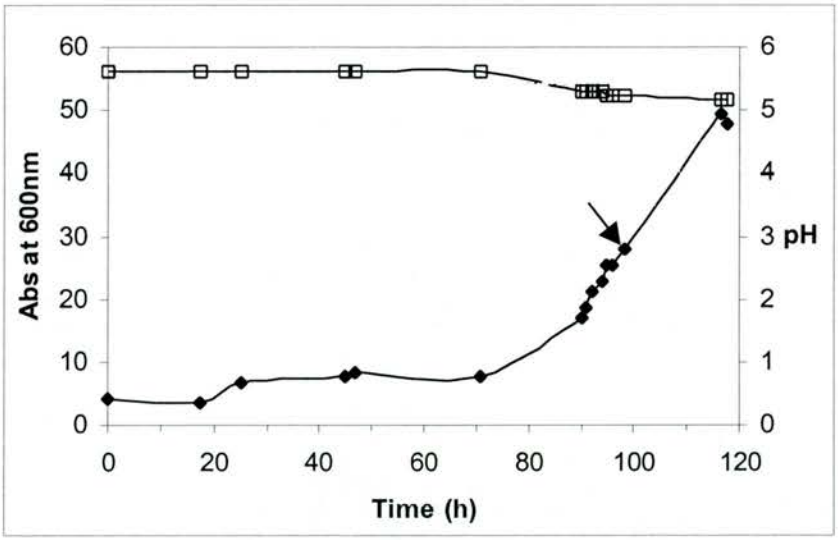

Figure 3.8. Fermentation of protease deficient *Pichia* expressing MAO A. The batch fermentation was at 30°C using basal salts media with 2% glucose and an addition of 100 mL 40% glucose with 2 mL/L trace salts at 98.5 h (marked by the arrow). The cells were harvested at an Abs_{600nm} (◆) of 48. The pH (⊟) did not decrease below 5. The air supply was 6 L/min with the agitation at 400 rpm.

Pichia fermentation starting with 2% glucose was performed to express MAO A. The pH and growth were monitored as shown in Figure 3.8. There was a very long lag phase that lasted over 70 hours. The rapid growth after that was accompanied by a decrease of the pH. An extra batch addition of glucose almost doubled the Abs_{600nm} in less than 20 hours. The harvested cells (276 g dry weight) corresponded to a yield of 27.6 g_{yeast}/L.

The long lag phase was suppressed by the addition of yeast extract and peptone to the original media (Figure 3.9). Four extra additions of glucose were made but only the first had a strong effect on the Abs_{600nm}. The final yield of cells was 31 g_{yeast}/L.

With the information gathered from these fermentations, it was possible to standardise the *Pichia* fermentation for this laboratory (see chapter 2.2.2). The original media consists of basal salts media, yeast extract, peptone and glucose. In about 24h the stationary phase is reached at an Abs_{600nm} of about 30 and a batch addition of glucose is made. The cells are harvested after another 24 h when the Abs_{600nm} is 45-50. The pH starts at about 5.5 and does not decrease to below 4.5. The yield would be about 30 g_{yeast}/L and the expression level of MAO A 0.2 U/g_{yeast}. Figure 3.10 shows a standard *Pichia* fermentation.

The protease deficient *Pichia* fermentation was later further improved by increasing the pH from 5 to 6.5. After 48h of fermentation the Abs_{600nm} reached 70 yielding 55 g_{yeast}/L in contrast to 30 g_{yeast}/L obtained before. The enzyme yield was still 0.2 U/g_{yeast}.

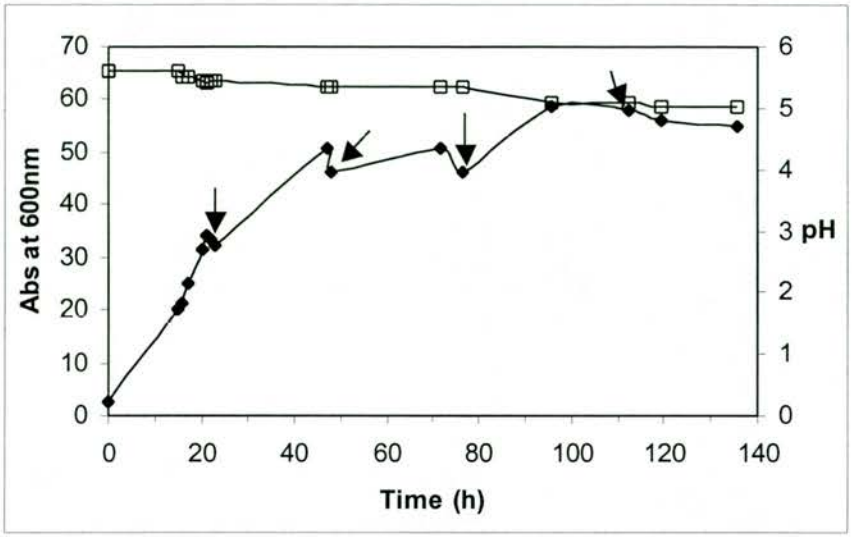

Figure 3.9. Yeast extract and peptone suppress the lag in fermentation of protease deficient *Pichia* expressing MAO A C374A. The batch fermentation was at 30°C using basal salts media plus 0.5% yeast extract and 1% peptone with 2% glucose. Additions of 40% glucose with 2 mL/L trace salts: 500 mL at 23 h, 200 mL at 48h, 500 mL at 76.5 h and 500 mL at 119.5 h (marked by the arrows). The cells were harvested at an Abs_{600nm} (◆) of 55. The pH (⊟) did not decrease below 5. The air supply was 6 L/min with the agitation at 400 rpm.

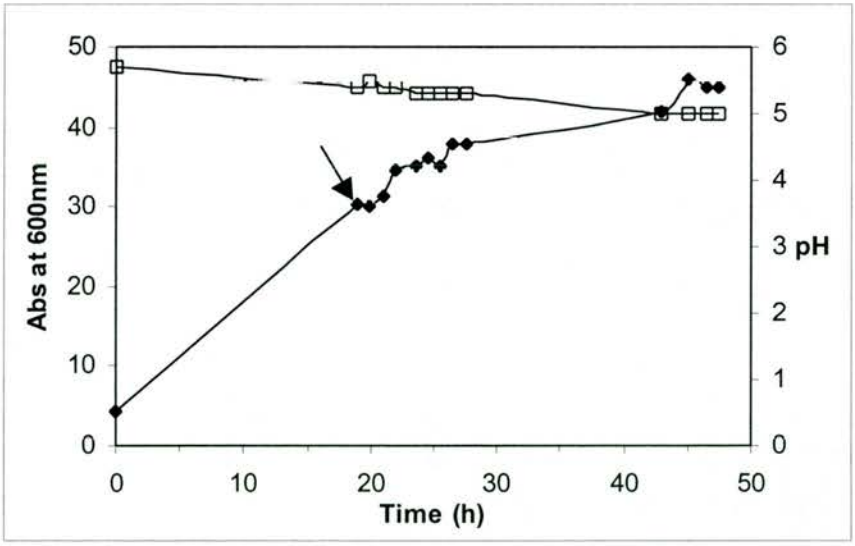

Figure 3.10. Standard fermentation of protease deficient *Pichia* expressing MAO A. The batch fermentation was at 30°C using basal salts media plus 0.5% yeast extract and 1% peptone with 2% glucose. 500 mL of 40% glucose with 2 mL/L trace salts were added at 20 h (marked by the arrow). The cells were harvested at an Abs_{600nm} (◆) of 45. The pH (⊟) did not decrease below 5. The air supply was 6-14 L/min with the agitation at 400-600 rpm.

3.3. Purification of MAO

The purification procedure of human liver MAO A expressed in *Saccharomyces cerevisiae* is described in (*48, 171*). This procedure was optimised for MAO expressed in *Pichia*. The major problems were on the cell breakage and on the critical extraction steps, especially the phospholipase one, which are very dependent on the protein determination.

Several small scale cell breakage methods were tried in an attempt to improve the yield of this step (Table 3.2). The best results were obtained with the cell disrupter at a high pressure of 40 kpsi. However, when 200-300 g of yeast cells were used, the cell breakage yield would go back down to 0.05 U/g_{yeast}. The only method found to be reproducible at large scale was the vortexing with glass beads with a yield of around 0.2 U/g_{yeast}.

To improve the enzyme recovery during the phospholipase extraction step, the mitochondrial membrane suspension was split in four and 0.2, 0.5, 1 and 2 times the usual amount of phospholipase A (PLA) (408816 U/L) were added. Table 3.3 summarizes the results and shows that 0.2 times the usual PLA amount gave the best recovery, but that the normal amount gave the best specific activity.

Another option was to change the usual amount of phospholipase C (PLC) of 100 mg/L and/or the usual protein concentration of 25 mg/mL. The conditions tried in a MAO B purification were half the usual amount of PLC, half both the PLC and the protein concentration and half the protein concentration (Table 3.4). The best activity recovery and specific activity were obtained diluting the protein content of the mitochondrial membrane suspension to 12.5 mg/mL without changing the PLC amount. The suspensions were kept separated for the next step, the Triton extraction. The condition 12.5 mg/mL protein was still the best as it resulted in the highest

specific activity of 110 mU/mg_{prot} and the least turbid suspension (*i.e.* less lipid content) in the spin after the Triton extraction.

The difference in specific activity values between the MAO A (Table 3.3) and MAO B (Table 3.4) is a factor of 10. This was due to the higher expression level for MAO B and good cell breakage yielding 0.7 U/g_{yeast} but also because the *Pichia* strain had been changed from the wild type (Table 3.3) to the protease deficient one for the purification of MAO B (Table 3.4).

To summarize, the changes made in order to improve the MAO purification procedure were: (a) the *Pichia* strain used was protease deficient; (b) the cell breakage was done using vortex with glass beads; (c) the phospholipase extraction step was done with a protein content of 12.5 mg/mL as determined by the BCA method.

Table 3.2. MAO A activity yield of small scale cell breakage step.

Cell breakage method	Yield (U/g_{yeast})
Glass beads and vortex	0.2
Glass beads in Braun homogeniser	0.05
Ultrasonication probe	0.02
Cell disrupter at 40kpsi	0.3

Table 3.3. PLA digestion of MAO A mitochondrial membranes.

Fraction of usual amount of PLA	Protein conc.* (mg/mL)	Specific act. ($mU/mg_{prot.}$)	Activity recovery (%)
0.2	93.3	2.9	86.2
0.5	44.2	2.9	77.2
1	38.5	4.5	78.0
2	52.6	3.4	76.4

*The protein concentration was determined with the BCA method.

Table 3.4. PLC digestion of MAO B mitochondrial membranes.

Condition	Protein conc.* (mg/mL)	Specific act. ($mU/mg_{prot.}$)	Activity recovery (%)
½ PLC	34.0	52	66
½ PLC & ½ protein	36.9	39	53
½ protein	35.7	66	78

*The protein concentration was determined with the BCA method.

3.3.1. MAO A and MAO A C374A

Table 3.5 and Table 3.6 show the purification results of MAO A and MAO A C374A, respectively. The low expression levels lead to the use of very high quantities of starting material, about 500 g of cells, which in practice is very cumbersome, especially in the breakage and ultracentrifuge steps. In both purifications, the activity yield of 100% was considered to be at the second step (when the membranes were harvested by high speed centrifugation) where the highest activity was detected. The high cell quantity yields high quantities of protein and leads to very turbid solutions. Even as diluted as much as the detection limit permits, the turbidity of these solutions interferes with the accuracy of the spectrophotometric activity assay, especially on the first step (low speed centrifugation). The yield of extracted enzyme was estimated to be about 0.2 U/g_{yeast}, as expected from the expression level tests.

In both purification procedures the Triton extraction step was repeated due to very low activity yield on the first one. The second Triton extraction was successful, especially on the MAO A purification giving an overall step yield close to 100%.

Figure 3.11 shows the elution profile for the DEAE column in MAO A C374A purification. MAO elutes from the column during the second half of the gradient. The first fractions are contaminated with heme protein as seen by the ratio of absorbance 450/280 profile and so they were pooled separately. The purest fractions (gradient 165-195 mM) were pooled together as the final main fraction. The side fractions (gradient 130-165 mM and 195-205 mM) were pooled together as the final lead fraction.

Table 3.5. Purification of MAO A

Step	Solution	Volume (mL)	Activity (Total U)	Protein (mg/mL)	Specific activity (mU/mg_{prot})	Step yield (%)	Activity yield (%)
Cell breakage	LSS	1040	90	20.9	4.1		
Mitochondria	HSS	890	1.1	14.8	0.1		
Separation	HSP	190	101.2	41	13	100	100
Phospholipase	PLS	585	0	4.7	-		
Extraction	PLP	178	82.6	33.9	14	81.6	81.6
1st Triton	TXP_1	182	44.9	28.2	9		
extraction	TXS_1	262	44	5	34	53.2	43.5
2nd Triton	TXP_2	140	0	31.3	-		
extraction	TXS_2	270	33.4	3.7	34	75.9	33
Total Triton ext.	TXS_T	532	77.4	4.3	34	93.7	76.5
Chromatography	Lead	1.1	2.2	26.9	70		
and concentration	Main	5.8	66.2	40	290		
Total at end			68.2				67.6

The purification of MAO A was done as described in chapter 2.3. The starting material was 460 g_{yeast}. The protein was measured by the BCA and Peterson-Lowry methods. The definition of activity unit (U) is μmol(product)/min using 1 mM kynuramine (Sigma) as substrate measured at 314 nm. Abbreviations: LSS- low speed supernatant; HSS and HSP- high speed supernatant and pellet; PLS and PLP- phospholipase extraction centrifuge supernatant and pellet; TXS and TXP- Triton extraction centrifuge supernatant and pellet; Lead and Main solutions are the column eluent fractions concentrated separately.

Table 3.6. Purification of MAO A C374A

Step	Solution	Volume (mL)	Activity (Total U)	Protein (mg/mL)	Specific activity (mU/mg_{prot})	Step yield (%)	Activity yield (%)
Cell breakage	LSS	975	109	17.9	6		
Mitochondria	HSS	855	3.6	13.3	0.3		
Separation	HSP	178	111.9	41.5	15	100	100
Phospholipase	PLS	650	0	3.4	-		
Extraction	PLP	182	111	23.9	26	99	99
1st Triton	TXP_1	136	58	23.3	15.9		
extraction	TXS_1	250	50	2.3	100	45	44.7
2nd Triton	TXP_2	146	25	21.7	7.8		
extraction	TXS_2	184	23	3.8	30	20	20.6
Total Triton ext.	TXS_T	434	73	2.9	58	65.8	65.2
Chromatography	Lead	5.0	18.3	11.9	310		
and concentration	Main	4.2	25.2	15.1	400		
Total at end			43.5				38.9

The purification of MAO A C374A was done as described in chapter 2.3. The starting material was 550 g_{yeast}. The protein was measured by the BCA and Peterson-Lowry methods. The definition of activity unit (U) is μmol(product)/min using 1 mM kynuramine (Sigma) as substrate measured at 314 nm. Abbreviations are as in Table 3.5.

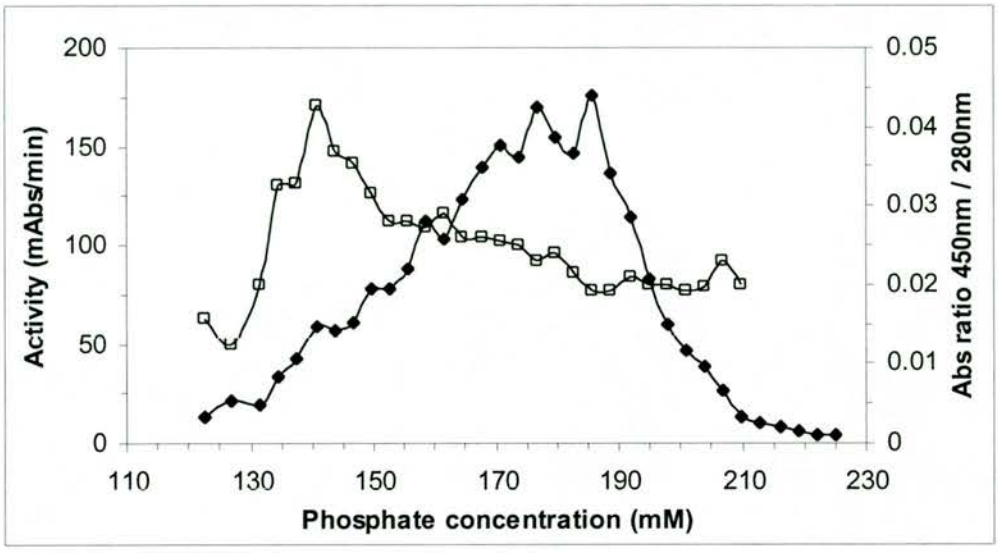

Figure 3.11. Chromatogram of MAO A C374A purification. The MAO A C374A was eluted from a DEAE sepharose column by a linear gradient of phosphate buffer from 20 mM to 225 mM at a flow rate of 1 mL/min (see chapter 2.3). The collection of the fractions (11mL) was started halfway the gradient, at a phosphate concentration of 122 mM. The lines show the activity of MAO using 1 mM kynuramine (◆) and the ratio of the absorbance at 450 nm and 280 nm (⊟). The pooled final main fraction corresponded to the gradient 165-195 mM. The pooled final lead fraction corresponded to the gradient 130-165 mM and 195-205 mM.

After concentration of the pooled fractions, the amount of total and active enzyme was determined from the spectrum of the bound flavin, by taking the ratio of the absorbance difference at 456 nm between the oxidised state (Figure 3.12, line 1) and the substrate-reduced state in the presence of kynuramine (Figure 3.12, line 2), and the absorbance difference between the oxidised state and the totally reduced state in the presence of dithionite (Figure 3.12, line 3). Table 3.7 shows the results calculated from the spectra in Figure 3.12.

To assess the final purity, aliquots of the concentrated pools were run on 10% polyacrylamide SDS-gels. Figure 3.13 shows 3 dilutions of the final lead and main fractions of the purified MAO C374A. Both fractions are estimated to be around 90% pure.

Table 3.7. Percentage of estimated active enzyme*

	MAO A		MAO A C374A	
Fraction	Lead	Main	Lead	Main
% active	84	92	86.4	86.7

*The percentage of active enzyme was calculated as the difference of absorbance at 456 nm upon reduction with kynuramine divided by the total difference of absorbance upon reduction with dithionite and multiplied by 100.

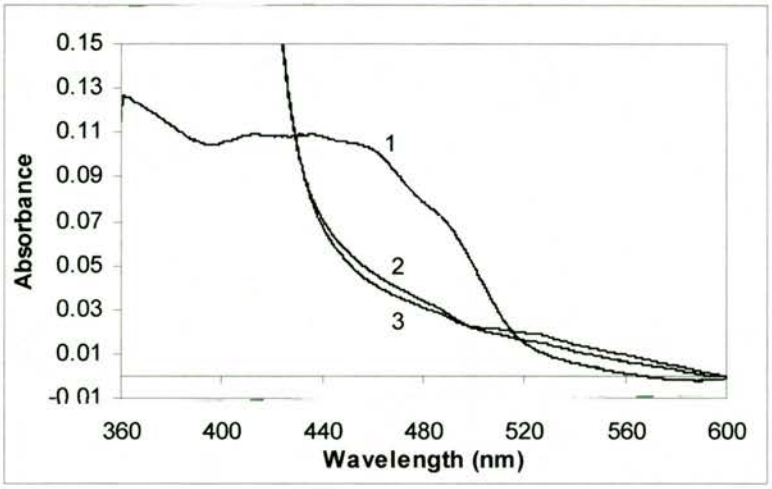

Figure 3.12. Reduction of the flavin of MAO A by substrate followed by dithionite. Anaerobic oxidised MAO A (1) was reduced by excess of kynuramine (2) and then completely reduced by addition of few crystals of sodium dithionite (3). MAO A C374A gave similar spectra.

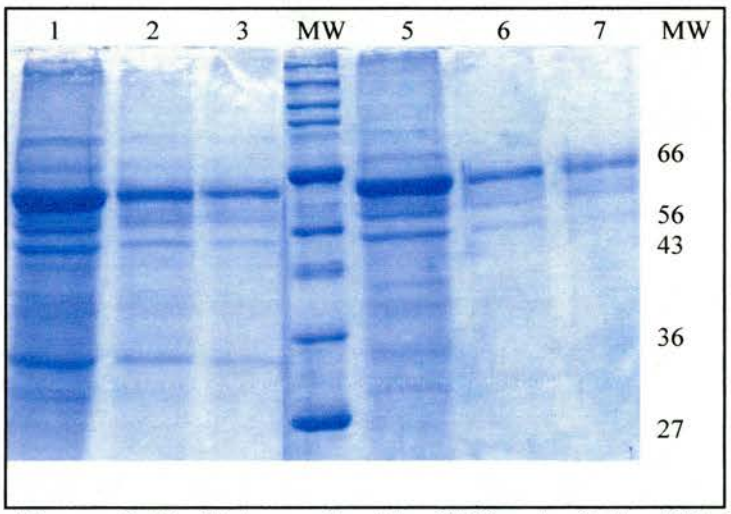

Figure 3.13. Polyacrylamide SDS-gel of the MAO A C374A main and lead fractions. Lanes 1 to 3 – 5, 1 and 0.5 μg of lead fraction; MW - protein markers; lanes 5 to 7 – 5, 1 and 0.5 μg of main fraction.

3.3.2. MAO A C398A and MAO A C374A & C398A

The inactive mutants MAO A C398A and MAO A C374A & C398A were purified based on what was previously done for MAO A and MAO A C374A (chapter 3.3.1). The final products were inactive but the spectra had absorbance at 400-500 nm region consistent with incorporation of the flavin (not shown). Although it was not detected on cell lysates (Figure 3.5), the western blots on the purified enzymes showed the MAO characteristic band at 60 kDa (Figure 3.14). Thus, although the clones were expressing the mutants, the enzymes were very sensitive to proteolysis as seen on the western blots with the cell lysates.

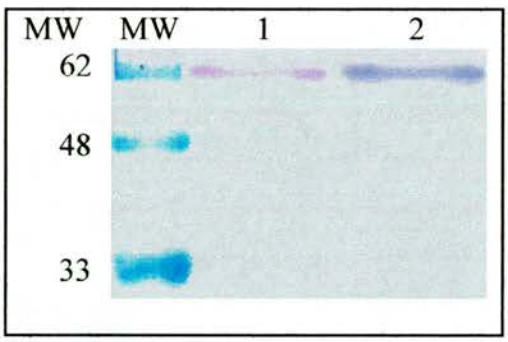

Figure 3.14. Western blots on purified MAO A C398A and MAO A C374A & C398A. Lane 1: pre-stained protein markers; lane 2 and 3: 10μg of purified MAO A C398A and MAO A C374A & C398A, respectively, with Ab A&B at a dilution of 1/1,000.

4. CHARACTERISATION OF MAO A AND THE MUTANT MAO A C374A AND COMPARISON OF THEIR PROPERTIES

Once MAO A and the mutant MAO A C374A were extracted and purified, it was possible to characterise the enzymes and look for differences in their redox, kinetic and mechanism-based inactivation properties due to the mutation of the cysteine.

4.1. Redox Properties

4.1.1. Reductive titrations with dithionite

Several reductive titrations of MAO A and MAO A C374A by dithionite were performed to assess any differences between them, particularly in the stabilisation of the semiquinone. If the cysteines and the flavin exchange electrons (*100*), changes in the redox behaviour would be expected with the mutation. The anaerobic titrations are shown in Figure 4.1 and Figure 4.2.

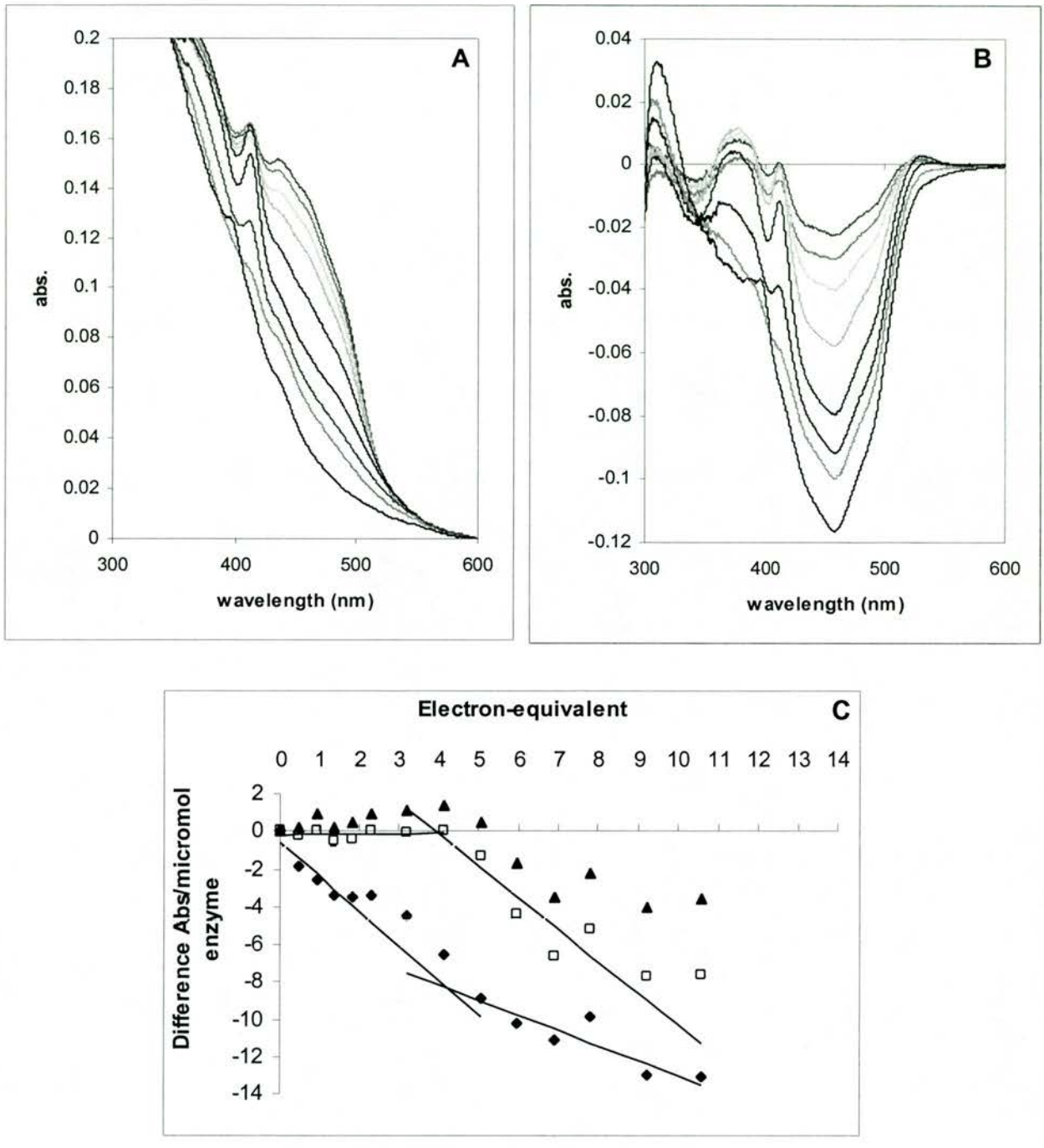

Figure 4.1. Anaerobic titrations on MAO A. ***A.*** Selected spectra recorded during reduction of 10.8 μM of enzyme with 1.03 mM dithionite. ***B.*** Selected difference spectra of reduced minus oxidised states. ***C.*** Difference of absorbances at 377 (▲), 412 (□) and 456 nm (◆) per μmol of enzyme against the number of electron-equivalents added. The lines represent the 2 phases of reduction (see text).

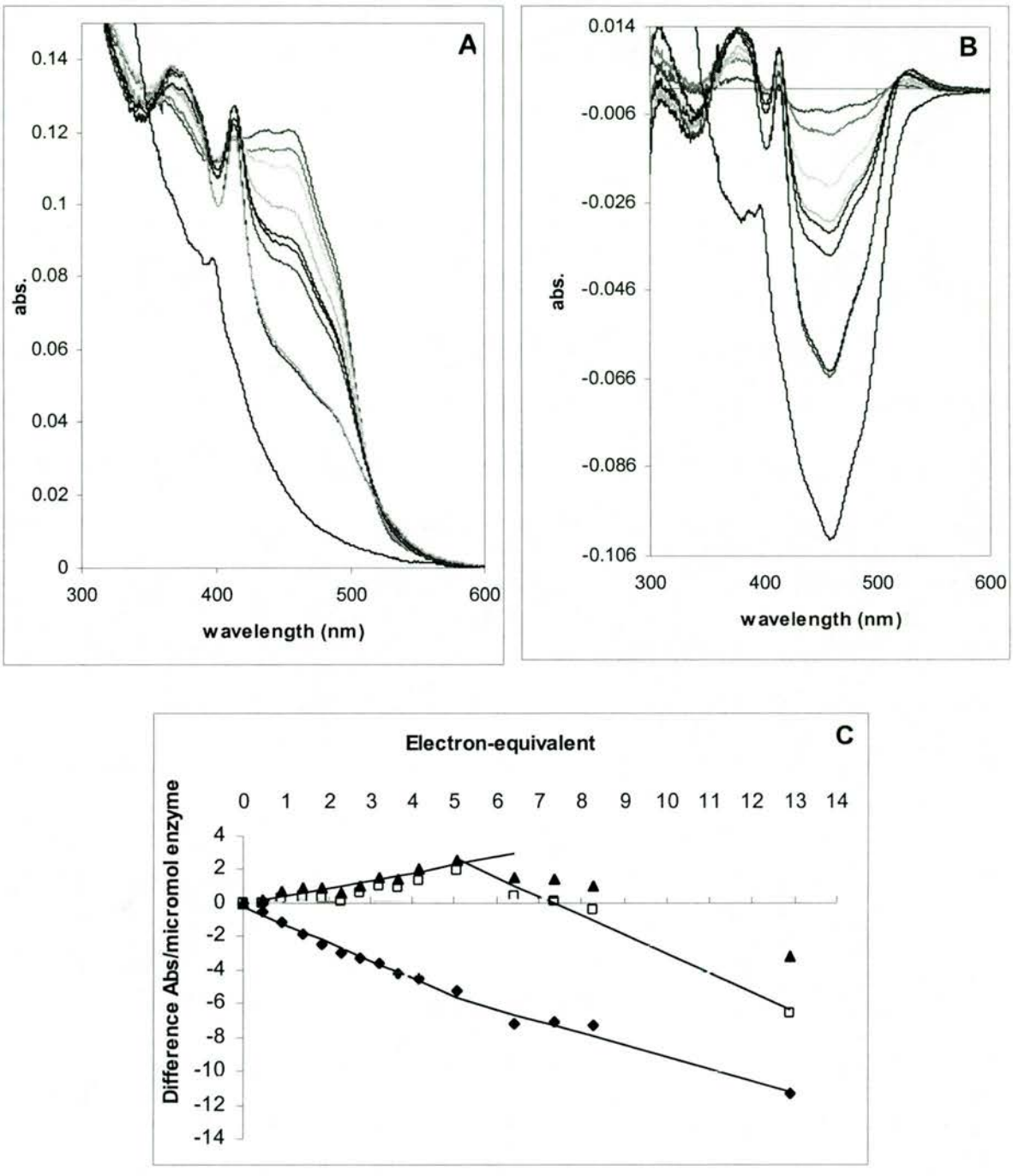

Figure 4.2. Anaerobic titrations on MAO A C374A. ***A.*** Selected spectra recorded during reduction of 9.4 μM of enzyme with 1.01 mM dithionite. ***B.*** Selected difference spectra of reduced minus oxidised states. ***C.*** Difference of absorbances at 377 (▲), 412 (□) and 456 nm (◆) per μmol of enzyme against the number of clectron-equivalents added. The lines represent the 2 phases of reduction (see text).

For both MAO A and MAO A C374A the formation of the semiquinone is observed at 412 nm (Figure 4.1.A. and Figure 4.2.A.). In the difference spectra (Figure 4.1.B. and Figure 4.2.B.) the main reduction effects (bleaching) are visible at 377, 412 and 456nm. The plots of the difference absorbance per μmol of enzyme against the electron-equivalent of dithionite added are shown in Figure 4.1.C. and Figure 4.2.C. In contrast to the 4-phase reduction previously reported (*100*), only 2 phases can be seen at 456 nm: (i) formation of the semiquinone using 5-6 electron-equivalents along with the reduction of the flavin; and (ii) disappearance of the semiquinone along with the total reduction of the flavin. However, the fact that the changes at 377 and 456 nm are not synchronised suggest complex steps in the reduction. Another unexpected feature is the need of much higher number of electron-equivalents than four for full reduction of the enzyme. This could be due to oxygen leak although all the precautions were made, including the addition of glucose and glucose oxidase / catalase mixture to consume any residual oxygen. Another possibility could be difficulty of reaching the equilibrium between the enzyme and dithionite, even though an electron-mediator (methyl viologen) was present in the reaction mixture. Further evidence of lack of equilibrium is presented below (chapter 4.1.2). Dithionite reduction of human liver MAO A inducibly expressed in *Pichia* required only two electron-equivalents for full reduction, with 50% yield of semiquinone at one electron-equivalent (*102*).

Nevertheless, the reductive titrations show no significant difference between MAO A and MAO A C374A in the extinction coefficient of any of the three wavelengths.

4.1.2. Redox potential

The redox potential is a highly sensitive probe of the active site alterations affecting the mechanism. Several attempts were made to determine the redox potentials of the two phases of the MAO A and MAO A C374A reduction.

The redox potentials for MAO A and MAO A C374A were estimated for the formation of the semiquinone. Figure 4.3 shows the reduction of both the enzyme and the reference dye by dithionite (bleaching at 456 nm and 610 nm, respectively) with the formation of the semiquinone (increase at 412 nm). The redox potential for FAD_{ox} / FAD_{sq} redox couple is determined from the double logarithmic plot (Figure 4.4). The difference between the potential for the enzyme and the potential for the reference dye, indigo disulphonate (-137 mV), was calculated by using the modified Nernst equation:

$\ln([E_{ox}]/[E_r]) = -E_m\left(N_e \frac{F}{RT}\right) + \frac{N_e}{N_d}\ln([D_{ox}]/[D_r])$, where E_{ox} and E_r are the oxidised and reduced forms of the enzyme; D_{ox} and D_r are the oxidised and reduced forms of the dye; and N_e and N_d are the number of electrons transferred onto the enzyme and the dye, respectively. The concentrations of the oxidised FAD and semiquinone $FAD^{\bullet}$ of MAO were calculated from the absorbance changes at the isosbestic points of the indigo disulphonate at 457 nm. The concentrations of the reduced and oxidised dye were calculated from the absorbance of the indigo disulphonate at 610 nm.

From Figure 4.3 and Figure 4.4 it was possible to estimate the midpoint potential for the formation of the semiquinone for MAO A. The same was done for MAO A C374A and the values are compared in Table 4.1. The MAO A and MAO A C374A midpoint potentials for the FAD_{ox} / FAD_{sq} redox couple obtained were similar, but the calculations may be compromised by the incomplete yield of the

semiquinone. When taking the total observed absorbance change at 456 nm, the slope given is probably higher than the real value, as the yield of the semiquinone does not reach 100% (Figure 4.3) and the same semiquinone starts going to fully reduced. However, the potential value obtained for the native enzyme is close to the one previously published of –159 mV (*97*). Furthermore, the number of electron-equivalents for the formation of the semiquinone obtained were close to 1 (Table 4.1), which corroborates what was found for the inducibly expressed MAO A in *Pichia* (*102*) and is consistent with the fact that no other putative electron acceptor group was found in the active site of MAO B (*122*).

It was not possible to reproduce these results due to difficulties in reaching the equilibrium between the enzyme and the dye and to oxygen leak and/or dithionite instability, even though methyl viologen (that facilitates the rate of electron transfer) and glucose oxidase / catalase (that consumes residual oxygen) were present in the mixture. The titrations were also tried with the xanthine and xanthine oxidase reductive system but with no improvement.

After addition of dithionite the dye was the first to receive the electrons as its absorbance decreased quickly. With time the enzyme was reduced, while the dye absorbance was partially increased. This observation suggests that the equilibrium in the system is very slow and explains the number of electrons greater than 1 (Table 4.1) and presumably the published data (*100*).

The mathematical significance could not be determined but the small difference in the midpoint potentials between MAO A and MAO A C374A, might be important as there were other kinetic small differences found between the enzymes (chapters 4.2 and 4.3).

The midpoint potentials for FAD_{sq} / FAD_{red} were not determined because after the long time necessary to reduce the first redox couple, the enzyme stability in solution decreased and the turbidity affected the spectra.

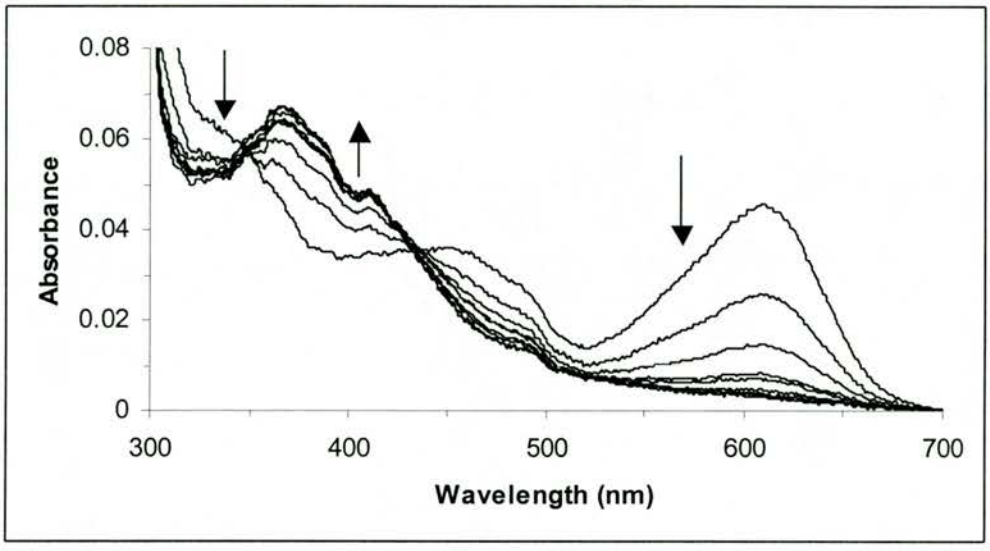

Figure 4.3. Spectra for the reduction of MAO A flavin in the presence of indigo disulphonate. The enzyme (7.7 μM) and the dye (5.1 μM) were incubated under anaerobic conditions at room temperature in 50 mM KPi, pH 7.2, 0.1% Brij-35 and 20 mM glucose and 5 μL glucose oxidase/catalase mixture (chapter 2.4.1). 2 μL aliquots of 0.63 mM dithionite were added and the spectra were run 30 min after each addition. The arrows indicate the direction of the changes of absorbance.

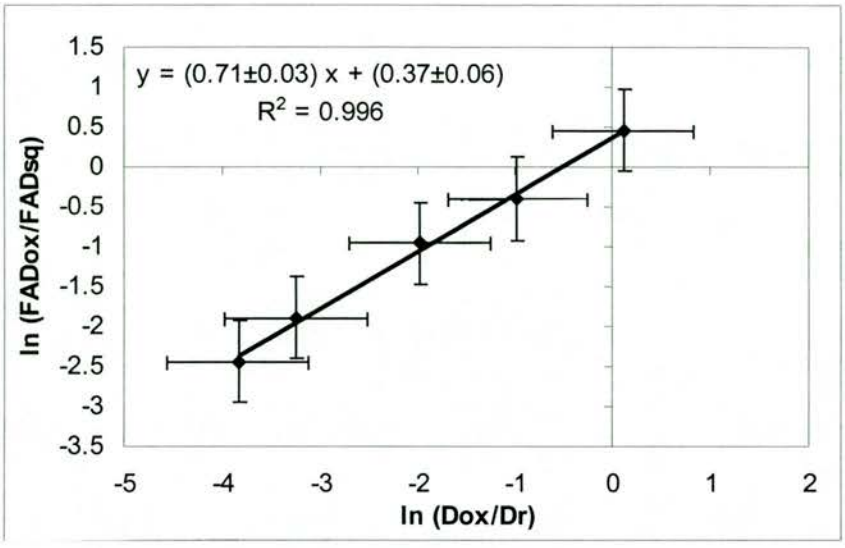

Figure 4.4. Determination of the MAO A redox potential for the FAD_{ox} / FAD_{sq} redox couple. The data were taken from Figure 4.3. Applying the Nernst equation, the N_e = slope × 2 and ΔE_m = - intercept / N_e × RT/F.

Table 4.1. Midpoint potentials for FAD_{ox} / FAD_{sq} in MAO A and MAO A C374A.

Enzyme	No. electrons	Redox potential (mV)
MAO A	1.4	-144
MAO A C374A	1.3	-125

4.2. Steady-State Kinetics

4.2.1. Substrates

Table 4.2 compares the kinetic behaviour of MAO A and MAO A C374A based on the Michaelis constant (K_m), the catalytic rate (k_{cat}), and the specificity constant (k_{cat}/K_m), for a series of substrates. The k_{cat} is defined as μmol(product) per μmol(flavin) per second and was calculated based on the concentration of active enzyme.

MAO A and the mutant MAO A C374A show small kinetic differences towards substrates. The substrates K_m values are increased for the mutant except for PEA. The specificity constant k_{cat}/K_m of the substrates decreases for the mutant except with MPTP where there is no change. In fact, the plot of the specificity constant for the mutant against that for the native (Figure 4.5) showed a correlation coefficient of 0.993 and a slope of 0.7, revealing a trend that the mutant had lower specificity constant (k_{cat}/K_m) than the native enzyme.

Theories of enzyme catalysis (*177*) suggest that many enzymes use binding energy to optimise k_{cat} rather than to decrease K_m below the level encountered in the cell. This is achieved by stabilization of the transition state. The differences in activation energies ($\Delta\Delta G^{\ddagger}$) for amine oxidation by the native and the mutant were analysed for the five substrates in Table 4.2. The values of $\Delta\Delta G^{\ddagger}$ ranging from 0 (no change in k_{cat}/K_m) to +1.34 kJ.mol^{-1} are relatively small differences but reflect the trend of the decrease in specificity constant for the mutant. It seems that this mutation does influence the catalytic process in the active site.

Table 4.2. MAO A and MAO A C374A steady-state parameters for substrates[1]

	K_m (mM)		k_{cat} (s^{-1})		k_{cat}/K_m ($s^{-1}.mM^{-1}$)		$\Delta\Delta G^{\ddagger}$ [2]
Substrates	MAO A	MAO A C374A	MAO A	MAO A C374A	MAO A	MAO A C374A	($kJ.mol^{-1}$)
MPTP	0.033±0.002	0.039±0.001	0.241±0.002	0.29±0.01	7.4±0.5	7.4±0.3	0
PEA	0.49±0.03	0.44±0.02	3.1±0.2	2.5±0.2	6.3±0.6	5.5±0.6	+0.34
Serotonin	0.43±0.01	0.51±0.04	18.6±0.5	16±1	44±4	31±3	+0.88
Kynuramine[3]	0.10±0.01	0.17±0.01	2.16±0.06	2.51±0.05	22±2	15±1	+0.96
Benzylamine[3]	0.42±0.02	0.61±0.01	0.09±0.01	0.079	0.22±0.02	0.129±0.003	+1.34

(1) The values are presented as the mean ± standard errors of three to five determinations. (2) $\Delta\Delta G^{\ddagger} = -RT\ln[(k_{cat}/K_m)_{mutant}/(k_{cat}/K_m)_{wild\text{-}type}]$ (*178*). (3) K_m and k_{cat}/K_m are significantly different at a 95% degree of confidence in a t-test.

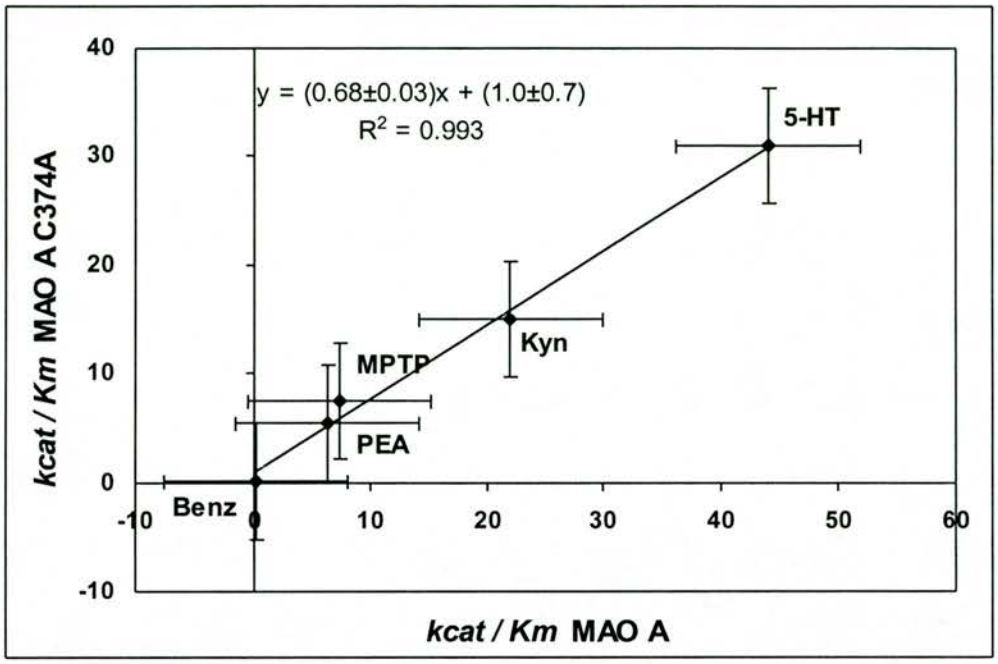

Figure 4.5. Kinetic differences between MAO A and the mutant MAO A C374A in the specificity constant for benzylamine (Benz), PEA, MPTP, kynuramine (Kyn) and serotonin (5-HT). The values were taken from Table 4.2.

4.2.2. Inhibitors

Although some significant differences are seen in the K_m alone, it must be remembered that the K_m for MAO A contains rate constants also. Competitive inhibitor constants estimate binding constants but even they are not simple constants because amphetamine and MPP^+ bind both to the oxidised and the reduced form of the enzyme (*63, 134*). The K_i values for three structurally different competitive inhibitors, D-amphetamine, MPP^+ and harman were determined. Inspection of Table 4.3 shows minor differences in the K_i values indicating that the influence of the mutation on the active site does not strongly affect the binding. Rather it is likely that the chemical steps in the catalysis are altered as reflected in the activation energy changes in Table 4.2.

Table 4.3. MAO A and MAO A C374A competitive inhibitor constants*

	K_i (μM)	
Inhibitors	**MAO A**	**MAO A C374A**
D-amphetamine	15±2	12±2
MPP^+	3.5±0.3	5±1
Harman	0.13±0.03	0.13±0.04

* The values ± standard errors were obtained from the best fit of $(Km/Vmax)_{app}$ vs. [I] with two times 7 inhibitor concentrations.

4.3. Mechanism-Based Inactivation by Cyclopropylamines

I visited Prof. Silverman's lab, in the Northwestern University, Evanston, USA, to start a study on a series of mechanism-based inactivators of MAO, the cyclopropylamines, to assess differences between MAO A and the mutant MAO A C374A. The compounds chosen were *N*-cyclopropyl-α-methylbenzylamine (N-CαMBA), 1-phenyl-cyclopropylamine (1-PCPA) and 2-phenyl-cyclopropylamine (2-PCPA) (Figure 1.8). This visit was funded by the William Ramsay Henderson Trust.

The mechanism of inactivation of MAO by the cyclopropylamines, suggested by Prof. Silverman, involves a one-electron transfer to the flavin and consequent ring opening of the inactivator, which in turn forms an adduct to a cysteine (Figure 1.10). The cysteine modified by N-CαMBA in MAO B was identified to be the 365, the equivalent to the cysteine 374 in MAO A (*95*).

4.3.1. Flavin spectra change by inactivation

Cyclopropylamines are mechanism-based inactivators that reduce the flavin during normal MAO catalysis. The reactive product may form adducts with the flavin and/or a cysteine (*46*). 1-PCPA and N-CαMBA form adducts to the flavin and to the cysteine, respectively, with MAO A from human placenta (*93*). A simple way to determine the modification target for inactivation is to follow the reduction of the flavin during inactivation by the cyclopropylamines and then see if reoxidation of the flavin occurs after denaturation of the protein. Reoxidation of the flavin means that the inactivator did not bind to it but to an amino acid residue.

All the inactivators studied reduced the flavin for both MAO A and the mutant MAO A C374A. Figure 4.6.A (left) is an example of this, where the absorbance at 456nm decreases over time after the addition of N-CαMBA. Once the

enzyme was less than 5% active, it was denaturated with urea leading to the reoxidation of the flavin. This is shown by the appearance of the riboflavin characteristic spectrum with peaks at 450 and 370nm (Figure 4.6.A, right).

In contrast, the reduction of the flavin by 1-PCPA is followed by the appearance of another species that cause two peak areas around 390 and 440nm (Figure 4.6.B, right). This species disappears linearly and very slowly after denaturation of the protein, which suggests a chemical decomposition. Nevertheless, the flavin does not reoxidise as, over a period of 16h, the total change at 450nm corresponds only to 10% of the expected change for the concentration of the flavin used and there is no change at 370nm (Figure 4.6.B, right). The modified flavin in MAO A C374A remains reduced, as for the native enzyme (*93*).

For the enzyme modified by 2-PCPA the oxidised flavin spectrum appears after denaturation (Figure 4.6.C). The same result was obtained with native MAO A (not shown). Thus, in both the native and the mutant, 2-PCPA does not modify the flavin, indicating that the inactivator is forming an adduct with one amino acid residue, most likely a cysteine.

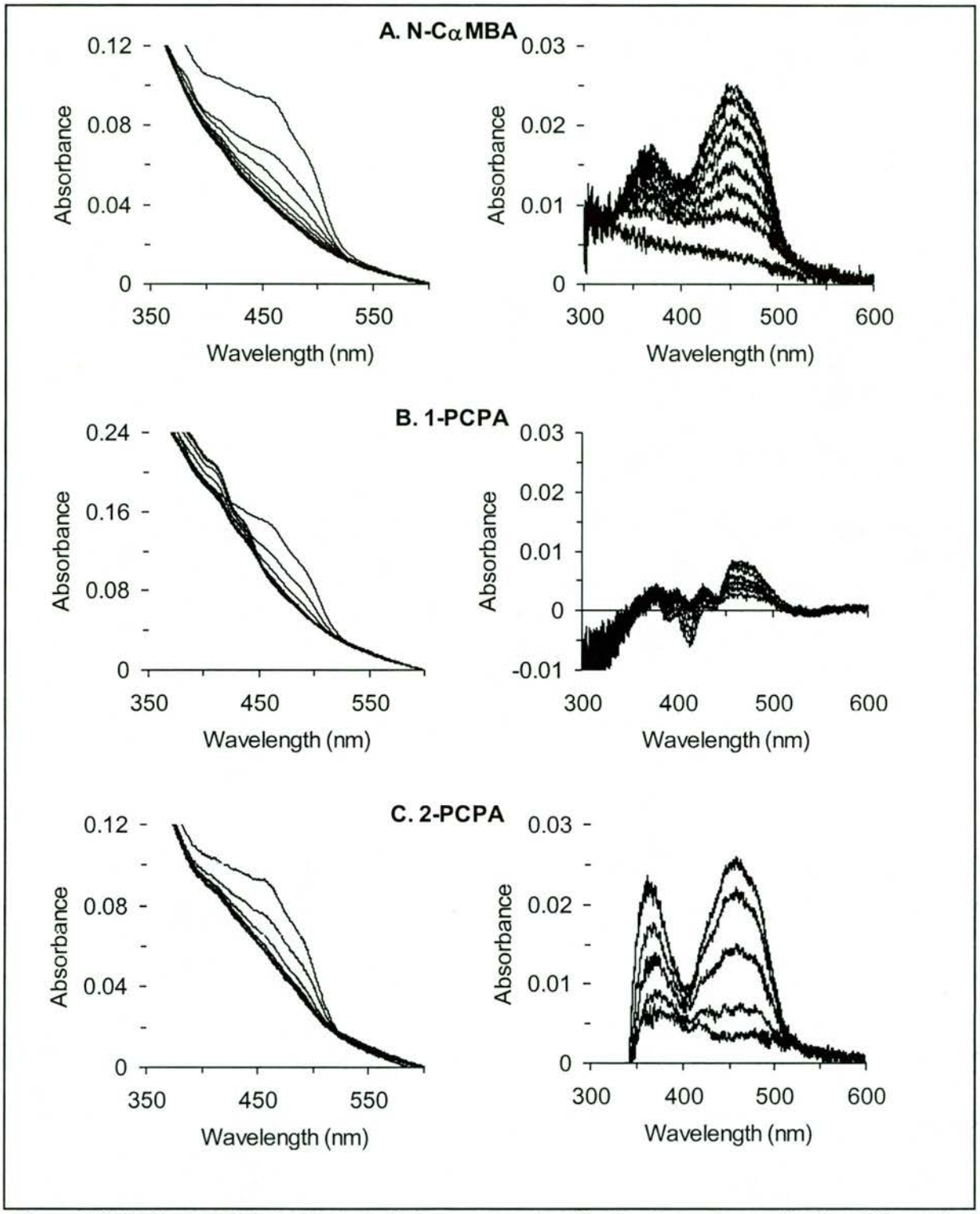

Figure 4.6. MAO A C374A flavin spectral changes upon inactivation by cyclopropylamines followed by protein denaturation. ***A.Left***. Reduction of the flavin by N-CαMBA. 2.5 mM of N-CαMBA were added to 3.5μM of MAO A C374A in 50mM potassium phosphate buffer, pH 7.2, 0.1% Brij-35 and spectra were recorded over a period of 3h. ***A.Right***. Difference spectra of flavin after denaturation. When the enzyme was more than 95% inactive, it was diluted 1/2 with saturated urea (11M). Spectra were recorded over a period of 1h, after wich the flavin was fully reoxidised. ***B.Left*** Reduction of the flavin by 1-PCPA. 5mM of 1-PCPA were added to 3.9μM of MAO A C374A as above and spectra were recorded over a period of 5h. ***B.Right*** Difference spectra of flavin after denaturation. The flavin remained reduced over a period of 16h. ***C.Left.*** Reduction of the flavin by 2-PCPA. 2mM of 2-PCPA were added to 3.4μM of MAO A C374A as above and spectra were recorded over a period of 2h. ***C.Right***. Difference spectra of flavin after denaturation. The flavin was fully reoxidised after 1h.

4.3.2. MAO cysteine content

Calculating the free cysteine content of the native and mutant enzymes and comparing it with the value after inactivation could confirm if N-CαMBA and 2-PCPA modify a cysteine.

The cysteine contents of MAO A and MAO A C374A before and after inactivation by N-CαMBA (amino acid modified) and 1-PCPA (flavin modified) are listed in Table 4.4. The native MAO A contained 8.3 cysteine residues per flavin, in agreement with previous determinations (*48, 93*). The mutant MAO A C374A contained only 6.9 free thiols, a decrease of one cysteine, as expected. Both MAO A and the mutant MAO A C374A inactivated by N-CαMBA have one less free cysteine residue than untreated enzyme, showing that one thiol has been modified. On the other hand, 1-PCPA that irreversibly modifies only the flavin does not alter the count of free cysteines, as expected. This experiment could not be done with 2-PCPA because the adduct formed is unstable, releasing cinnamaldehyde (*89*) that interferes with the assay. However, this inactivator does not modify the flavin of MAO A and the mutant (Figure 4.6.C), but one amino acid residue, which could be a cysteine as in MAO B (*88*).

Table 4.4. Cysteine content[a] of MAO A and MAO A C374A before and after inactivation by N-CαMBA and 1-PCPA

	MAO A	MAO A C374A
Native	8.0±0.3	6.9±0.3
N-CαMBA – inactivated	7.0±0.1	5.8±0.3
1-PCPA – inactivated	8.2[b]	6.8±0.2

[a]Number of cysteine residues per enzyme molecule (average of 4 experiments ± standard errors). [b]Taken from (*93*)

4.3.3. Kinetics of inactivation

Table 4.5 compares the inactivation kinetics for the cyclopropylamines between MAO A and the mutant MAO A C374A. The K_I and k_{inact} are the inactivation constant and inactivation rate at saturation, respectively. Their values were determined by plotting the $t_{1/2}$ values for each inactivator concentration versus the reciprocal of the inactivator concentration (Figure 4.7.A).

For both the wild-type and mutant enzymes the order of inactivation potency is 2-PCPA > N-CαMBA > 1-PCPA, as the K_I increases and the k_{inact} decreases (Table 4.5). Although the inactivation rates are very similar between MAO A and the mutant MAO A C374A, the K_I values are higher for the mutant, especially for the N-CαMBA. This is similar with what was found for the Michaelis-Menten parameters (Table 4.2). The k_{inact}/K_I for the mechanism-based inactivators reflect the same decrease for the mutant as for substrates confirming the alterations in the catalytic efficiency as seen with substrates. Since the inactivation depends on the catalytic turnover the same factors should indeed be influenced by the mutation.

The competitive inhibition constants, K_i, were also determined for each inactivator from the initial rates at various concentrations of inactivator and substrate (kynuramine) and at fixed oxygen saturation (Table 4.5, Figure 4.7.B). The values of K_m / V_{max} were plotted against inactivator concentration to obtain the K_i (*179*). The K_i values for 1-PCPA and 2-PCPA are similar in the wild-type and the mutant, as found for other competitive inhibitors (Table 4.3), but for N-CαMBA the K_i for the mutant is double that found for the wild-type.

For both the wild-type and mutant enzymes the K_i values increase in the order 2-PCPA > N-CαMBA > 1-PCPA, which is the same trend found with the catalytic inactivation.

The partition ratio, *PR*, represents the number of equivalents of inactivator necessary to inactivate the enzyme, *i.e.*, the number of inactivator molecules turned over for each enzyme molecule inactivated. Apart from 2-PCPA, the partition ratios for cyclopropylamines inactivation of the mutant are about half of the native. The partition ratio for N-CαMBA changes from 5:1 for MAO A to 2:1 for MAO A C374A (Table 4.5, Figure 4.8). Thus, the probability of the inactivation of MAO A C374A by N-CαMBA is higher than non-modifying turnover. This does not mean that the mutant is more rapidly inactivated, as the k_{inact} does not change, but that the mutation causes a change that influences the number of hits. Given that the life-time of the reactive product of catalysis can be assumed to be unchanged, the residue(s) modified in the mutant must be more susceptible or available than in the native enzyme. This might be due to a change on the enzyme structure and/or on the cysteine modified by the inactivator. As the mutant MAO A C374A is also inactivated by N-CαMBA is unlikely that the cysteine modified in MAO A is the 374, the correspondent to the MAO B C365, but it is not certain as in the absence of this cysteine another on the surface could be modified.

Table 4.5. Comparison of kinetic properties for 2-PCPA, *N*-CαMBA and 1-PCPA with MAO A and MAO A C374A*

	K_I (mM)[1]		k_{inact} (min^{-1})[1]		k_{inact}/K_I (min^{-1}. mM^{-1})		K_i (mM)[2]		*PR*[3]	
Inactivator	MAO A	MAO A C374A	MAO A	MAO A C374A	MAO A	MAO A C374A	MAO A	MAO A C374A	MAO A	MAO A C374A
N-CαMBA	1.5±0.6	3±1	1.0±0.6	1.0±0.5	0.65±0.03	0.38±0.01	0.12±0.03	0.28±0.05	4.7	1.6
1-PCPA	7±3	12±6	0.5±0.2	0.6±0.3	0.068±0.005	0.047±0.003	0.60±0.04	0.52±0.06	11.5	5.6
2-PCPA	0.20±0.04	0.30±0.09	4.1±0.8	5±1	20.1±0.4	16.5±0.3	0.041±0.005	0.035.4±0.003	3.2	2.9

(1) The values ± standard errors were obtained from the best fit of $t_{1/2}$ vs. 1/[Inact] with two times 7 inactivator concentrations. (2) The values ± standard errors were obtained from the best fit of $(Km/Vmax)_{app}$ vs. [Inact] with two times 7 inactivator concentrations. (3) Partition ratio.

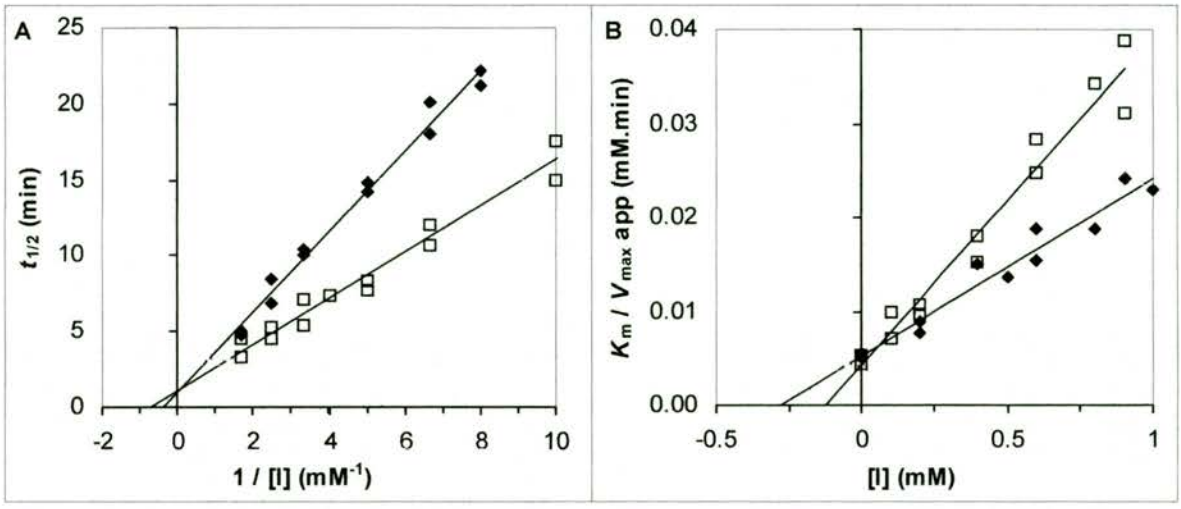

Figure 4.7. Inactivation kinetics by N-CαMBA. ***A.*** MAO A (⊟) and MAO A C374A (◆) were incubated with different concentrations of N-CαMBA and the half-life times ($t_{1/2}$) were determined. The $t_{1/2}$ plotted against the inverse of the inactivator concentration give a straight line (Kitz & Wilson replot), where the K_I equals the slope over the intercept and the k_{inact} equals the inverse of the intercept. ***B.*** MAO A (⊟) and MAO A C374A (◆) were assayed using a constant range of kynuramine concentrations (0.1 to 0.9mM) in the presence of different concentrations of N-CαMBA. The apparent K_m/V_{max} values plotted against the concentration of inactivator give a straight line, where K_i equals minus the intercept at the *x* axis.

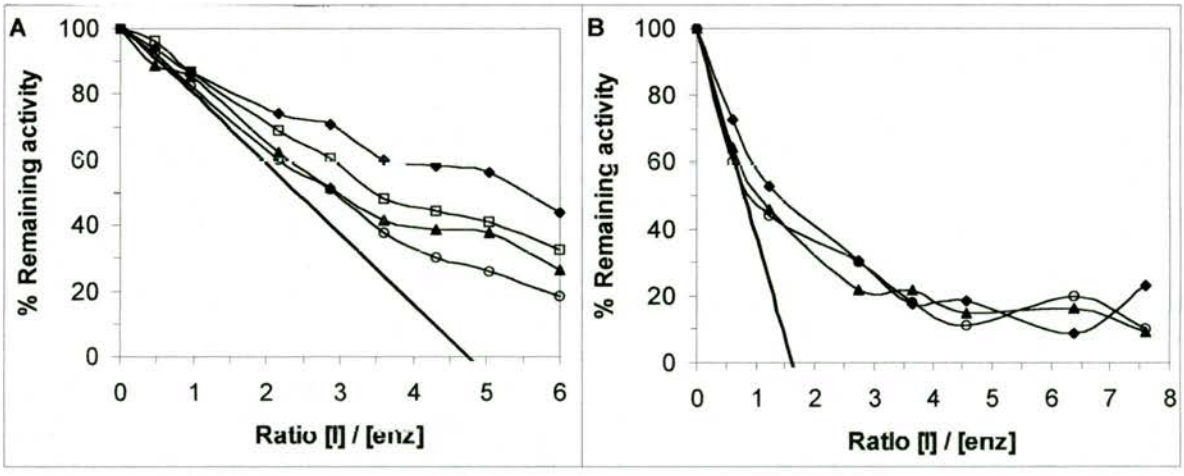

Figure 4.8. Partition ratios for N-CαMBA inactivation of MAO A and MAO A C374A. ***A.*** MAO A (2.1μM) was incubated with increasing concentrations of N-CαMBA from 0 to 6.25μM in 100mM KPi, pH 7.2, 0.2% Triton, 20% glycerol. Aliquots were assayed periodically, at days 2 (◆), 4 (⊟), 5 (▲) and 7 (⊖), until there was no change in the PR value (—). *B.* MAO A C374A (1.7μM) was incubated with increasing concentrations of N-CαMBA as above.

4.3.4. Identification of modified MAO A cysteine by N-CαMBA

To identify which cysteine in MAO A is modified by N-CαMBA, inactivated MAO A was sent to the Harvard Microchemistry Institute for localization of the adduct and sequencing of the peptide modified. Trypsin digest of the inactivated enzyme and mass spectrometry permitted coverage of 83% of the protein (Figure 4.9). The peptides covered included the cysteines 165, 266, 306 and 374, but no modification by the inactivator was found. Thus, C374, the equivalent to C365 identified in MAO B, is excluded as a single specific site. The modification could be in any of the non-recovered peptides that contain the cysteines 201, 321, 323 and 398. The modification of thiol groups by biotinylatilated NEM, demonstrated that inactivation by this thiol reagent was accompanied by variable modification of multiple thiols (*180*). Seven MAO A thiol groups were modified in 5 hours whereas only 2 MAO B thiols were modified in 25 hours. Furthermore, amphetamine protects 4 cysteines in MAO A from inactivation by DPDS (unpublished results from this laboratory). It is therefore likely that MAO A inactivation could result from multiple or alternate sites of modification.

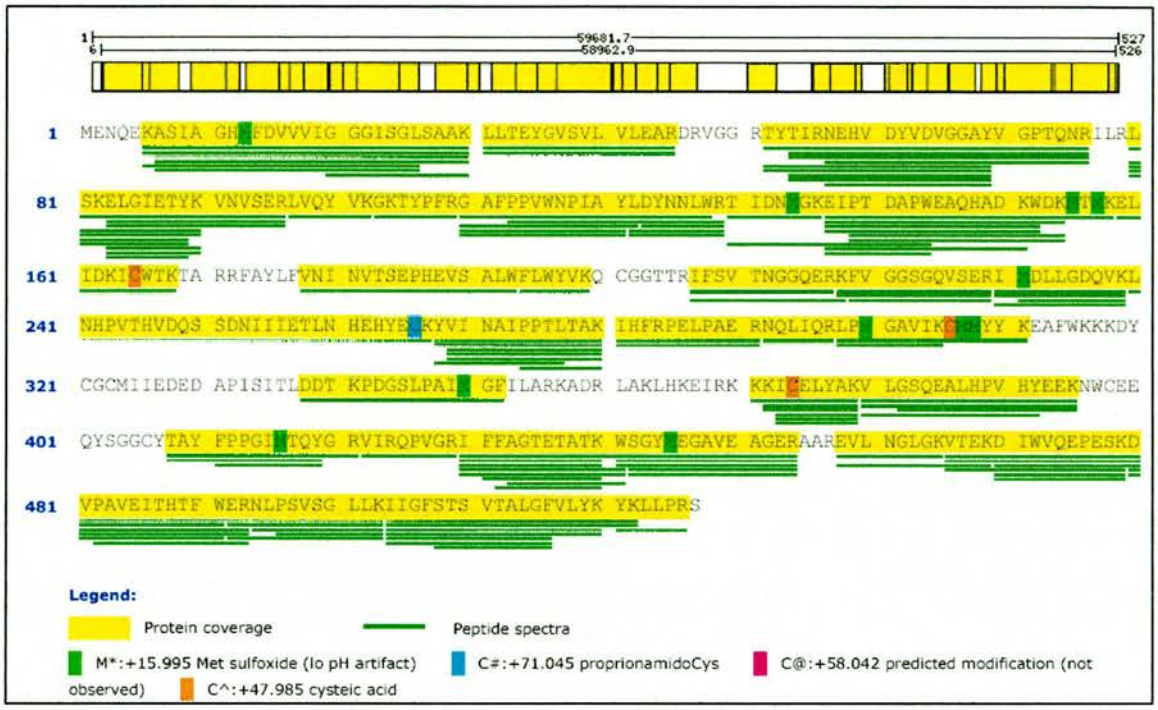

Figure 4.9. Analysis of the tryptic digest of N-CαMBA-inactivated MAO A. MAO A was inactivated by N-CαMBA and the adduct stabilised as described in chapter 2.6.6. The respective gel bands were sent to the Harvard Microchemistry Institute where the protein was digested with trypsin and the peptides analysed by mass spectrometry.

5. REVISED MECHANISM OF MAO INACTIVATION BY CYCLOPROPYLAMINES

The fact that the MAO B C365A mutant was active is consistent with the finding that this cysteine is not in the active site of MAO B but on the surface of the protein. What is surprising is that modification of this cysteine inactivates the enzyme. The C365 modified by N-CαMBA gives a 3-hydroxypropylcysteine (**5**, Figure 5.2), which is much larger than the alanine mutation and could possibly affect the putative loop movements on the entrance to the active site. This in addition to the influence on the catalytic process, as found for the MAO A C374A mutant, might be the cause for complete inactivation.

However, the inactivation mechanism by N-CαMBA proposed before (*95*) can no longer accommodate the two facts revealed by the MAO B crystal structure (*122*): (a) there is no active site residue that can act as a base and (b) the modified cysteine is not in the active site.

It is possible that the flavin itself is acting as a base after reduction. If this is the case, there will be a concerted one-electron transfer and α–proton loss (Figure 5.1). The free amine radical cation intermediate is bypassed and the second electron transfer takes place.

To account for the second fact, the oxidation of N-CαMBA has to produce an activated species capable of travelling from the flavin before becoming attached to an amino acid residue. So, again, there is a concerted electron transfer and deprotonation, giving species **3** (Figure 5.2). The cysteine thiolate undergoes a Michael addition to the conjugated double bond of **3**, followed by protonation, giving **4**. Hydrolysis of the imine adduct **4** was shown to occur studying the mechanism of

MAO B inactivation by N-(1-methylcyclopropyl)benzylamine (*181*) and **5** has been identified by mass spectrometry (*95*).

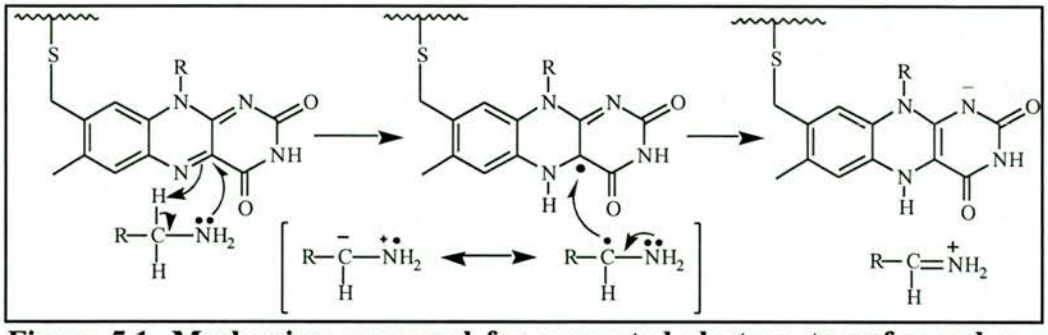

Figure 5.1. Mechanism proposed for concerted electron transfer and α-proton loss.

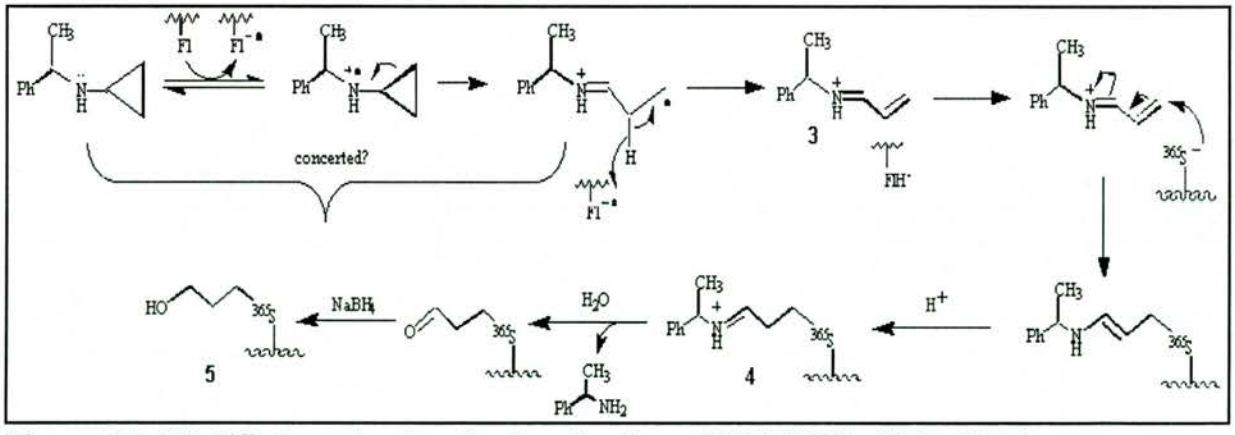

Figure 5.2. Modified mechanism for inactivation of MAO B by N-CαMBA.

6. CONCLUSIONS

Monoamine oxidases are flavoproteins that are important for the development of drugs for the treatment of depression, Parkinson's and Alzheimer diseases and other behaviour disorders and neurodegenerative diseases. Thus, full understanding of the catalytic mechanism of the enzyme is crucial for the design of new, selective and efficient drugs. The chemical mechanism of MAO has been extensively studied but remains controversal as different research groups defend two opposing theories: the nucleophilic and the one-electron transfer mechanisms (*12, 139*). An obscure element is the role of the cysteine residues in the MAO catalysis:

- Thiol modification inactivates the enzyme (*48*)
- Thiol modification changes the redox properties of the flavin (*100*)
- Ligands prevent thiol modification (*48*)
- Cysteine to serine mutants expressed in mammalian cells retain partial or no activity (*111*)
- Chemical modification of the MAO B cysteine 365 inactivates the enzyme (*95*)

However,

- The crystal structure of MAO B shows that cysteine 365 is on the surface of the protein and not in the active site (*122*)

To find the influence of certain cysteine residues on MAO catalysis, single and double cysteine to alanine mutants were constructed and constitutively expressed in *Pichia pastoris*. The chosen cysteine residues were MAO A C374 and C398 and the correspondent MAO B C365 and C389. The mutants MAO A C374A, MAO B C365A and MAO B C389A were active whereas the mutants MAO A C398A, MAO

A C374A & C398A and MAO B C365A & C389A had no detectable activity (Table 3.1). Thus, MAO A C374 and the correspondent MAO B C365 are not essential for activity, in contrast to previous report (*111*). In fact, like the MAO B C365, the correspondent cysteine 374 in MAO A is most unlikely to be in the active site. The loss of activity of other mutants could be attributed to instability and higher susceptibility to proteolysis, as seen on western blots (Figure 3.5 and Figure 3.6), and not directly to the absence of the respective cysteines.

Although the expression levels of MAO A and the mutant MAO A C374A were found to be relatively low (Table 3.1), with the fermentation and purification conditions adapted to the *Pichia* constitutive system, it was possible to extract and purify the enzymes (Table 3.5 and Table 3.6) at levels that permitted analysis of the redox, kinetic and mechanism-based inactivation properties.

The reductive titrations of MAO A and the mutant MAO A C374A showed no apparent differences in the flavin redox behaviour (Figure 4.1 and Figure 4.2). However, the redox potential for the FAD_{ox} / FAD_{sq} couple was slightly higher for the mutant (Table 4.1). The flavin redox potential is very sensitive to changes in its environment (*1*), so it is possible that the mutation of the cysteine 374 is influencing the active site and thus causing a small change in the flavin redox properties not detected through simple reductive titrations.

The steady-state kinetics on a series of substrates showed only small differences between MAO A and the mutant MAO A C374A (Table 4.2). However, a prominent trend was found of decreasing specificity constant values for the mutant. The same trend was reflected in the differences between wild-type and mutant for the activation energies for amine oxidation. These data suggest that the catalytic process of MAO A is changed by the absence of the cysteine 374. This change is not likely to

be influencing the ligand binding as the K_i values for three structurally different inhibitors are similar between MAO A and the mutant and do not show an apparent trend (Table 4.3).

In collaboration with Prof. Richard Silverman, from the Northwestern University, the mechanism-based inactivators of MAO, the cyclopropylamines, were used to further investigate the differences between MAO A and the mutant MAO A C374A. The cyclopropylamines inactivate the enzyme by modifying the flavin and/or a cysteine. The site of modification by N-CαMBA (cysteine), 1-PCPA (flavin) and 2-PCPA (cysteine) is not changed by the mutation of cysteine 374 (Table 4.4 and Figure 4.6). However, the mutant MAO A C374A is still inactivated by N-CαMBA (Table 4.5). This suggests that the cysteine modified in MAO A is not the C374 (the corresponding to C365 in MAO B), although MAO A inactivation could result from multiple or alternate sites of modification. The identification of the MAO A cysteines modified by N-CαMBA was attempted as it had been done with MAO B. In the peptides that could be recovered from the tryptic digest of inactivated MAO A, no modification was detected (Figure 4.9), leaving four cysteines as potential candidates (201, 321, 323 and 398). Although the C374 was found not to be modified, it could still be a possible modification site but with low probability to be hit.

The kinetics of inactivation by mechanism-based inactivators was also studied (Table 4.5). As with the substrates, specificity constants for the cyclopropylamines in the mutant were less than in the native enzyme. This was not surprising, as the mechanism-based inactivators are also turned-over by the enzyme and thus, suffer from the same alterations in the catalytic efficiency. The alteration in the PR is another matter. For N-CαMBA the PR is decreased by more than 50%. As

a possible modification site, the absence of C374 alters the hit probability status, making the cysteine(s) with higher influence on the inactivation of the enzyme more prone to being hit. Thus, C374 could be a possible but not essential modification site.

In the whole, it can be concluded that, although the cysteine 374 in MAO is presumably located on the surface of the protein, its mutation alters the normal catalytic process in the active site.

In collaboration with Prof. Silverman, we have proposed a revised mechanism of MAO inactivation by cyclopropylamines involving a concerted one-electron transfer to the flavin and substrate α-proton loss (Figure 5.2).

As a final note I would like to remind the reader that although solving the protein crystal structure can give much important information, it is not more than a snapshot and that most of the times it does not answer all the questions about the catalytic mechanism of the enzyme. These answers are closer to reach, when the information taken from crystal structure is complemented by other biochemical studies, including mutational and kinetic analysis.

7. APPENDIX

7.1. MAO A cDNA sequence and its translation

```
                                                                          Tth111 I
1    atg gaa aac caa gaa aag gct atc tct gcg ggc cac atg ttc   gac gta gtc gtg atc gga ggt   ggc att tca
1    M   E   N   Q   E   K   A   S   I   A   G   H   M   F     D   V   V   V   I   G   G     G   I   S
73   gga cta tct gct gcc aaa ctc ttg act gaa tat ggc gtt agt   gtt ttg gtt tta gaa gct cgg   gac agg gtt
25   G   L   S   A   A   K   L   L   T   E   Y   G   V   S     V   L   V   L   E   A   R     D   R   V
145  gga gga aga aca tat act ata agg aat gag cat gtt gat tac   gta gat gtt ggt gga gct tat   gtg gga cca
49   G   G   R   T   Y   T   I   R   N   E   H   V   D   Y     V   D   V   G   G   A   Y     V   G   P
217  acc caa aac aga atc tta cgc ttg tct aag gag ctg ggc ata   gag act tac aaa gtg aat gtc   agt gag cgt
73   T   Q   N   R   I   L   R   L   S   K   E   L   G   I     E   T   Y   K   V   N   V     S   E   R
                                                   Ban I/Kas I/Nar I/Ehe I/Bbe I/Msl I
289  ctc gtt caa tat gtc aag ggg aaa aca tat cca ttt cgg ggc   gcc ttt cca cca gta tgg aat   ccc att gca
97   L   V   Q   Y   V   K   G   K   T   Y   P   F   R   G     A   F   P   P   V   W   N     P   I   A
     Xcm I
361  tat ttg gat tac aat aat ctg tgg agg aca ata gat aac atg   ggg aag gag att cca act gat   gca ccc tgg
121  Y   L   D   Y   N   N   L   W   R   T   I   D   N   M     G   K   E   I   P   T   D     A   P   W
                                                               EcoICR I/Sac I
433  Gag gct caa cat gct gac aaa tgg gac aaa atg acc atg aaa   gag ctc att gac aaa atc tgc   tgg aca aag
145  E   A   Q   H   A   D   K   W   D   K   M   T   M   K     E   L   I   D   K   I   C165  W   T   K
505  Act gct agg cgg ttt gct tat ctt ttt gtg aat atc aat gtg   acc tct gag cct cac gaa gtg   tct gcc ctg
169  T   A   R   R   F   A   Y   L   F   V   N   I   N   V     T   S   E   P   H   E   V     S   A   L
                                         Ban I
577  Tgg ttc ttg tgg tat gtg aag cag tgc ggg ggc acc act cgg   ata ttc tct gtc acc aat ggt   ggc cag gaa
193  W   F   L   W   Y   V   K   Q   C   G   G   T   T   R     I   F   S   V   T   N   G     G   Q   E
649  Cgg aag ttt gta ggt gga tct ggt caa gtg agc gaa cgg ata   atg gac ctc ctc gga gac caa   gtg aag ctg
217  R   K   F   V   G   G   S   G   Q   V   S   E   R   I     M   D   L   L   G   D   Q     V   K   L
721  Aac cat cct gtc act cac gtt gac cag tca agt gac aac atc   atc ata gag acg ctg aac cat   gaa cat tat
241  N   H   P   V   T   H   V   D   Q   S   S   D   N   I     I   I   E   T   L   N   H     E   H   Y
```

```
                                  Vsp I
793   Gag  tgc  aaa  tac  gta  att  aat  gcg  atc  cct  ccg  acc  ttg  act   gcc  aag  att  cac  ttc  aga  cca   gag  ctt  cca
265   E    C    K    Y    V    I    N    A    I    P    P    T    L    T     A    K    I    H    F    R    P     E    L    P
864   Gca  gag  aga  aac  cag  tta  att  cag  cgt  ctt  cca  atg  gga  gct   gtc  att  aag  tgc  atg  atg  tat   tac  aag  gag
289   A    E    R    N    Q    L    I    Q    R    L    P    M    G    A     V    I    K    C    M    M    Y     Y    K    E
937   Gcc  ttc  tgg  aag  aag  aag  gat  tac  tgt  ggc  tgc  atg  atc  att   gaa  gat  gaa  gat  gct  cca  att   tca  ata  acc
313   A    F    W    K    K    K    D    Y    C    G    C    M    I    I     E    D    E    D    A    P    I     S    I    T
1009  Ttg  gat  gac  acc  aag  cca  gat  ggg  tca  ctg  cct  gcc  atc  atg   ggc  ttc  att  ctt  gcc  cgg  aaa   gct  gat  cga
337   L    D    D    T    K    P    D    G    S    L    P    A    I    M     G    F    I    L    A    R    K     A    D    R
                                                                            EcoICR I/Sac I                    BamH I
1081  Ctt  gct  aag  cta  cat  aag  gaa  ata  agg  aag  aag  aaa  atc  tgt   gag  ctc  tat  gcc  aaa  gtg  ctg   gga  tcc  caa
361   L    A    K    L    H    K    E    I    R    K    K    K    I    C374  E    L    Y    A    K    V    L     G    S    Q
      Hind III                                                                                Sca I
1153  Gaa  gct  tta  cat  cca  gtg  cat  tat  gaa  gag  aag  aac  tgg  tgt   gag  gag  cag  tac  tct  ggg  ggc   tgc  tac  acg
385   E    A    L    H    P    V    H    Y    E    E    K    N    W    C398  E    E    Q    Y    S    G    G     C    Y    T
                                  BspH I
1225  gcc  tac  ttc  cct  cct  ggg  atc  atg  act  caa  tat  gga  agg  gtg   att  cgt  caa  ccc  gtg  ggc  agg   att  ttc  ttt
409   A    Y    F    P    P    G    I    M    T    Q    Y    G    R    V     I    R    Q    P    V    G    R     I    F    F
                                       Van91 I
1297  gcg  ggc  aca  gag  act  gcc  aca  aag  tgg  agc  ggc  tac  atg  gaa   ggg  gca  gtt  gag  gct  gga  gaa   cga  gca  gct
433   A    G    T    E    T    A    T    K    W    S    G    Y    M    E     G    A    V    E    A    G    E     R    A    A
                                            BstE II
1369  agg  gag  gtc  tta  aat  ggt  ctc  ggg  aag  gtg  acc  gag  aaa  gac   atc  tgg  gta  caa  gaa  cct  gaa   tca  aag  gac
457   R    E    V    L    N    G    L    G    K    V    T    E    K    D     I    W    V    Q    E    P    E     S    K    D
1441  gtt  cca  gcg  gta  gaa  atc  acc  cac  acc  ttc  tgg  gaa  agg  aac   ctg  ccc  tct  gtt  tct  ggc  ctg   ctg  aag  atc
481   V    P    A    V    E    I    T    H    T    F    W    E    R    N     L    P    S    V    S    G    L     L    K    I
1513  att  gga  ttt  tcc  aca  tca  gta  act  gcc  ctg  ggg  ttt  gtg  ctg   tac  aaa  tac  aag  ctc  ctg  cca   cgg  tct  tga
505   I    G    F    S    T    S    V    T    A    L    G    F    V    L     Y    K    Y    K    L    L    P     R    S    *
                                                                                                 Ssp I
1585  agt  tct  gtt  ctt  atg  ctc  tct  gct  cac  tgg  ttt  tca  ata  cca   cca  aga  gga  aaa  tat  tga  caa   gtt  taa  agg
1657  ctg  tgt  cat  tgg  gcc  atg  ttt  aag  tgt  act  gga  ttt  aac  tac   ctt  tgg  ctt  aat  tcc  aat  cat   tgt  taa  agt
                                            Vsp I
1729  aaa  aac  aat  tca  aag  aat  cac  cta  att  aat  ttc  agt  aag  atc   aag  ctc  cat  ctt  att  tgt  cag   tgt  aga  tca
1801  act  cat  gtt  aat  tga  tag  aat  aaa  gcc  ttg  tga  tca  ctt  tct   gaa  att  cac  aaa  gtt  aaa  cgt   gat  gtg  ctc
1873  atc  aga  aac
```

7.2. MAO B cDNA sequence and its translation

```
                    BstAP I         Tth111 I
1    atg  agc  aac  aaa  tgc  gac  gtg  gtc  gtg  gtg  ggg  ggc  ggc  atc  tca  ggt  atg  gca  gca  gcc  aaa  ctt  ctg  cat
1    M    S    N    K    C    D    V    V    V    V    G    G    G    I    S    G    M    A    A    A    K    L    L    H
                                                                  Sma I
73   gac  tct  gga  ctg  aat  gtg  gtt  gtt  ctg  gaa  gcc  cgg  gac  cgt  gtg  gga  ggc  agg  act  tac  act  ctt  agg  aac
25   D    S    G    L    N    V    V    V    L    E    A    R    D    R    V    G    G    R    T    Y    T    L    R    N
                                                       BamH I
145  caa  aag  gtt  aaa  tat  gtg  gac  ctt  gga  gga  tcc  tat  gtt  gga  cca  acc  cag  aat  cgt  atc  ttg  aga  tta  gcc
49   Q    K    V    K    Y    V    D    L    G    G    S    Y    V    G    P    T    Q    N    R    I    L    R    L    A
217  aag  gag  cta  gga  ttg  gag  acc  tac  aaa  gtg  aat  gag  gtt  gag  cgt  ctg  atc  cac  cat  gta  aag  ggc  aaa  tca
73   K    E    L    G    L    E    T    Y    K    V    N    E    V    E    R    L    I    H    H    V    K    G    K    S
289  tac  ccc  ttc  agg  ggg  cca  ttc  cca  cct  gta  tgg  aat  cca  att  acc  tac  tta  gat  cat  aac  aac  ttt  tgg  agg
97   Y    P    F    R    G    P    F    P    P    V    W    N    P    I    T    Y    L    D    H    N    N    F    W    R
                                                                  Nco I
361  aca  atg  gat  gac  atg  ggg  cga  gag  att  ccg  agt  gat  gcc  cca  tgg  aag  gct  ccc  ctt  gca  gaa  gag  tgg  gac
121  T    M    D    D    M    G    R    E    I    P    S    D    A    P    W    K    A    P    L    A    E    E    W    D
433  aac  atg  aca  atg  aag  gag  cta  ctg  gac  aag  ctc  tgc  tgg  act  gaa  tct  gca  aag  cag  ctt  gcc  act  ctc  ttt
145  N    M    T    M    K    E    L    L    D    K    L    C    W    T    E    S    A    K    Q    L    A    T    L    F
                         Pst I
505  gtg  aac  ctg  tgt  gtc  act  gca  gag  acc  cat  gag  gtc  tct  gct  ctc  tgg  ttc  ctg  tgg  tat  gtg  aag  cag  tgt
169  V    N    L    C    V    T    A    E    T    H    E    V    S    A    L    W    F    L    W    Y    V    K    Q    C
577  gga  ggc  aca  aca  aga  atc  atc  tcg  aca  aca  aat  gga  gga  cag  gag  agg  aaa  ttt  gtg  ggc  gga  tct  ggt  caa
193  G    G    T    T    R    I    I    S    T    T    N    G    G    Q    E    R    K    F    V    G    G    S    G    Q
649  gtg  agt  gag  cgg  ata  atg  gac  ctc  ctt  gga  gac  cga  gtg  aag  ctg  gag  agg  cct  gtg  atc  tac  att  gac  cag
217  V    S    E    R    I    M    D    L    L    G    D    R    V    K    L    E    R    P    V    I    Y    I    D    Q
721  aca  aga  gaa  aat  gtc  ctt  gtg  gag  acc  cta  aac  cat  gag  atg  tat  gag  gct  aaa  tat  gtg  att  agt  gct  att
241  T    R    E    N    V    L    V    E    T    L    N    H    E    M    Y    E    A    K    Y    V    I    S    A    I
793  cct  cct  act  ctg  ggc  atg  aag  att  cac  ttc  aat  ccc  cct  ctg  cca  atg  atg  aga  aac  cag  atg  atc  act  cgt
265  P    P    T    L    G    M    K    I    H    F    N    P    P    L    P    M    M    R    N    Q    M    I    T    R
                                                            Psi I
864  gtg  cct  ttg  ggt  tca  gtc  atc  aag  tgt  ata  gtt  tat  tat  aaa  gag  cct  ttc  tgg  agg  aaa  aag  gat  tac  tgt
289  V    P    L    G    S    V    I    K    C    I    V    Y    Y    K    E    P    F    W    R    K    K    D    Y    C
937  gga  acc  atg  att  att  gat  gga  gaa  gaa  gct  cca  gtt  gcc  tac  acg  ttg  gat  gat  acc  aaa  cct  gaa  ggc  aac
```

```
313  G    T    M    I    I    D    G    E    E    A    P    V    A    Y    T    L    D    D    T    K    P    E    G    N
1009 tat  gct  gcc  ata  atg  gga  ttt  atc  ctg  gcc  cac  aaa  gcc  aga  aaa  ctg  gca  cgt  ctt  acc  aaa  gag  gaa  agg
337  Y    A    A    I    M    G    F    I    L    A    H    K    A    R    K    L    A    R    L    T    K    E    E    R
1081 ttg  aag  aaa  ctt  tgt  gaa  ctc  tat  gcc  aag  gtt  ctg  ggt  tcc  cta  gaa  gct  ctg  gag  cca  gtg  cat  tat  gaa
361  L    K    K    L    C365 E    L    Y    A    K    V    L    G    S    L    E    A    L    E    P    V    H    Y    E
                                                Sca I                                                  BamH I
1153 gaa  aag  aac  tgg  tgt  gag  gag  cag  tac  tct  ggg  ggc  tgc  tac  aca  act  tat  ttc  ccc  cct  ggg  atc  ctg  act
385  E    K    N    W    C389 E    E    Q    Y    S    G    G    C397 Y    T    T    Y    F    P    P    G    I    L    T
                                                                                  Ban I
1225 caa  tat  gga  agg  gtt  cta  cgc  cag  cca  gtg  gac  agg  att  tac  ttt  gca  ggc  acc  gag  act  gcc  aca  cac  tgg
409  Q    Y    G    R    V    L    R    Q    P    V    D    R    I    Y    F    A    G    T    E    T    A    T    H    W
                                                                                            Sph I/Nco I
1297 agc  ggc  tac  atg  gag  ggg  gct  gta  gag  gcc  ggg  gag  aga  gca  gcc  cga  gag  atc  ctg  cat  gcc  atg  ggg  aag
433  S    G    Y    M    E    G    A    V    E    A    G    E    R    A    A    R    E    I    L    H    A    M    G    K
                                                     Bsg I
1369 att  cca  gag  gat  gaa  atc  tgg  cag  tca  gaa  cca  gag  tct  gtg  gat  gtc  cct  gca  cag  ccc  atc  acc  acc  acc
457  I    P    E    D    E    I    W    Q    S    E    P    E    S    V    D    V    P    A    Q    P    I    T    T    T
     Xcm I                                                     Bpu10 I
1441 ttt  ttg  gag  aga  cat  ttg  ccc  tcc  gtg  cca  ggc  ctg  ctc  agg  ctg  att  gga  ttg  acc  acc  atc  ttt  tca  gca
481  F    L    E    R    H    L    P    S    V    P    G    L    L    R    L    I    G    L    T    T    I    F    S    A
1513 acg  gct  ctt  ggc  ttc  ctg  gcc  cac  aaa  agg  ggg  cta  ctt  gtg  aga  gtc  taa
505  T    A    L    G    F    L    A    H    K    R    G    L    L    V    R    V    *
```

8. REFERENCES

1. **Ghisla, S., and Massey, V.** (1989). "Mechanism of flavoprotein-catalyzed reactions". *Eur J Biochem 181*, pp 1-17.

2. **Kemal, C., Chan, T. W., and Bruice, T. C.** (1977). "Reaction of 3O2 with dihydroflavins. 1. N3,5-Dimethyl-1,5-dihydrolumiflavin and dihydroisoallxazines". *J Am Chem Soc 99*, pp 7272-7286.

3. **Massey, V.** (1994). "Activation of molecular oxygen by flavins and flavoproteins". *J Biol Chem 269*, pp 22459-22462.

4. **Ghisla, S., and Massey, V.** (1986). "New flavins for old: artificial flavins as active site probes of flavoproteins". *Biochem J 239*, pp 1-12.

5. **Porter, D. J., Voet, J. G., and Bright, H. J.** (1973). "Direct evidence for carbanions and covalent N 5 -flavin-carbanion adducts as catalytic intermediates in the oxidation of nitroethane by D-amino acid oxidase". *J Biol Chem 248*, pp 4400-4416.

6. **Jensen, K. F.** (2002) "The divergent family of dihydroorotate dehydrogenases" in *Flavins and flavoproteins 2002*, pp 481-490 (Chapman, S. K., Perham, R. N., and Scrutton, N. S., Eds.), Rudolf Weber, Berlin.

7. **Buffoni, F.** (1995). "Semicarbazide-sensitive amine oxidase: some biochemical properties and general considerations". *Prog Brain Res 106*, pp 323-331.

8. **Buffoni, F., Ignesti, G., and Agresti, A.** (1978). "Some quantum chemical considerations on the substrates of pig plasma benzylamine oxidase". *Ital J Biochem 27*, pp 354-357.

9. **Buffoni, F., Coppi, C., Ignesti, G., and D., W.** (1981). "pH variation of isotope effect on the catalytic activity of pig plasma benzylamine oxidase". *Biochem Intern 3*, pp 391-397.

10. **Tanizawa, K., Matsuzaki, R., Shimizu, E., Yorifuji, T., and Fukui, T.** (1994). "Cloning and sequencing of phenylethylamine oxidase from Arthrobacter globiformis and implication of Tyr-382 as the precursor of its covalently bound quinone cofactor". *Biochem Biophys Res Commun 199*, pp 1096-1102.

11. **Seiler, N.** (1995). "Polyamine oxidase, properties and functions". *Prog Brain Res 106*, pp 333-344.

12. **Binda, C., Mattevi, A., and Edmondson, D. E.** (2002). "Structure-function relationships in flavoenzyme-dependent amine oxidations: a comparison of polyamine oxidase and monoamine oxidase". *J Biol Chem 277*, pp 23973-23976.

13. **Binda, C., Coda, A., Angelini, R., Federico, R., Ascenzi, P., and Mattevi, A.** (1999). "A 30A long U-shaped catalytic tunnel in the crystal structure of polyamine oxidase". *Structure Fold Des 7*, pp 265-276.

14. **Simondsen, R. P., and Tollin, G.** (1980). "Structure-function relations in flavodoxins". *Mol Cell Biochem 33*, pp 13-24.

15. **Moonen, C. T., and Muller, F.** (1984). "On the intermolecular electron transfer between different redox states of flavodoxin from *Megasphaera elsdenii*. A 500MHz 1H NMR study." *Eur J Biochem 140*, pp 303-309.

16. **Massey, V.** (1995). "Introduction: flavoprotein structure and mechanism". *FASEB J 9*, pp 473-5.

17. **Zanetti, G., and Williams, C. H., Jr.** (1967). "Characterization of the active center of thioredoxin reductase". *J Biol Chem 242*, pp 5232-5236.

18. **Williams, C. H., Jr.** (1995). "Mechanism and structure of thioredoxin reductase from *Escherichia coli*". *FASEB J 9*, pp 1267-1276.

19. **Mattevi, A., Schierbeek, A. J., and Hol, W. G.** (1991). "Refined crystal structure of lipoamide dehydrogenase from *Azotobacter vinelandii* at 2.2A resolution. A comparison with the structure of glutathione reductase." *J Mol Biol 220*, pp 975-994.

20. **Pai, E. F., and Schulz, G. E.** (1983). "The catalytic mechanism of glutathione reductase as derived from the X-ray difraction analyses of reaction intermediates". *J Biol Chem 258*, pp 1752-1757.

21. **Wang, P. F., Arscott, L. D., Gilberger, T. W., Muller, S., and Williams, C. H., Jr.** (1999). "Thioredoxin reductase from *Plasmodium falciparum*: evidence for interaction between the C-terminal cysteine residues and the active site disulfide-dithiol". *Biochemistry 38*, pp 3187-3196.

22. **Davioud-Charvet, E., McLeish, M. J., Veine, D., Giegel, D., Andricopulo, A. D., Becker, K., Muller, S., Schirmer, R. H., Williams, C. H., Jr., and Kenyon, G. L.** (2002) "Mechanism-based inactivation of thioredoxin reductase from *Plasmodium falciparum* by Mannich bases. Implications for drug design." in *Flavins and flavoproteins 2002*, pp 845-851 (Chapman, S. K., Perham, R. N., and Scrutton, N. S., Eds.), Rudolf Weber, Berlin.

23. **Xia, Z.-X., Shamala, N., Bethge, P. H., Lim, L. W., Bellamy, H. D., Xuong, N. H., Lederer, F., and Mathews, F. S.** (1987). "Three-dimensional structure of flavocytochrome b2 from baker's yeast at 3.0A resolution". *Proc Natl Acad Sci U S A 84*, pp 2629-2633.

24. **Fischmann, T. O., Hruza, A., Niu, X. D., Fosseta, J. D., Lunn, C. A., Dolphin, E., Prongay, A. J., Reichert, P., Lundell, D. J., Narula, S. K., and Weber, P. C.** (1999). "Structural characterization of nitric oxide synthase isoforms reveals striking active site conservation". *Nat Struct Biol 6*, pp 233-242.

25. **Xia, Z.-X., and Mathews, F. S.** (1990). "Molecular structure of flavocytochrome b_2 at 2.4A resolution". *J Mol Biol 212*, pp 837-863.

26. **Sinclair, R., Reid, G. A., and Chapman, S. K.** (1998). "Re-design of *Saccharomyces cerevisiae* flavocytochrome b_2: Introduction of L-mandelate dehydrogenase activity". *Biochem J 333*, pp 117-120.

27. **Mowat, C. G., Wehenkel, G. A., Reid, G. A., Walkinshaw, M. D., Green, A. J., and Chapman, S. K.** (2002) "Structural insights into substrate binding and mechanism in flavocytochrome b_2" in *Flavins and flavoproteins 2002*, pp 305-310 (Chapman, S. K., Perham, R. N., and Scrutton, N. S., Eds.), Rudolf Weber, Berlin.

28. **Enroth, C., Eger, B. T., Okatomo, K., Nishino, T., Nishino, T., and Pai, E. F.** (2000). "Crystal structure of bovine milk xanthine dehydrogenase and xanthine oxidase: structure-based mechanism of conversion". *Proc Natl Acad Sci U S A 97*, pp 10723-10728.

29. **Correl, C. C., Batie, C. J., Ballou, D. P., and Ludwig, M. L.** (1985). "Crystalographic characterization of phthalate oxygenase reductase, an iron-sulfur flavoprotein from *Pseudomonas cepacia*". *J Biol Chem 260*, pp 14633-14635.

30. **Howes, B. D., Bray, R. C., Richards, R. L., Turner, N. A., Bennett, B., and Lowe, D. J.** (1996). "Evidence favoring molybdenum-carbon bond formation in xanthine oxidase action: 17O- and 13C-ENDOR and kinetic studies". *Biochemistry 35*, pp 1432-1443.

31. **Xia, M., Dempski, R., and Hille, R.** (1999). "The reductive half-reaction of xanthine oxidase. Reaction with aldehyde substrates and identification of the catalytically labile oxygen". *J Biol Chem 274*, pp 3323-3330.

32. **Porras, A. G., Olson, J. S., and Palmer, G.** (1981). "The reaction of reduced xanthine oxidase with oxygen. Kinetics of peroxide and superoxide formation." *J Biol Chem 256*, pp 9006-9103.

33. **Page, C. C., Moser, C. C., Chen, X., and Dutton, P. L.** (1999). "Natural engineering principles of electron tunnelling in biological oxidation-reduction". *Nature 402*, pp 47-52.

34. **Stockert, A. L., Shinde, S. S., Anderson, R. F., and Hille, R.** (2002). "The reaction mechanism of xanthine oxidase: evidence for two-electron chemistry rather than sequential one-electron steps". *J Am Chem Soc 124*, pp 14554-14555.

35. **Hare, M. L. C.** (1928). "Tyramine Oxidase I. A new enzyme system in liver". *Biochem J 22*, pp 968-972.

36. **Suzuki, H., Katsumata, Y., and Oya, M.** (1979) "Characterization of some biogenic monoamine as substrates for type A and type B monoamine oxidase" in *Monoamine Oxidase: Structure, Functions and Altered Functions* (Singer, T. P., Von Korff, R. W., and Murphy, D. L., Eds.), Academic Press, New York.

37. **O'Carroll, A. M., Anderson, M. C., Tobbia, I., Phillips, J. P., and Tipton, K. F.** (1989). "Determination of the absolute concentrations of monoamine oxidase A and B in human tissues". *Biochem Pharmacol 38*, pp 901-905.

38. **Schnaitman, C., Erwin, V. G., and Greenawalt, J. W.** (1967). "The submitochondrial localization of monoamine oxidase. An enzymatic marker for the outer membrane of rat liver mitochondria". *J. Cell Biol. 32*, pp 719-735.

39. **Johnston, J. P.** (1968). "Some Observations Upon a New Inhibitor of Monoamine Oxidase in Brain Tissue". *Biochem Pharm 17*, pp 1285-1297.

40. **Knoll, J., and Magyar, K.** (1972). "Some puzzling pharmacological effects of monoamine oxidase inhibitors". *Adv Biochem Psycopharm 5*, pp 393-408.

41. **Westlund, K. N., Denney, R. M., Kochersperger, L. M., Rose, R. M., and Abell, C. W.** (1985). "Distinct monoamine oxidase A and B populations in primate brain". *Science 230*, pp 181-183.

42. **Murphy, D. L.** (1978). "Substrate-selective monoamine oxidases - Inhibitor, tissue, species and functional differences". *Biochem Pharm 27*, pp 1889-1893.

43. **Denney, R. M., Fritz, R. R., Patel, N. T., and Abell, C. W.** (1982). "Human liver MAO-A and MAO-B separated by immunoaffinity chromatography with MAO-B-specific monoclonal antibody". *Science 215*, pp 1400-1403.

44. **Singer, T. P.** (1991) "Monoamine Oxidases" in *Chemistry and Biochemistry of Flavoenzymes II*, pp 437-470 (Muller, F., Ed.), CRC Press, Boca Raton, FL.

45. **Ramsay, R. R., and Singer, T. P.** (1991). "The kinetic mechanisms of monoamine oxidases A and B". *Biochem Soc Trans 19*, pp 219-223.

46. **Silverman, R. B.** (1992). "Electron transfer chemistry of monoamine oxidase". *Adv. in Elect. Trans. Chem. 2*, pp 177-213.

47. **Weyler, W., Hsu, H. P., and Breakefield, X. O.** (1990). "Biochemistry and genetics of monoamine oxidase". *Pharmac Ther 47*, pp 391-417.

48. **Weyler, W., and Salach, J. I.** (1985). "Purification and properties of mitochondrial monoamine oxidase type A from human placenta". *J. Biol. Chem. 260*, pp 13199-13207.

49. **Donnelly, C. H., and Murphy, D. L.** (1977). "Substrate- and inhibitor-related characteristics of human platelet monoamine oxidase". *Pharmacology 26*, pp 853-858.

50. **Minamiura, N., and Yasunobu, K. T.** (1978). "Bovine liver monoamine oxidase. A modified purification procedure and preliminary evidence for two subunits and one FAD". *Arch Biochem Biophys 189*, pp 481-489.

51. **Oreland, L.** (1971). "Purification and properties of pig liver mitochondrial monoamine oxidase". *Arch Biochem Biophys 146*, pp 410-421.

52. **Erwin, V. G., and Hellerman, L.** (1967). "Mitochondrial monoamine oxidase 1. Purification and characterization of the bovine kidney enzyme". *J Biol Chem 242*, pp 4230-4238.

53. **Chuang, H. Y. K., Patek, D. R., and Hellerman, L.** (1974). "Mitochondrial monoamine oxidase. Inactivation by pargyline. Adduct formation". *J Biol Chem 249*, pp 2381-2384.

54. **Salach, J. I.** (1979). "Monoamine oxidase from beef liver mitochondria: Simplified isolation procedure, properties and determination of its cysteinyl flavin content". *Arch Biochem Biophys 192*, pp 128-137.

55. **Weyler, W.** (1989). "Monoamine oxidase A from human placenta and monoamine oxidase B from bovine liver both have one FAD per subunit". *Biochem J 260*, pp 725-729.

56. **Kearney, E. B., Salach, J. I., Walker, W. H., Seng, R. L., Kenney, W., Zeszotek, E., and Singer, T. P.** (1971). "The covalently-bound flavin of hepatic monoamine oxidase 1. Isolation and sequence of a flavin peptide and evidence for binding at the 8α position". *Eur J Biochem 24*, pp 321-327.

57. **Walker, W. H., Kearney, E. B., Seng, R. L., and Singer, T. P.** (1971). "The covalently-bound flavin of hepatic monoamine oxidase 2. Identification and properties of cysteinyl riboflavin". *Eur J Biochem 24*, pp 328-331.

58. **Cohen, G.** (1987). "Monoamine oxidase, hydrogen peroxide, and Parkinson's disease". *Adv Neurol 45*, pp 119-125.

59. **Parkinson Study Group**. (1989). "Effect of (-)deprenyl on the progression of disability in early Parkinson's disease". *New Engl J Med 321*, pp 1480-1482.

60. **Yu, P. H., and Davis, A. B.** (1988). "Stereospecific deamination of benzylamine catalysed by different amine oxidases". *Int J Biochem 20*, pp 1197-1201.

61. **Wouters, J.** (1998). "Structural aspects of monoamine oxidase and its reversible inhibition". *Curr Med Chem 5*, pp 137-62.

62. **Chiba, K., Trevor, A., and Castagnoli, N., Jr.** (1984). "Metabolism of the neurotoxic tertiary amine, MPTP, by brain monoamine oxidase". *Biochem Biophys Res Commun 120*, pp 574-578.

63. **Tan, A. K., and Ramsay, R. R.** (1993). "Substrate-specific enhancement of the oxidative half-reaction of monoamine oxidase". *Biochemistry 32*, pp 2137-2143.

64. **Krueger, M. J., Efange, S. M., Michelson, R. H., and Singer, T. P.** (1992). "Interaction of flexible analogs of N-methyl-4-phenyl-1,2,3,6-tetrahydropyridine and

of N-methyl-4-phenylpyridinium with highly purified monoamine oxidase A and B". *Biochemistry 31*, pp 5611-5615.

65. **Efange, S. M. N., Michelson, R. H., Tan, A. K., Krueger, M. J., and Singer, T. P.** (1993). "Molecular size and flexibility as determinants of selectivity in the oxidation of *N*-methyl-4-phenyl-1,2,3,6-tetrahydropyridine analogs by monoamine oxidase A and B". *J Med Chem 36*, pp 1278-1283.

66. **Sablin, S. O., Krueger, M. J., Singer, T. P., Bachurin, S. O., Khare, A. B., Efange, S. M., and Tkachenko, S. E.** (1994). "Interaction of tetrahydrostilbazoles with monoamine oxidase A and B". *J Med Chem 37*, pp 151-157.

67. **Squires, R. F.** (1972). "Multiple forms of monoamine oxidase in intact mitochondria as characterized by selective inhibitors a nd thermal stability: a comparison of eight mammalian species". *Adv Biochem Psycopharm 5*, pp 355-370.

68. **Inoue, H., Castagnoli, K., van der Schyf, C., Mabic, S., Igarashi, K., and Castagnoli, J., N.** (1999). "Species-dependent differences in monoamine oxidase A and B-catalysed oxidation of various C4 substituted 1-methyl-4-phenyl-1,2,3,6-tetrahydropyridinyl derivatives". *J Pharm Exp Therap 291*, pp 856-864.

69. **Benedetti, S., and Dostert, P.** (1985). "Stereochemical aspects of MAO interactions: Reversible and selective inhibitors of monoamine oxidase". *TIPS*, pp 246-251.

70. **Mai, A., Artico, M., Esposito, M., Sbartella, G., Massa, S., Befani, O., Turini, P., Giovanni, V., and Mondovi, B.** (2002). "3-(1*H*-Pyrrol-1-yl)-2-oxazolidinones as reversible, highly potent and selective inhibitors of monoamine oxidase type A". *J Med Chem 45*, pp 1180-1183.

71. **Lebreton, L., Curet, O., Gueddari, S., Mazouz, F., Bernard, S., Burstein, C., and Milcent, R.** (1995). "Selective and potent monoamine oxidase type B inhibitors: 2-substituted 5-aryltetrazole derivatives". *J Med Chem 38*, pp 4786-4792.

72. **Rendenbach-Muller, B., Schlecker, R., Traut, M., and Weifenbach, H.** (1994). "Synthesis of coumarins as subtype-selective inhibitors of monoamine oxidase". *Bioorg Med Chem Lett 4*, pp 1195-1198.

73. **Mazouz, F., Gueddari, S., Burstein, C., Mansuy, D., and Milcent, R.** (1993). "5-[4-(benzyloxy)phenyl]-1,3,4-oxadiazol-2(3H)-one derivatives and related analogues: new reversible, highly potent, and selective monamine oxidase type B inhibitors". *J Med Chem 36*, pp 1157-1167.

74. **Krueger, M. J., Mazouz, F., Ramsay, R. R., Milcent, R., and Singer, T. P.** (1995). "Dramatic species differences in the susceptibility of monoamine oxidase B to a group of powerful inhibitors". *Biochem Biophys Res Commun 206*, pp 556-562.

75. **Egashira, T., Takayama, F., and Yamanaka, Y.** (1999). "The inhibition of monoamine oxidase activity by various antidepressants: Differences found in various mammalian species". *Jpn J Pharmacol 81*, pp 115-121.

76. **Medvedev, A. E., Kirkel, A. A., Kamyshanskaya, N. S., Moskvitina, T. A., Axenova, L. N., Gorkin, V. Z., Andreeva, N. I., Golovina, S. M., and Mashkovsky, M. D.** (1994). "Monoamine oxidase inhibition by novel antidepressant tetrindole". *Biochem Pharmacol 47*, pp 303-308.

77. **Thull, U., Kneubuhler, S., Gaillard, P., Carrupt, P., Testa, B., Altomare, C., Carotti, A., Jenner, P., and McNaught, K. S. P.** (1995). "Inhibition of monoamine oxidase by isoquinoline derivatives". *Biochem Pharm 50*, pp 869-877.

78. **Singer, T. P., Salach, J. I., and Crabtree, D.** (1985). "Reversible inhibition and mechanism-based irreversible inactivation of monoamine oxidases by 1-methyl-4-phenyl-1,2,3,6-tetrahydropyridine (MPTP)". *Biochem Biophys Res Commun 127*, pp 707-712.

79. **Singer, T. P., Salach, J. I., Castagnoli, N., Jr., and Trevor, A.** (1986). "Interactions of the neurotoxic amine 1-methyl-4-phenyl-1,2,3,6-tetrahydropyridine with monoamine oxidases". *Biochem J 235*, pp 785-789.

80. **Medvedev, A. E., Ramsay, R. R., Ivanov, A. S., Veselovsky, A. V., Shvedov, V. I., Tikhonova, O. V., Barradas, A. P., Davidson, C. K., Moskvitina, T. A., Fedotova, O. A., and Axenova, L. N.** (1999). "Inhibition of monoamine oxidase by pirlindole analogues: 3D-QSAR analysis". *Neurobiology (Bp) 7*, pp 151-158.

81. **Curet, O., Damoiseau, G., Aubin, N., Sontag, N., Rovei, V., and Jarreau, F. X.** (1996). "Befloxatone, a new reversible and selective monoamine oxidase A inhibitor. 1.Biochemical profile". *J Pharm Exp Therap 277*, pp 253-264.

82. **Kim, H., Sablin, S. O., and Ramsay, R. R.** (1997). "Inhibition of monoamine oxidase A by beta-carboline derivatives". *Arch Biochem Biophys 337*, pp 137-142.

83. **Jin, Y. Z., Ramsay, R. R., Youngster, S. K., and Singer, T. P.** (1990). "A new class of powerful inhibitors of monamine oxidase A". *Biochem Biophys Res Commun 172*, pp 1338-1341.

84. **McIntosh, C. M., Niemz, A., and Rotello, V. M.** (1999) "Supramolecular models of flavoenzyme redox processes" in *Flavins and Flavoproteins 1999* (Ghisla, S., Kroneck, P., Sund, H., and Macheroux, P., Eds.).

85. **Ramsay, R. R., and Hunter, D. J.** (2002). "Inhibitors alter the spectrum and redox properties of monoamine oxidase A". *Biochim Biophys Acta 1601*, pp 178-184.

86. **Singer, T. P.** (1981) "Suicide inhibitors: An overview" in *Molecular Basis of Drug Action* (Yu, P. H., and et al, Eds.).

87. **Murphy, D. L.** (1976) "Clinical, genetic, hormonal and drug influences on the activity of human platelet monoamine oxidase" in *Monoamine Oxidase and Its*

Inhibition, pp 341-351 (Wolstenholme, G. E., and Knight, J., Eds.), Elsevier, Amsterdam.

88. **Paech, C., Salach, J. I., and Singer, T. P.** (1980). "Suicide inactivation of monoamine oxidase by *trans*-phenylcyclopropylamine". *J. Biol. Chem. 255*, pp 2700-2704.

89. **Silverman, R. B.** (1983). "Mechanism of inactivation of monoamine oxidase by trans-2-phenylcyclopropylamine and the structure of the enzyme-inactivator adduct". *J. Biol. Chem. 258*, pp 14766-14769.

90. **Silverman, R. B., and Zieske, P. A.** (1985). "Mechanism of inactivation of monoamine oxidase by 1-phenylcyclopropylamine". *Biochemistry 24*, pp 2128-2138.

91. **Silverman, R. B., and Zieske, P. A.** (1986). "Identification of the amino acid bound to the labile adduct formed during inactivation of monoamine oxidase by 1-phenylcyclopropylamine". *Biochem Biophys Res Commun 135*, pp 154-159.

92. **Mitchell, D. J., Nikolic, D., van Breemen, R. B., and Silverman, R. B.** (2001). "Inactivation of monoamine oxidase B by 1-phenylcyclopropylamine: mass spectral evidence for the flavin adduct". *Bioorg Med Chem Lett 11*, pp 1757-1760.

93. **Silverman, R. B., and Hiebert, C. K.** (1988). "Inactivation of monoamine oxidase A by the monoamine oxidase B inactivators 1-phenylcyclopropylamine, 1-benzylcyclopropylamine, and N-cyclopropyl-alpha-methylbenzylamine". *Biochemistry 27*, pp 8448-8453.

94. **Silverman, R. B.** (1984). "Effect of alpha-methylation on inactivation of monoamine oxidase by N-cyclopropylbenzylamine". *Biochemistry 23*, pp 5206-5213.

95. **Zhong, B., and Silverman, R. B.** (1997). "Identification of the active site cysteine in bovine liver monoamine oxidase B". *J Am Chem Soc 119*, pp 6690-6691.

96. **Ramsay, R. R., Sablin, S. O., and Singer, T. P.** (1995). "Redox properties of the flavin cofactor of monoamine oxidases A and B and their relationship to the kinetic mechanism". *Prog Brain Res 106*, pp 33-9.

97. **Sablin, S. O., and Ramsay, R. R.** (2001). "Substrates but not inhibitors alter the redox potentials of monoamine oxidases". *Antioxid Redox Signal 3*, pp 723-729.

98. **Draper, R. D., and Ingraham, L. L.** (1968). "A potentiometric study of the flavin semiquinone equilibrium". *Arch Biochem Biophys 125*, pp 802-808.

99. **Cleveland, O. H.** (1968). *Handbook of biochemistry* (Sober, H.A., Ed.), The Chemical Rubber Co.

100. **Sablin, S. O., and Ramsay, R. R.** (1998). "Monoamine oxidase contains a redox-active disulfide". *J. Biol. Chem. 273*, pp 14074-14076.

101. **Miller, J. R., and Edmondson, D. E.** (1999). "Structure-activity relationships in the oxidation of para-substituted benzylamine analogues by recombinant human liver monoamine oxidase A". *Biochemistry 38*, pp 13670-13683.

102. **Li, M., Hubalek, F., Newton-Vinson, P., and Edmondson, D. E.** (2002). "High-level expression of human liver monoamine oxidase A in *Pichia pastoris*: comparison with the enzyme expressed in *Saccharomyces cerevisiae*". *Protein Expr Purif 24*, pp 152-162.

103. **Hsu, Y. P., Weyler, W., Chen, S., Sims, K. B., Rinehart, W. B., Utterback, M. C., Powell, J. F., and Breakefield, X. O.** (1988). "Structural features of human monoamine oxidase A elucidated from cDNA and peptide sequences". *J Neurochem 51*, pp 1321-1324.

104. **Bach, A. W., Lan, N. C., Johnson, D. L., Abell, C. W., Bembenek, M. E., Kwan, S. W., Seeburg, P. H., and Shih, J. C.** (1988). "cDNA cloning of human liver monoamine oxidase A and B: molecular basis of differences in enzymatic properties". *Proc Natl Acad Sci U S A 85*, pp 4934-4938.

105. **Wouters, J., and Baudoux, G.** (1998). "First partial three-dimensional model of human monoamine oxidase A". *Proteins 32*, pp 97-110.

106. **Lan, N. C., Heinzmann, C., Gal, A., Klisak, I., Orth, U., Lai, E., Grimsby, J., Sparkes, R. S., Mohandas, T., and Shih, J. C.** (1989). "Human monoamine oxidase A and B genes map to Xp 11.23 and are deleted in a patient with Norrie disease". *Genomics 4*, pp 552-559.

107. **Grimsby, J., Chen, K., Wang, L. J., Lan, N. C., and Shih, J. C.** (1991). "Human monoamine oxidase A and B genes exhibit identical exon-intron organization". *Proc Natl Acad Sci U S A 88*, pp 3637-3641.

108. **Sablin, S. O., Yankovskaya, V., Bernard, S., Cronin, C. N., and Singer, T. P.** (1998). "Isolation and characterization of an evolutionary percursor of human monoamine oxidases A and B". *Eur J Biochem 253*, pp 270-279.

109. **Singer, T. P., and Barron, E. S.** (1945). "Studies on biological oxidations". *J Biol Chem 157*, pp 241-253.

110. **Gomes, B., Kloepfer, H. G., Oi, S., and Yasunobu, K. T.** (1976). "The reaction of the sulphyldryl reagents with bovine hepatic monoamine oxidase. Evidence for the presence of two cysteine residues essential for activity." *Biochim. et Biophys. Acta 438*, pp 347-357.

111. **Wu, H. F., Chen, K., and Shih, J. C.** (1993). "Site-directed mutagenesis of monoamine oxidase A and B: role of cysteines". *Mol. Pharmacol. 43*, pp 888-893.

112. **Cesura, A. M., Gottowik, J., Lahm, H., Imhof, R., Malherbe, P., Rothlisberger, U., and Da Prada, M.** (1996). "Investigation on the structure of the active site of monoamine oxidase B by affinity labelling with selective inhibitor lazabemide and site-directed mutagenesis". *Eur J Biochem 236*, pp 996-1002.

113. **Hiramatsu, A., Tsurushiin, S., and Yasunobu, K. T.** (1975). "Evidence for essential histidine residues in bovine liver mitochondrial monoamine oxidase". *Eur J Biochem 57*, pp 587-583.

114. **Nandigama, R. K., Miller, J. R., and Edmondson, D. E.** (2001). "Loss of serotonin oxidation as a component of the altered substrate specificity in the Y444F mutant of recombinant human liver MAO A". *Biochemistry 40*, pp 14839-14846.

115. **Nandigama, R. K., and Edmondson, D. E.** (2000). "Influence of FAD structure on its binding and activity with the C406A mutant of recombinant human liver monoamine oxidase A". *J Biol Chem 275*, pp 20527-20532.

116. **Hiro, I., Tsugeno, Y., Hirashiki, I., Ogata, F., and Ito, A.** (1996). "Characterization of rat monoamine oxidase A with noncovalently-bound FAD expressed in yeast cells". *J Biochem (Tokyo) 120*, pp 759-765.

117. **Tsugeno, Y., Hirashiki, I., Ogata, F., and Ito, A.** (1995). "Regions of the molecule responsible for substrate specificity of monoamine oxidase A and B: a chimeric enzyme analysis". *J Biochem (Tokyo) 118*, pp 974-980.

118. **Grimsby, J., Zentner, M., and Shih, J. C.** (1996). "Identification of a region important for human monoamine oxidase B substrate and inhibitor selectivity". *Life Sci 58*, pp 777-787.

119. **Geha, R. M., Chen, K., and Shih, J. C.** (2000). "Phe(208) and Ile(199) in human monoamine oxidase A and B do not determine substrate and inhibitor specificities as in rat". *J Neurochem 75*, pp 1304-1309.

120. **Tsugeno, Y., and Ito, A.** (1997). "A key amino acid responsible for substrate selectivity of monoamine oxidase A and B". *J Biol Chem 272*, pp 14033-14036.

121. **Wouters, J., Ramsay, R. R., Goormaghtigh, E., Ruysschaert, J. M., Brasseur, R., and Durant, F.** (1995). "Secondary structure of monoamine oxidase by FTIR spectroscopy". *Biochem Biophys Res Commun 208*, pp 773-778.

122. **Binda, C., Newton-Vinson, P., Hubalek, F., Edmondson, D. E., and Mattevi, A.** (2002). "Structure of human monoamine oxidase B, a drug target for the treatment of neurological disorders". *Nat Struct Biol 9*, pp 22-26.

123. **Shiloff, B. A., Behrens, P. Q., Kwan, S. W., Lee, J. H., and Abell, C. W.** (1996). "Monoamine oxidase B isolated from bovine liver exists as large oligomeric complexes *in vitro*". *Eur J Biochem 242*, pp 719-735.

124. **Pawelek, P. D., Cheah, J., Coulombe, R., Macheroux, P., Ghisla, S., and Vrielink, A.** (2000). "The structure of L-amino acid oxidase reveals the substrate trajectory into enantiomerically conserved active site". *EMBOJ 19*, pp 4204-4215.

125. **Mitoma, J., and Ito, A.** (1992). "Mitochondrial targeting signal of rat liver monoamine oxidase B is located at its carboxy terminus". *J Biochem (Tokyo) 111*, pp 20-24.

126. **von Heijne, G.** (1992). "Membrane protein structure prediction. Hydrophobicity analysis and the positive-inside rule". *J Mol Biol 225*, pp 487-494.

127. **Veselovsky, A. V., Medvedev, A. E., Tikhonova, O. V., Skvortsov, V. S., and Ivanov, A. S.** (2000). "Modeling of substrate-binding region of the active site of monoamine oxidase A". *Biochemistry (Mosc) 65*, pp 910-916.

128. **Geha, R. M., Chen, K., Wouters, J., Ooms, F., and Shih, J. C.** (2002). "Analysis of conserved active site residues in monoamine oxidase A and B and their three-dimensional molecular modeling". *J Biol Chem 277*, pp 17209-17216.

129. **Hynson, R. M. G., Ramsay, R. R., and Philp, D.** (2002) "Inhibitor interactions with the active site redox cofactor of MAO A" in *Flavins and flavoproteins 2002*, pp 867-871 (Chapman, S. K., Perham, R. N., and Scrutton, N. S., Eds.), Rudolf Weber, Berlin.

130. **Wouters, J., Moureau, F., Vercauteren, D. P., Evrard, G., Durant, F., Koenig, J. J., Ducrey, F., and Jarreau, F. X.** (1994). "Experimental and theoretical study of reversible monoamine oxidase inhibitors: structural approach of the active site of the enzyme". *J Neural Transm Suppl 41*, pp 313-319.

131. **Husain, M., Edmondson, D. E., and Singer, T. P.** (1982). "Kinetic studies on the catalytic mechanism of liver monoamine oxidase". *Biochemistry 21*, pp 595-600.

132. **Pearce, L. B., and Roth, J. A.** (1985). "Human brain monoamine oxidase type B: Mechanism of deamination as probed by steady-state methods". *Biochemistry 24*, pp 1821-1826.

133. **Ramsay, R. R., Koerber, S. C., and Singer, T. P.** (1987). "Stopped-flow studies on the mechanism of oxidation of N-methyl-4-phenyltetrahydropyridine by bovine liver monoamine oxidase B". *Biochemistry 26*, pp 3045-3050.

134. **Ramsay, R. R.** (1991). "Kinetic mechanism of monoamine oxidase A". *Biochemistry 30*, pp 4624-4629.

135. **Singer, T. P., and Ramsay, R. R.** (1995). "Flavoprotein structure and mechanism 2. Monoamine oxidases: old friends hold many surprises". *FASEB J 9*, pp 605-610.

136. **Houslay, M. D., and Tipton, K. F.** (1975). "Rat liver mitochondrial monoamine oxidase. A change in the reaction mechanism on solubilization". *Biochem J 145*, pp 311-321.

137. **Edmondson, D. E., Bhattacharyya, A. K., and Walker, M. C.** (1993). "Spectral and kinetic studies of imine product formation in the oxidation of p-(N,N-

dimethylamino)benzylamine analogues by monoamine oxidase B". *Biochemistry 32*, pp 5196-51202.

138. **Weyler, W.** (1987). "2-Chloro-2-phenylethylamine as a mechanistic probe and active site directed inhibitor of monoamine oxidase from bovine liver mitochondria". *Arch Biochem Biophys 255*, pp 400-408.

139. **Silverman, R. B.** (1995). "Radical ideas about monoamine oxidase". *Acc. Chem. Res. 28*, pp 335-342.

140. **Hamilton, G. A.** (1971) "The proton in biological redox reactions" in *Progress in Bioorganic Chemistry*, pp 83-157 (Kaiser, E. T., and Kedzy, F. J., Eds.), Wiley-Interscience, New York.

141. **Silverman, R. B., and Lu, X.** (1994). "Evidence against a nucleophilic mechanism for monoamine oxidase-catalyzed amine oxidation". *J Am Chem Soc 116*, pp 4129-4130.

142. **Silverman, R. B., Lu, X., Zhou, J. J., and Swihart, A.** (1994). "Monoamine oxidase B-catalyzed oxidation of cinnamylamine-2,3-oxide. Further evidence against a nucleophilic mechanism". *J Am Chem Soc 116*, pp 11590-11591.

143. **Silverman, R. B., and Zieske, P. A.** (1986). "1-Phenylcyclobutylamine, the first in a new class of monoamine oxidase inactivators. Further evidence for a radical intermediate". *Biochemistry 25*, pp 341-346.

144. **Miller, J. R., and Edmondson, D. E.** (1999). "Structure-activity relationships in the oxidation of para-substituted benzylamine analogues by recombinant human liver monoamine oxidase A". *Biochemistry 38*, pp 13670-83.

145. **Tomilov, A. P., Maironovskii, S. G., Fioshin, M. Y., and Smirnov, V. A.** (1972). *Electrochemistry of Organic Compounds*, Haldsted Press, New York.

146. **Miller, J. R., Edmondson, D. E., and Grissom, C. B.** (1995). "Mechanistic probes of monoamine oxidase B catalysis: rapid-scan stopped-flow and magnetic independence of the reductive half-reaction". *J Am Chem Soc 117*, pp 7830-7831.

147. **Yelekci, K., Lu, X., and Silverman, R. B.** (1989). "Electron spin resonance studies of monoamine oxidase B. First evidence for a substrate radical intermediate". *J Am Chem Soc 111*, pp 1138-1140.

148. **Walker, M. C., and Edmondson, D. E.** (1987) "Kinetic probes of the proposed radical mechanism of monoamine oxidase" in *Flavins and Flavoproteins 1987*, pp 699-703 (McCormick, D. B., Ed.), Walter de Gruyter, Berlin.

149. **Parkinson Study Group**. (2000). "A controlled clinical trial of rasagiline in early Parkinson's disease". *Am Neurol Assoc.*

150. **Youdim, M. B. H., Gross, A., and Finberg, J. P.** (2001). "Rasagiline (N-propagyl-1R(+)-aminoindan), a selective and potent inhibitor of mitochondrial monoamine oxidase B". *Br J Pharmacol 132*, pp 500-506.

151. **Tatton, N. A., and Chalmers-Redman, R. M. E.** (1996). "Modulation of gene expression rather than monoamine oxidase inhibition: (-)-deprenyl-related compounds in controlling neurodegeneration". *Neurobiology 44(suppl.3)*, pp S171-183.

152. **Youdim, M. B. H., Wadia, A., Tatton, N. A., and Weinstock, M.** (2001). "The antiparkinson drug rasagiline and its cholinesterase inhibitor derivatives exert neuroprotection unrelated to MAO inhibition in cell culture and *in vivo*". *Ann NY Acad Sci 931*, pp 450-458.

153. **Irwin, I., and Langston, J. W.** (1985). "Selective accumulation of MPP^+ in the substantia nigra: a key to neurotoxicity?" *Life Sci 36*, pp 207-212.

154. **Langston, J. W., Ballard, P., Tetrud, J. W., and Irwin, I.** (1983). "Chronic parkinsonism in humans due to a product of meperidine-analog synthesis". *Science 219*, pp 979-980.

155. **Saura, J., Luque, J. M., Cesura, A. M., Da Prada, M., Chan-Palay, V., Huber, G., Loffler, J., and Richards, J. G.** (1994). "Increased monoamine oxidase B activity in plaque-associated astrocytes of Alzheimer brains revealed quantitative enzyme radioautography". *Neuroscience 62*, pp 15-30.

156. **Thomas, T.** (2000). "Monoamine oxidase-B inhibitors in the treatment of Alzheimers disease". *Neurobiol Aging 21*, pp 343-348.

157. **Youdim, M. B. H., and Weinstock, M.** (2002). "Novel neuroprotective anti-Alzheimer drugs with anti-depressant activity derived from the anti-Parkinson drug, rasagiline". *Mechan Ageing Develop 123*, pp 1081-1086.

158. **Bruhlmann, C., Ooms, F., Carrupt, P., Testa, B., Catto, M., Leonetti, F., Altomare, C., and Carotti, A.** (2001). "Coumarins derivatives as dual inhibitors of acetylcholinesterase and monoamine oxidase". *J Med Chem 44*, pp 3195-3198.

159. **Brunner, H. G., Nelen, M., Breakefield, X. O., Ropers, H. H., and van Oost, B. A.** (1993). "Abnormal behavior associated with a point mutation in the structural gene for monoamine oxidase A". *Science 262*, pp 578-580.

160. **Cases, O., Seif, I., Grimsby, J., Gaspar, P., Chen, K., Pournin, S., Muller, U., Aguet, M., Babinet, C., Shih, J. C., and et al.** (1995). "Aggressive behavior and altered amounts of brain serotonin and norepinephrine in mice lacking MAOA". *Science 268*, pp 1763-1766.

161. **Kim, J. J., Shih, J. C., Chen, K., Chen, L., Bao, S., and al, e.** (1997). "Selective enhancement of emotional, but not motor, learning in monoamine oxidase A-deficient mice". *Proc Natl Acad Sci USA 94*, pp 5929-5933.

162. **Grimsby, J., Toth, M., Chen, K., Kumazawa, T., Klaidman, L., and al, e.** (1997). "Increased stress response and β-phenylethylamine in MAO B-deficient mice". *Nature Genet 17*, pp 1-5.

163. **Fowler, J. S., Volkow, N. D., Wang, G. J., Pappas, N., Logan, J., MacGregor, R., Alexoff, D., Shea, C., Schlyer, D., Wolf, A. P., Warner, D., Zezulkova, I., and Cilento, R.** (1996). "Inhibition of monoamine oxidase B in the brain of smokers". *Nature 379*, pp 733-736.

164. **Fowler, J. S., Volkow, N. D., Wang, G. J., Pappas, N., Logan, J., Shea, C., Alexoff, D., MacGregor, R., Schlyer, D., Zezulkova, I., and Wolf, A. P.** (1996). "Brain monoamine oxidase A inhibition on cigarette smokers". *Proc Natl Acad Sci USA 93*, pp 14065-14069.

165. **Yu, P. H., and Boulton, A. A.** (1987). "Irreversible inhibition of monoamine oxidase by some components of cigarette smoke". *Life Sci 41*, pp 675-682.

166. **Honig, L. S.** (1999). "Smoking and Parkinson's Disease". *Neurology 53*, pp 1158.

167. **Promega** (1996). *Protocols and Applications Guide* (3rd, Ed.), Promega Corporation.

168. **Boehm, T., Pirie-Shepherd, S., Trinh, L.-B., Shiloach, J., and Folkman, J.** (1999). "Disruption of the KEX1 gene in *Pichia pastoris* allows expression of full-length murine and human endostatin". *Yeast 15*, pp 563-572.

169. **Pompon, D., Louerat, B., Bronine, A., and Urban, P.** (1996). "Yeast Expression of Animal and Plant P450s in Optimized Redox Environments". *Methods Enzymol. 272*, pp 51-64.

170. **Bollag, D. M., Rozycki, M. D., and Edelstein, S. J.** (1996). *Protein Methods* (2nd, Ed.), Wiley-Liss.

171. **Tan, A. K., Weyler, W., Salach, J. I., and Singer, T. P.** (1991). "Differences in Substrate Specificities of Monoamine Oxidase A from Human liver and Placenta". *Biochem. Biophys. Res. Commun. 181*, pp 1084-1088.

172. **Higgins, D. R., and Cregg, J. M.** (1998). "Introduction to *Pichia pastoris*". *Methods Mol Biol 103*, pp 1-15.

173. **Waterham, H. R., Diggan, M. E., Koutz, P. J., Lair, S. V., and Cregg, J. M.** (1997). "Isolation of the *Pichia pastoris* glyceraldehyde-3-phosphate dehydrogenase gene and regulation and use of its promoter". *Gene 186*, pp 37-44.

174. **Gottowik, J., Cesura, A. M., Malherbe, P., Lang, G., and Da Prada, M.** (1993). "Characterization of wild-type and mutant forms of human monoamine oxidase A and B expressed in a mammalian cell line". *FEBS Lett 317*, pp 152-156.

175. **Newton-Vinson, P., Hubalek, F., and Edmondson, D. E.** (2000). "High-level expression of human liver monoamine oxidase B in Pichia pastoris". *Protein Expr Purif 20*, pp 334-45.

176. **Cereghino, J. L., and Cregg, J. M.** (2000). "Heterologous protein expression in the methylotrophic yeast *Pichia pastoris*". *FEMS Microbiol Rev 24*, pp 45-66.

177. **Fersht, A. R.** (1977). *Enzyme structure and mechanism*, W. H. Freeman, San Francisco.

178. **Wilkinson, A. J., A.R., F., Blow, D. M., and Winter, G.** (1983). "Site-directed mutagenesis as a probe of enzyme structure and catalysis: tyrosyl-tRNA synthetase cysteine-35 to glycine-35 mutation". *Biochemistry 22*, pp 3581-3586.

179. **Segel, I. H.** (1975). *Enzyme kinetics. Behaviour and analysis of rapid-equilibrium and steady-state enzyme systems*. pp 767-783, Wiley-Interscience, USA.

180. **Hubalek, F., and Edmondson, D. E.** (2002) "Thiol reactivities as probes of MAO A and MAO B structures and function" in *Flavins and flavoproteins 2002*, pp 217-222 (Scrutton, N. S., Ed.), Rudolf Weber, Berlin.

181. **Silverman, R. B., and Yamasaki, R. B.** (1984). "Mechanism-based inactivation of mitochondrial monoamine oxidase by N-(1-methylcyclopropyl)benzylamine". *Biochemistry 23*, pp 1322-1332.